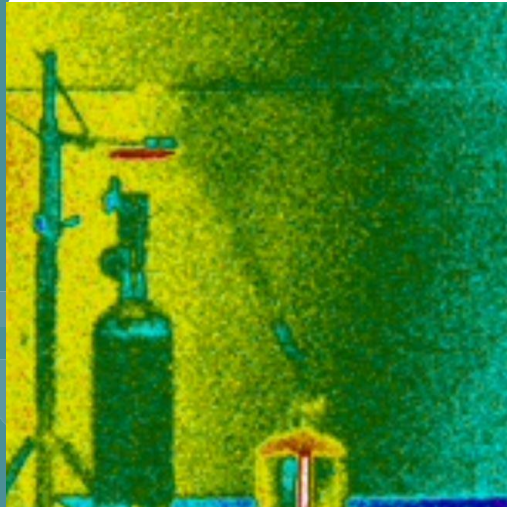


# A REPORT ON USING FORWARD LOOKING INFRARED RADIATION (FLIR) TECHNOLOGY AS AN EFFECTIVE PCE/TCE SCREENING TOOL FOR VAPOR INTRUSION SAMPLING



U.S. EPA  
Office of Research and Development  
National Risk Management Research Laboratory  
Land and Materials Management Division  
Remediation and Technology Evaluation Branch

and

U.S. EPA Region 6  
Superfund Division

*This page intentionally left blank.*

September 2018

# **A Report on Using Forward Looking Infrared Radiation (FLIR) Technology as an Effective PCE/TCE Screening Tool for Vapor Intrusion Sampling**

Land and Materials Management Division  
National Risk Management Research Laboratory  
Cincinnati, OH, 45268

and

Superfund Division  
U.S. EPA Region 6  
Dallas, TX, 75202

# Authors

## **Primary Authors**

### **David Eppler**

US Environmental Protection Agency  
Superfund Division  
1445 Ross Ave.  
Dallas, TX 75202

### **David Ferguson**

US Environmental Protection Agency  
Land and Materials Management Division  
National Risk Management Research Laboratory  
26 W. Martin Luther King Dr.  
Cincinnati, OH 45268

### **Michael Torres**

US Environmental Protection Agency  
Superfund Division  
1445 Ross Ave.  
Dallas, TX 75202

### **Daniel Young**

US Environmental Protection Agency  
Land and Materials Management Division  
National Risk Management Research Laboratory  
26 W. Martin Luther King Dr.  
Cincinnati, OH 45268

### **Raghuraman Venkatapathy**

Pegasus Technical Services, Inc.  
46 E. Hollister Street  
Cincinnati, OH 45219

# Notice/Disclaimer Statement

This report is a review of available methods for using Forward Looking Infrared Radiation (FLIR) technology as an effective PCE/TCE screening tool for vapor intrusion sampling. The inclusion of or affirmative statements regarding any method, data, or model included in this review does not imply endorsement by the U.S. Environmental Protection Agency. The quality of the methods, data, or models has not been evaluated by the U.S. EPA for any specific application. Upon review, approval does not signify the contents reflect the views of the U.S. EPA, nor does mention of trade names or commercial products constitute endorsement or recommendation for use.

# Foreword

The U.S. Environmental Protection Agency (US EPA) is charged by Congress with protecting the Nation's land, air, and surface water and groundwater resources. Under a mandate of national environmental laws, the US EPA strives to formulate and implement actions leading to a compatible balance between human activities and the ability of natural systems to support and nurture life. To meet this mandate, US EPA's research program is providing data and technical support for solving environmental problems today and building a science knowledge base necessary to manage our ecological/environmental resources wisely, understand how pollutants affect our health, and prevent or reduce public health and environmental threats/risks in the future.

The Superfund Division within US EPA Region 6 implements and enforces the federal Comprehensive Environmental Response, Compensation and Liability Act, the Superfund Amendments and Reauthorization Act, and the Oil Pollution Act and the Brownfields program. EPA's Superfund program is responsible for cleaning up some of the nation's most contaminated land and responding to environmental emergencies, oil spills and natural disasters. To protect public health and the environment, the Superfund program focuses on making a visible and lasting difference in communities, ensuring that people can live and work in healthy, vibrant places. EPA risk managers provide the technical risk assessments the Superfund program uses to determine whether remediation is required for a Superfund site. EPA Region 6 provides the risk management assessments to clean up contaminated sites located in Arkansas, Louisiana, New Mexico, Oklahoma, Texas and 66 Tribes.

The National Risk Management Research Laboratory (NRMRL) within the Office of Research and Development (ORD) is the Agency's center for investigation of technological and management approaches for preventing and reducing risks from pollution that threaten human health and the environment. The focus of the Laboratory's research program is on methods and their cost-effectiveness for prevention and control of pollution to air, land, water, and subsurface resources; protection of water quality in public water systems; remediation of contaminated sites, sediments, and ground water; prevention and control of indoor air pollution; and restoration of ecosystems. NRMRL collaborates with both public and private sector partners to foster technologies that reduce the cost of compliance and to anticipate emerging problems. NRMRL's research provides solutions to environmental problems by: 1) developing and promoting technologies that protect and improve the environment; 2) advancing scientific and engineering information to support regulatory and policy decisions; and 3) providing the technical support and information transfer to ensure implementation of environmental regulations and strategies at the national, state, and community levels.

This report is a summary of the experiments conducted in support of using FLIR technology as a screening tool for detecting tetrachloroethylene (PCE) and trichloroethylene (TCE) vapor intrusion into indoor or outdoor settings. Research to support this effort was conducted at the EPA Region 6 Addison Facility in Texas. Development of this project arose through close collaboration of ORD and EPA Region 6. Findings in this report represent an evaluation of the FLIR GF-306 and FLIR GF-320 VOC camera systems to detect PCE, TCE and other gases of interest under various scenarios, including flow through systems that simulate a vapor intrusion leak, and static systems that mimic confined spaces.

Cynthia Sonich-Mullin, Director  
National Risk Management Research Laboratory

Carl E. Edlund, P.E., Director  
Superfund Division, US EPA, Region 6

## Table of Contents

Authors .....	iv
Notice/Disclaimer Statement .....	v
Table of Contents .....	vii
Executive Summary .....	xv
Acknowledgments .....	xvii
1. INTRODUCTION .....	1
1.1 Objectives .....	7
2. BACKGROUND .....	9
3. EXPERIMENTAL APPROACH .....	14
3.1 Materials .....	14
3.1.1 Chemicals Used .....	14
3.1.2 Camera Systems .....	14
3.2 Methods .....	18
3.2.1 Leak Detection Experiments .....	18
3.3 Databases .....	21
3.3.1 NIST WebBook .....	21
3.3.2 Pacific Northwest National Laboratory IR Database .....	22
3.3.3 Response Factor (RF) Calculator .....	22
4. QUALITY ASSURANCE/QUALITY CONTROL .....	25
5. RESULTS AND DISCUSSION .....	26
5.1 Camera Performance Check .....	26
5.2 PCE and TCE Leak Detection .....	32
5.3 Determination of Gas Detection Capabilities for each Camera System .....	35
5.4 PCE and TCE Gas Detection Capabilities for each Camera System .....	37
5.5 Determination of Gas Leak Detection Limits .....	40
5.5.1 Determination of Detection Limits using the RF Calculator .....	41
5.5.2 Estimation of Detection Limits using IR Spectra .....	43
5.6 Static Detection of Gas using the Two Camera Systems .....	44
5.7 Implications for Testing Vapor Intrusion Scenarios .....	57
6. CONCLUSIONS .....	64
7. RECOMMENDATIONS .....	66
8. REFERENCES .....	68

## Table of Figures

Figure 1.1: The PCE Plume Superfund Site located in Roswell, NM. The purple circles represent soil gas sampling locations, and the contours represent PCE isoconcentrations, with the innermost contour in red having the highest soil gas PCE concentration (Niemet <i>et al.</i> , 2012). .....	2
Figure 1.2: The PCE Plume Superfund Site located in Roswell, NM. The purple circles represent soil gas sampling locations, and the contours represent PCE isoconcentrations, with the innermost contour in red having the highest soil gas PCE concentration. In addition, the black contours represent groundwater contamination, with the innermost black contour having groundwater PCE concentrations higher than 1000 parts per billion (Niemet <i>et al.</i> , 2012). .....	3
Figure 1.3: The PCE Plume Superfund Site located in Roswell, NM. The red squares represent outdoor air sampling locations, and the contours represent PCE isoconcentrations, with the innermost contour having the highest indoor air PCE concentration or $>50 \mu\text{g}/\text{m}^3$ , and site OD-11 having the highest PCE concentration in the air at $57.9 \mu\text{g}/\text{m}^3$ (Niemet <i>et al.</i> , 2012). .....	4
Figure 1.4: Schematic illustrating vapor intrusion into a typical home. ....	5
Figure 2.1: Schematic illustrating the electromagnetic spectrum from ionizing radiation at the far left (high frequency, short wavelength) to radio waves at the far right (low frequency, long wavelength). ....	9
Figure 2.2: A ball and stick figure of TCE, which has two carbon atoms (gray balls), three chlorine atoms (green balls) and a hydrogen atom (white ball). The sticks connecting the balls represent the type of bond, with the single stick representing a single bond, and the two parallel sticks between the two carbon atoms representing a double bond. ....	10
Figure 2.3: A ball and stick figure of PCE, which has two carbon atoms (gray balls) and four chlorine atoms (green balls). The sticks connecting the balls represent the type of bond, with the single stick representing a single bond, and the two parallel sticks between the two carbon atoms representing a double bond. ....	11
Figure 2.4: Illustration of stretching and bending vibrations in a carbon atom connected to two other atoms via a single bond. Source: <a href="http://shodor.org/succeed-1.0/compchem/labs/vibrations/">http://shodor.org/succeed-1.0/compchem/labs/vibrations/</a> .....	11
Figure 2.5: Vibrational modes of a chemical molecule that is similar to PCE and TCE. Source: Lochter <i>et al.</i> , 2012. A molecule similar to PCE and TCE will have 12 unique vibrational modes, and each of these frequencies will be different for different molecules. ....	12
Figure 2.6: IR spectrum of 1,1-difluoroethylene. ....	12
Figure 3.1: A FLIR GF-306 long-range IR camera (Source: FLIR Systems) that can detect ammonia and sulfur hexafluoride among other gases. ....	16
Figure 3.2: A FLIR GF-320 medium-range IR camera (Source: FLIR Systems) that is designed to detect VOC gases. ....	19
Figure 3.4: Experiment set up at the EPA Region 6 Addison Texas Facility. Gas canisters and bottles or vials containing chemicals such as ammonium hydroxide, dichloromethane, and	

hexanes were opened in the hood, and the camera was focused on the opening. The camera was placed exactly 8 feet from the hood. ....	20
Figure 3.3: Experiment set up at the EPA Region 6 Addison Texas Facility. Ventilation in the hood was turned off between experiments using the switch that can be seen on the right wall. ....	21
Figure 3.5: Screenshot of the Vibrational Energy search interface of the NIST WebBook database. Cameras can detect chemicals whose vibrational energies fall within their sensor's spectral range. ....	22
Figure 3.6: IR spectrum of PCE at 25 °C as shown in the PNNL database. PCE is referred to as perchloroethylene in the database. The inset shows the highest absorbance of PCE is approximately 920 cm <sup>-1</sup> (10.9 μm). ....	23
Figure 3.7: Relation between vapor pressure (Torr) and temperature (°C) for PCE as shown in the PNNL database. PCE is referred to as 1,1,2,2-Tetrachloroethene in the database. This relationship can be used to correct the IR spectra for other temperatures. ....	24
Figure 5.1: IR spectrum of propane as shown in the NIST WebBook database. The y-axis depicts percent light transmittance (1.0 indicates light is fully transmitted), while the x-axis shows the wavelength in micrometers. The amount of light absorbed is 100% minus the amount of light transmitted. The figure indicates that propane absorbs a majority of the light in the IR region between 2 – 4 μm wavelengths, while minor amounts are absorbed between 6 – 8 μm. ....	26
Figure 5.2: IR spectrum of ammonia as shown in the NIST WebBook database. The y-axis depicts percent light transmittance, while the x-axis shows the wavelength in micrometers. The figure indicates that ammonia absorbs most of the light in the IR range between 10 – 11 μm wavelengths. ....	26
Figure 5.3: IR image of an open propane tank using the black is hot palette. The gas plume is seen as black clouds against a white background. ....	27
Figure 5.4: IR image of an open propane tank using the white is hot palette. The gas plume is seen as white clouds against a black background. ....	28
Figure 5.5: IR image of an open propane tank using the rainbow color palette. The gas plume is seen as a black cloud against a yellow background. ....	29
Figure 5.6: IR image of an open vial containing ammonium hydroxide using the black is hot palette. A black plume is seen at the top of the vial as the liquid ammonium hydroxide vaporizes and is released into the air. ....	30
Figure 5.7: IR image of an open vial containing ammonium hydroxide using the white is hot palette. A white plume is seen rising from the top of the vial. ....	31
Figure 5.8: IR image of an open vial containing ammonium hydroxide using the rainbow color palette. The ammonia vapors are harder to see with the rainbow or any of the other available color palettes. ....	32
Figure 5.9: IR image of the top of a TCE gas canister using the black is hot palette. TCE, if detected, would show up as a black cloud above the nozzle that is pointed upwards. ....	33
Figure 5.10: IR image of the top of a TCE gas canister using the color palette. TCE, if detected, would show up as a blue cloud above the nozzle that is pointed upwards. ....	34
Figure 5.11: IR image of the top of a TCE gas canister using the white is hot palette. TCE, if detected,	

	would show up as a white cloud above the nozzle that is pointed upwards. A lack of a white cloud above the nozzle indicates the camera was not able to detect TCE. ....	35
Figure 5.12:	IR spectra of propane close to the 3.2 – 3.4 $\mu\text{m}$ spectral range. Since propane has a transmittance peak with a minima at approximately 3.36 $\mu\text{m}$ with approximately 30% transmittance (the minima are close to the 0.3 transmittance line in the y-axis), the GF-320 VOC camera can detect propane. ....	36
Figure 5.13:	IR spectra of propane close to the 10.3 – 10.7 $\mu\text{m}$ spectral range. Since the transmittance is very close to 1 for propane in this spectral range, the GF-306 camera, whose absorbance falls within this spectral range, cannot detect propane. ....	36
Figure 5.14:	IR spectra of ammonia close to the 10.3 – 10.7 $\mu\text{m}$ spectral range (shown using dark blue lines parallel to the y-axis). Even though ammonia has a transmittance peak with a minima at approximately 10.75 $\mu\text{m}$ , which is outside the spectral range of the GF-306 camera, the gas has some absorbance within the spectral range (60% transmittance close to 10.4 $\mu\text{m}$ and approximately 60% transmittance at 10.7 $\mu\text{m}$ ), the GF-306 camera can detect ammonium hydroxide vapors, which has a spectra similar to ammonia.....	37
Figure 5.15:	IR spectra of ammonia close to the 3.2 – 3.4 $\mu\text{m}$ spectral range. Since the transmittance is very close to 1 for ammonia in this spectral range, the GF-320 VOC camera, whose absorbance falls within this spectral range, cannot detect ammonium hydroxide vapors.....	37
Figure 5.16:	IR spectrum of TCE from the NIST WebBook database.....	38
Figure 5.17:	IR spectrum of PCE from the NIST WebBook database.....	38
Figure 5.18:	IR spectrum of TCE in the 10.3 – 10.7 $\mu\text{m}$ spectral region. The GF-306 camera can detect TCE molecules whose transmittance is in the shaded region. ....	39
Figure 5.19:	IR spectrum of TCE in the 3.2 – 3.4 $\mu\text{m}$ spectral region. The GF-320 VOC camera can detect TCE molecules whose transmittance is in this region.....	39
Figure 5.20:	IR spectrum of PCE in the 10.3 – 10.7 $\mu\text{m}$ spectral region. Though the PCE IR spectrum shows a transmittance peak in the figure, the dip in the transmittance starts at approximately 10.7 $\mu\text{m}$ . The transmittance is close to 100% in the 10.3 – 10.7 $\mu\text{m}$ spectral region, which is the spectral range of the GF-306 camera sensor. Hence, the camera is not able to detect PCE.....	40
Figure 5.21:	IR spectra of PCE in the 3.2 – 3.4 $\mu\text{m}$ spectral region. The transmittance is close to 100% in the 3.2 – 3.4 $\mu\text{m}$ spectral region, which is the spectral range of the GF-320 VOC camera sensor. Hence, the VOC camera is not able to detect PCE. ....	40
Figure 5.22:	The Response Factor (RF) Calculator website ( <a href="http://rfcalc.providencelphotonics.com/">http://rfcalc.providencelphotonics.com/</a> ). Appropriate selections were made for the camera, chemical and CL.....	42
Figure 5.23:	RF calculations results for PCE. Calculated results indicate that PCE is 1000 times less sensitive than the reference chemical, propane.....	42
Figure 5.24:	IR spectrum for propane in the spectral range of the FLIR GF-320 VOC camera system. .	43
Figure 5.25:	IR spectrum for TCE in the spectral range of the FLIR GF-320 VOC camera system. The area of the shaded region for TCE in this figure is approximately 5% of the area for propane (shown in Figure 5.24), suggesting the sensitivity of TCE is approximately	

5% of that of propane as detected by the GF-320 VOC camera.....	44
Figure 5.26: A schematic illustrating the importance of concentration and dimensions of the plume on the sensitivity of the camera towards a gas plume (Source: FLIR Systems, Inc.). If the vertical line closest to the camera lens can be considered to be the 100 cm line, and the line farthest away can be considered the 1 m line, the amount of gas seen by the camera at the 100 cm line is much smaller than the amount of gas seen at the 1 m line, leading to better sensitivity at the 1m line. ....	45
Figure 5.27: An inverted beaker and other glass jars were tested to “capture” PCE or TCE gas. In the picture, an open bottle containing ammonium hydroxide that was placed inside one of the glass jars could not be “seen” by the FLIR GF-306 camera as the outside glass jar was made of borosilicate glass, which blocks IR radiation from passing through. ....	46
Figure 5.28: An IR image of an empty 60 ml HDPE bottle using the rainbow color palette taken with the FLIR GF-306 camera. The bottle containing air was indistinguishable from the background.....	47
Figure 5.29: An IR image of a 60 ml HDPE bottle containing a few drops of ammonium hydroxide using the rainbow color palette. The ammonia vapors inside the HDPE bottle was easily distinguished by the FLIR GF-306 camera. ....	48
Figure 5.30: IR spectrum of hexane from the NIST WebBook database. The transmittance of hexane decreases in the 3.2 – 3.4 $\mu\text{m}$ spectral region, which can be detected by the FLIR-320 VOC camera. There is no reduction in transmittance in the 10.3 – 10.7 $\mu\text{m}$ spectral region, which indicates the GF-306 camera will be not be able to detect hexane.....	49
Figure 5.31: An IR image of a 60 ml HDPE bottle containing a few drops of hexane using the rainbow color palette. The hexane and its vapors inside the HDPE bottle was not detected by the FLIR GF-306 camera. ....	50
Figure 5.32: An IR image of a 60 ml HDPE bottle containing a few drops of ammonium hydroxide using the rainbow color palette. The cap on the nozzle was opened, and the bottle gently squeezed, releasing ammonia vapors in a jet stream, which is seen as a red plume.....	51
Figure 5.33: An IR image of a 60 ml HDPE bottle containing a few drops of ammonium hydroxide using the rainbow color palette. The cap on the nozzle was opened, and the bottle gently squeezed, releasing ammonia vapors in a jet stream, which is a red plume emanating from the nozzle. (The investigator’s hand and arm are seen as color palette with blue is hot.) .....	52
Figure 5.34: A setup to detect TCE gas in a 60 ml HDPE bottle. Two bottles were placed side by side on top of two glass jars to keep the HDPE bottles in line with the camera lens. The bottle on the left contained air while the bottle on the right contained 125 ppb TCE. ....	53
Figure 5.35: An IR image of two 60 ml HDPE bottles, the one on the right containing 125 ppb TCE, and the one on the left containing air using the rainbow color palette. The bottle containing TCE is bluish green, while the one containing air is yellow.....	54
Figure 5.36: An IR image of two 60 ml HDPE bottles, the one on the right containing 125 ppb TCE, and the one on the left containing air using the “black is hot” palette. The bottle containing TCE is darker in color, while the background and the one containing air are lighter in color. ....	55

Figure 5.37: An IR image of two 60 ml HDPE bottles, the one on the right containing 125 ppb TCE, and the one on the left containing air using the “white is hot” palette. The bottle containing TCE is lighter in color, while the background and the one containing air are darker in color. .... 55

Figure 5.38: A setup to detect TCE gas in a 60 ml HDPE bottle. Two bottles were placed side by side on top of two glass jars to keep the HDPE bottles in line with the camera lens. The bottle on the left contained air while the bottle on the right contained 125 ppb TCE. An IR image of the two bottles can be seen on the camera’s LCD screen in the foreground. .... 56

Figure 5.39: A setup to detect TCE gas in a 60 ml HDPE bottle. Two bottles were placed side by side on top of two glass jars to keep the HDPE bottles in line with the camera lens. The bottle on the left contained air while the bottle on the right contained 125 ppb TCE. An IR image of the two bottles can be seen on the camera’s LCD screen in the foreground. .... 57

Figure 7.1: PCE IR spectrum in the 10 – 14  $\mu\text{m}$  range. A VarioCAM with the wider spectral range will be able to take advantage of both transmittance peaks. .... 66

Figure 7.2: TCE IR spectrum in the 10 – 14  $\mu\text{m}$  range. A VarioCAM with the wider spectral range will be able to take advantage of all three transmittance peaks as opposed to half of one for the GF-306 camera. .... 66

# Tables

Table 3.1: Protective levels for PCE and TCE under residential air and worker air exposure scenarios	14
Table 3.2: Regional Screening Levels for TCE (US EPA, 2016)	14
Table 3.3: Technical specifications for the FLIR GF 306 camera	15
Table 3.4: Technical specifications for the FLIR GF 320 camera system	17
Table 3.5: Minimum Detected Leak Rate (MDLR) for various VOCs as determined by a third-party laboratory	18
Table 5.1: List of chemicals that can be detected by the FLIR GF 306 camera	59
Table 5.2: List of chemicals that can be detected by the FLIR GF 320 VOC camera	60

# Acronyms and Abbreviations

<b>AWBERC</b>	Andrew W. Breidenbach Environmental Research Center
<b>CL</b>	Product of concentration and length (depth) of gas plume as seen by a camera
<b>DCM</b>	Dichloromethane
<b>FLIR</b>	Forward Looking Infrared Radiation
<b>g/hr.</b>	Grams per hour, a measure of MDLR for gases
<b>GPS</b>	Global Positioning System
<b>HDMI</b>	High Definition Multimedia Interface
<b>HDPE</b>	High Density Polyethylene
<b>Hz</b>	Hertz (unit of frequency)
<b>InSb</b>	Indium antimonide
<b>IP</b>	Ingress Protection; IP 54 signifies a high level of protection against dust particles
<b>IR</b>	Infrared Radiation
<b>JPG/JPEG</b>	Joint Photographic Experts Group (a working group that sets picture formats)
<b>LCD</b>	Liquid Crystal Display
<b>lpm</b>	Liters per minute
<b>MCL</b>	Maximum Contamination Level
<b>MDLR</b>	Minimum Detected Leak Rate
<b>mK</b>	milli-Kelvin (a measure of detecting temperature differences by IR camera sensors)
<b>MP</b>	Megapixels
<b>MPEG</b>	Moving Picture Experts Group (a working group that sets movie formats)
<b>NETD</b>	Noise Equivalent Temperature Difference (units: mK)
<b>NRMRL</b>	National Risk Management Research Laboratory
<b>OGI</b>	Optical Gas Imaging
<b>OLED</b>	Organic Light Emitting Diode
<b>ORD</b>	Office of Research and Development
<b>PCE</b>	Perchloroethylene or tetrachloroethylene. Referred to as “perc”
<b>ppb</b>	Parts Per Billion
<b>ppm</b>	Parts Per Million
<b>ppt</b>	Parts Per Trillion
<b>QAPP</b>	Quality Assurance Project Plan
<b>QOGI</b>	Quantitative Optical Gas Imaging
<b>QWIP</b>	Quantum Well Infrared Photo Detector
<b>R6</b>	US EPA Region 6
<b>RF</b>	Response Factor
<b>TCE</b>	Trichloroethylene
<b>US EPA</b>	United States Environmental Protection Agency
<b>VI</b>	Vapor Intrusion

# Executive Summary

The information in this document is from a collaborative effort between the U.S. EPA, Region 6 Superfund Division and the Office of Research and Development, National Risk Management Research Laboratory. Research was conducted at the US EPA Region 6 Addison Texas Facility. The findings represent an evaluation of forward looking infrared radiation (FLIR) camera technology as a tool in screening of locations that suffer from tetrachloroethylene (PCE; International Union of Pure and Applied Chemistry (IUPAC) name: tetrachloroethene) and trichloroethylene (TCE; IUPAC name: trichloroethene) vapor intrusion (VI) into indoor air spaces prior to using costlier conventional sampling technologies in residential and commercial/industrial settings, where the potential for PCE and TCE short-term health effects are more difficult to assess. Research summarized in this report may provide a novel and innovative method to yield expeditious PCE and TCE screening levels to improve risk management decisions, which for far too long have relied on decades old sampling and analysis methods. There has been no use of the FLIR technology at the EPA to determine whether the instrument has screening capabilities in VI to indoor air risk assessment work and monitoring to assess and verify the performance and effectiveness of the remediation systems and interim measures.

PCE and TCE are industrial chemicals that may be released into the air, water and soil in locations close to their manufacture or use. Humans may be exposed to PCE and TCE by breathing air contaminated with PCE/TCE vapors (inhalation), drinking contaminated water (ingestion), or through activities such as showering (dermal/inhalation). One of the major sources of exposure to PCE and TCE is through VI from PCE and TCE contaminated ground water and soils into buildings through gaps or cracks in the building foundation, through porous concrete or through open doors and windows.

Conventional methods for determining VI typically follows EPA Method 21, which involves prescreening potential locations using a portable volatile organic carbon (VOC) analyzer, placing sample canisters at a location for a period of time, followed by analysis in a laboratory. As an alternative to EPA Method 21, Optical Gas Imaging (OGI) techniques that involve the use of infrared (IR) cameras that are designed to capture IR images and video in the IR spectral ranges of the leaking gases may be used. The primary objective of this study was to determine if OGI can be used to detect PCE and TCE in VI scenarios. In particular, two cameras manufactured by FLIR Systems Inc. were used to detect PCE and TCE at six different concentrations within EPA's risk management range for a cleanup, three of which were related to a residential air exposure scenario, and the remaining three were related to a worker air exposure scenario – the FLIR GF-320 VOC camera system, which is a mid-wave IR camera in the 3.2 – 3.4 micrometer ( $\mu\text{m}$ ) spectral range, and the FLIR GF-306 camera system, which is a long wave IR camera in the 10.3 – 10.7  $\mu\text{m}$  spectral range.

All leak detection experiments were conducted in a standard open-sash 4 feet  $\times$  4 feet chemical fume hood located at the EPA Region 6 Addison Texas Facility. A FLIR camera was positioned 8 feet in front of the hood, and the camera lens was in line with the outlet from a gas canister of known PCE or TCE concentration that represented the source of the leak inside the chemical fume hood. In all cases, including the highest concentrations of PCE (125 ppm) and TCE (125 ppb) tested, neither of the two camera systems could detect the gas vapors. In the case of PCE, this is likely because the absorbance range of PCE (10.8 – 13  $\mu\text{m}$ ) was just outside the spectral range of the GF-306 camera, while PCE does not have any absorbance in the spectral range of the GF-320 VOC camera (3.2 – 3.4  $\mu\text{m}$ ). In the case of TCE, though the spectral ranges of both the mid- and the long-wave camera system encompass at least a portion of TCE's absorbance wavelengths, this is likely because the concentration of the highest standard used (125 ppb) was likely much lower than the likely detection limit (estimated to be 500 ppm

by volume or higher based on Trefiak, 2016). Based on these results and the camera specifications, it is theorized that though neither of the two cameras will likely be able to detect PCE at any concentration, a camera system with a wider spectral range in the long wave IR region (e.g., 7.5 – 15  $\mu\text{m}$ ) might be able to detect both gases. However, the two camera systems were successful in detecting other vapor plumes, including ammonia and propane.

The detection capability or the sensitivity of a camera system is highly dependent on the concentration of gas in the plume and the cross-sectional length of the plume along the camera axis. Since the testing laboratory did not have the means to increase the plume size and the amount of gas for testing purposes was limited, the path length of a gas plume was artificially increased by capturing the gas (or liquids) in a plastic bottle. Under this scenario, the two cameras could detect ammonia and TCE vapors inside the plastic bottle, and were able to differentiate chemical vapors from a plastic bottle containing air. The ability to detect vapors under this so-called “static” scenario will be useful in situations such as confined spaces where a lack of air movement will cause the gas to remain in place long enough to be detected by an IR camera.

Though this study was not successful in detecting PCE and TCE vapor intrusions at both the worker and residential air exposure scenarios; this research was successful in demonstrating the capability of FLIR technology to safely detect gas leaks from a location relatively far from the source. In addition, the study was useful in determining the effect of flow rates of gas plumes and cross-sectional length of the plume with respect to the camera axis on a camera’s detection capabilities. However, based on their IR spectra and information provided by the manufacturer, detection of gases such as methane, propane and butane; gasoline fumes; solvents such as benzene and methylene chloride; and common water pollutants such as trihalomethanes are well within the capabilities of the two experimental camera systems. Other means to increase detector sensitivity include using a camera lens with a longer focal length, and controlling environmental factors such as wind, humidity and background.

# Acknowledgments

The partnership established between the U.S.EPA Region 6, Superfund Division and the Office of Research & Development National Risk Management Research Laboratory over the course of this project is a testimony to mutually sustained interdepartmental collaboration and trust.

The primary contractor for this project, Pegasus Technical Services, Inc., procured laboratory supplies, participated in experiments conducted at the EPA Region 6 Addison Facility in Texas, and contributed in the analyses associated with this project. His patience in closely-collaborating with EPA Region 6 and attention to detail in performing complex field phases coupled with proficient synthesizing of the information into several interpretable data reports were key factors in the success of this cooperative work.

The authors of this report, Co-Principal Investigators David Eppler and Michael Torres, EPA Region 6, Superfund Division; David Ferguson and Daniel Young, ORD/NRMRL Division; and Raghuraman Venkatapathy, Pegasus Technical Services, Inc., express their appreciation to the RARE program and the following individuals for their substantial contributions and support to this RARE program research project: Carl E. Edlund, P.E., EPA Region 6, Superfund Division Director; Cynthia Sonich-Mullin, ORD/NRMRL Division Director; Randy Parker, ORD Life Cycle and Decision Support Branch Chief; Michael Gonzalez, ORD Emerging Chemistry and Engineering Branch Chief; Michael Morton, EPA Region 6, Science Liaison to ORD; Walter Helmick, EPA Region 6, Quality Assurance (QA) Officer; and Jim Voit, former ORD/LMMD QA Manager. The authors also thank William Barrett of ORD/NRMRL and Alethea Tsui-Bowen of EPA Region 6 for their invaluable comments.

# 1. INTRODUCTION

Tetrachloroethylene (PCE) and trichloroethylene (TCE) are nonflammable and colorless chlorinated solvents that are typically used for dry-cleaning, extraction of vegetable oils, and as a degreaser in metals and electronics manufacturing plants. PCE and TCE may be released into the air, water and soil in locations close to their manufacture or use, including release into ground water. PCE and TCE in surface waters or shallow soils typically evaporates into the air, where they can remain stable and be transported for long distances, while solvents deeper in the soil can be transported to the ground water (a typical source of drinking water for many communities in the U.S.), where they can form up to mile-long plumes with PCE or TCE concentrations above the Safe Drinking Water Maximum Contamination Level (MCL) of 5 parts per billion (ppb). Soils and ground water are the primary sources of vapor forming chemicals, and human exposure to these chemicals. TCE may be present in the soil or ground water aquifer as a solvent or PCE can be transformed to TCE and/or lesser chlorinated byproducts under typical reducing subsurface environments. PCE and TCE vapors from contaminated soils may be released to the indoor air of buildings or other structures built on contaminated sites through cracks in basements and foundations, through conduits such as sewers, drain lines, access vaults, storage sheds, pump houses) and through cracks and other openings (U.S. EPA, 2006; McDonald & Wertz, 2007; U.S. EPA, 2015a). A Superfund response action is warranted when vapor-forming chemicals are present in the soil and ground water. Risk management to address the vapor intrusion (VI) exposure pathway when it poses unacceptable human health risks typically entails a combination of response actions. Figure 1.1 shows one such PCE contaminated site in EPA Region 6 that is located at McGaffey & Main St. (Hwy US 285) in Roswell, NM, presumed to be due to the use of PCE in three known dry-cleaning facilities, one of which was still active up to 2012 (Niemet *et al.*, 2012).

The McGaffey & Main Groundwater Plume Superfund Site was listed in the National Priorities List (NPL) in October 2002; remedial investigation activities occurred between 2003 – 2006, and a Record of Decision to mitigate the PCE contamination was reached in 2008 (Niemet *et al.*, 2012). The purple circles in Figure 1.1 shows soil gas sampling locations at the contaminated site, with PCE concentrations (in  $\mu\text{g}/\text{m}^3$ ) measured in 2010 listed in the call-out boxes next to each purple circle. PCE concentrations at the site range from non-detects at site SV-34 to 11,900,000  $\mu\text{g}/\text{m}^3$  at site SV-23 (Figure 1.1). The figure also shows isoconcentration contours at the PCE contaminated site, with the blue contour and outlying areas denoting concentrations of 370  $\mu\text{g}/\text{m}^3$  or less, concentrations between 370 and 10,000  $\mu\text{g}/\text{m}^3$  in areas encompassing the blue and green contours, concentrations between 10,000 and 100,000  $\mu\text{g}/\text{m}^3$  in the areas encompassing the green and purple contours, concentrations between 100,000 and 1,000,000  $\mu\text{g}/\text{m}^3$  in the areas encompassing purple and orange contours, and >10,000,000  $\mu\text{g}/\text{m}^3$  in areas within the red contour. The red contour is close to the last active dry cleaner facility at the corner of McGaffey & Main streets. In addition to the soil, PCE was also found in ground water within the area (Figure 1.2) as well as VI to indoor air of various facilities around the site (Figure 1.3); the exhaust from the dry cleaner at the last active dry cleaning facility (2,200  $\mu\text{g}/\text{m}^3$  in 2010) was estimated to contribute 84% of PCE to indoor air in the immediate area, with the remaining amount estimated to be due to subsurface VI from groundwater (Niemet *et al.*, 2012). The contributions from subsurface vapor intrusion was estimated to be higher than emission from the active dry cleaner at locations that are farther away from the dry cleaning facility. The Superfund site is in a mixed residential and commercial use area (Niemet *et al.*, 2012). Response actions to address exposure to VI in commercial and residential areas when it poses unacceptable human health risks at sites such as the McGaffey & Main PCE contaminated site include remediation to reduce or eliminate subsurface vapor sources, engineered exposure controls for specific buildings to reduce VI or reduce concentrations of vapor-forming chemicals that have already entered the building, monitoring to assess and verify the performance and

effectiveness of the remediation systems and engineered exposure controls, and institutional controls to restrict land use and/or to alert parties of the presence of subsurface sources of vapor-forming chemicals and to foster operation, maintenance, and monitoring of the remediation systems and engineered exposure controls (U.S. EPA, 2015a). Exposure to very high concentrations of vapor-forming chlorinated compounds may cause headaches, dizziness, confusion, nausea, unconsciousness, or death. The US EPA considers PCE and TCE to be carcinogens for humans. PCE and/or TCE have been found in at least 945 of the 1699 NPL sites identified by the EPA (U.S. EPA, 2018).

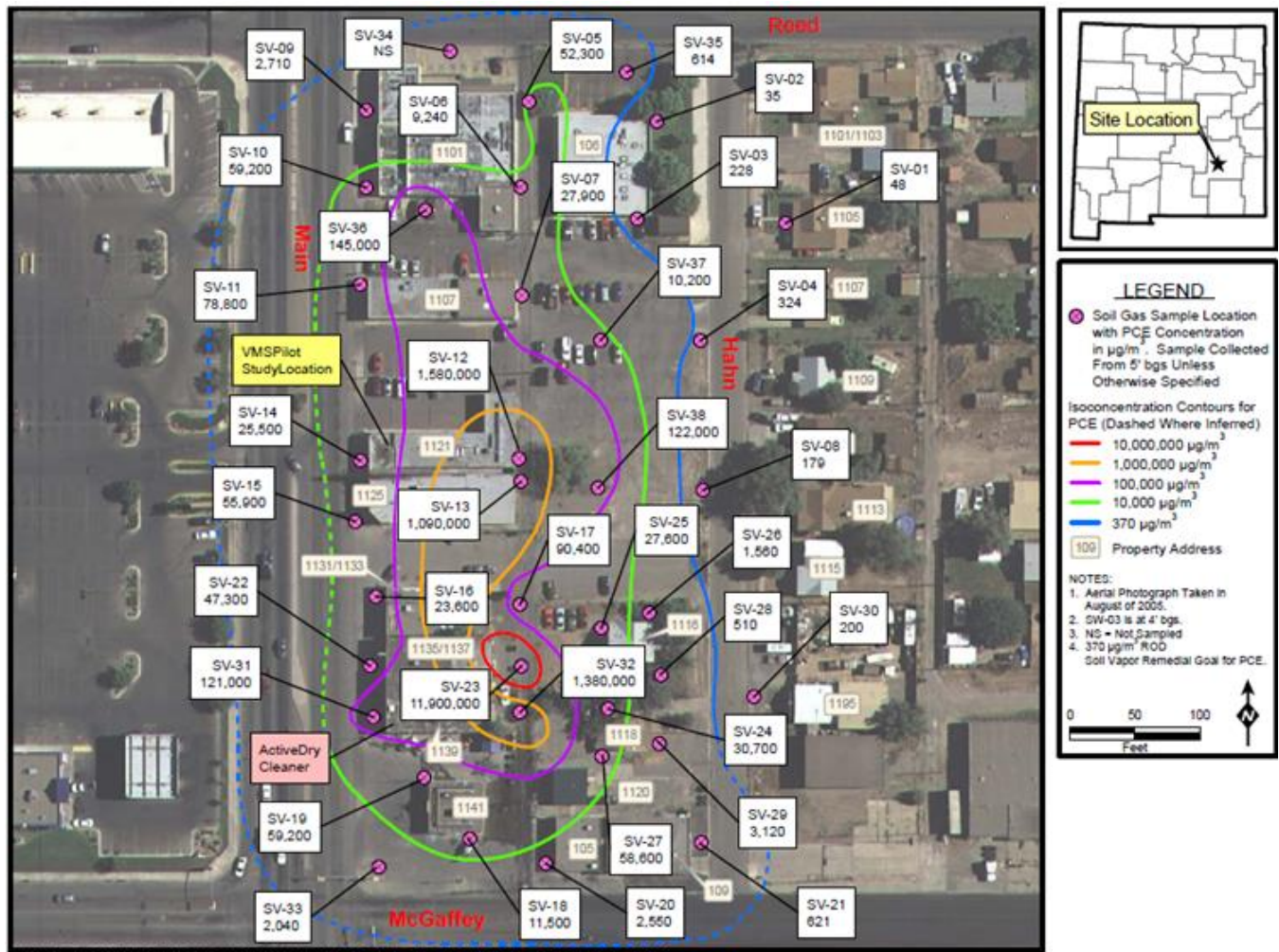


Figure 1.1: The McGaffey & Main Groundwater Plume Superfund Site located in Roswell, NM. The purple circles represent soil gas sampling locations, and the contours represent PCE isoconcentrations, with the innermost contour in red having the highest soil gas PCE concentration (Niemet et al., 2012).

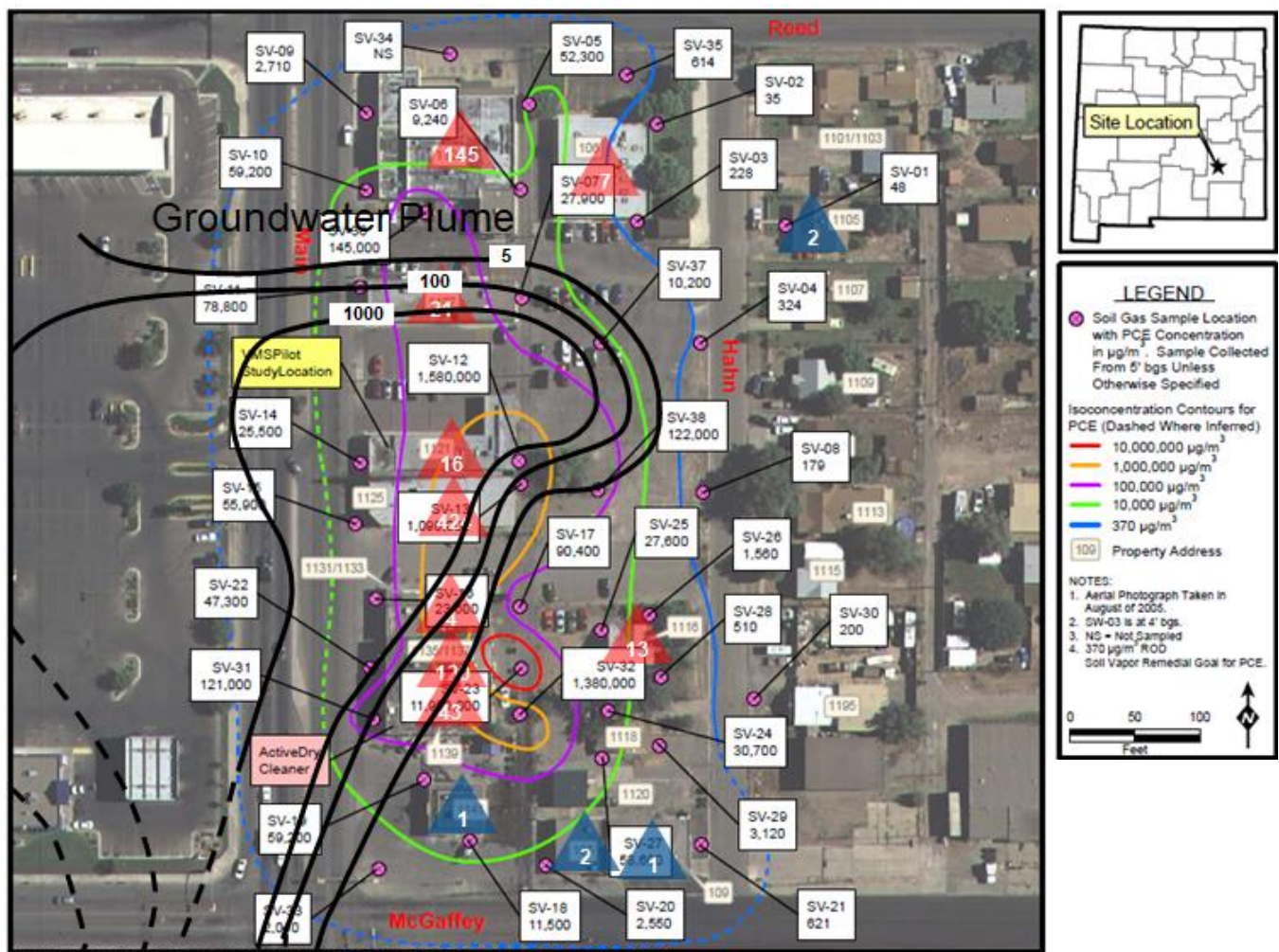


Figure 1.2: The McGaffey & Main Groundwater Plume Superfund Site located in Roswell, NM. The purple circles represent soil gas sampling locations, and the contours represent PCE isoconcentrations, with the innermost contour in red having the highest soil gas PCE concentration. In addition, the black contours represent ground water contamination, with the innermost black contour having ground water PCE concentrations higher than 1000 parts per billion (Niemet et al., 2012).

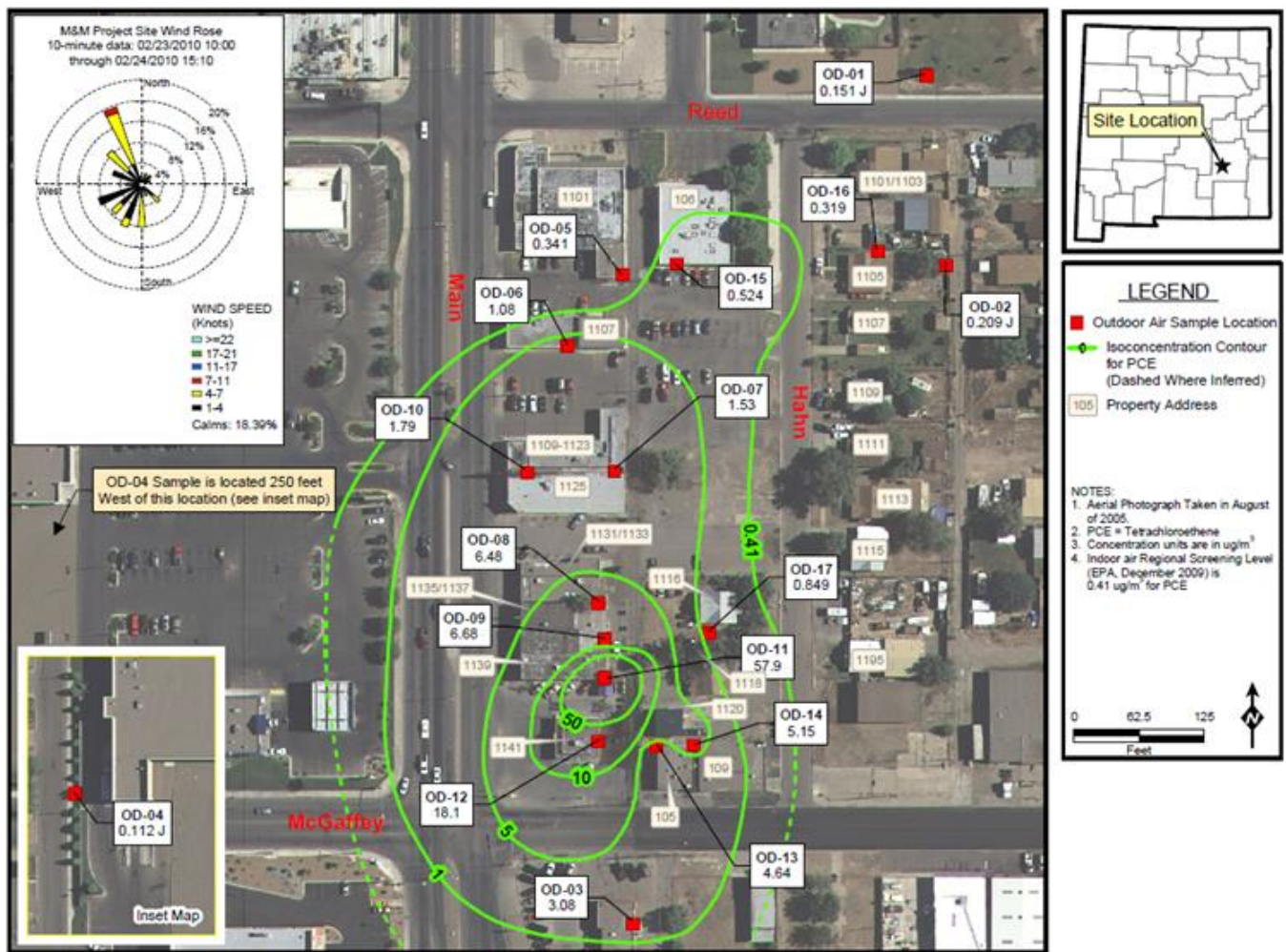


Figure 1.3: The McGaffey & Main Groundwater Plume Superfund Site located in Roswell, NM. The red squares represent outdoor air sampling locations, and the contours represent PCE isoconcentrations, with the innermost contour having the highest indoor air PCE concentration or  $>50 \mu\text{g}/\text{m}^3$ , and site OD-11 having the highest PCE concentration in the air at  $57.9 \mu\text{g}/\text{m}^3$  (Niemet et al., 2012).

Humans may be exposed to PCE and TCE by breathing air contaminated with PCE/TCE vapors (inhalation), drinking contaminated water (ingestion), or through activities such as showering (dermal/inhalation). Soil and ground water contaminated with volatile organic chemicals are two of the most common sources of vapor-forming chemical intrusion into indoor air. The most common source of exposure to PCE and TCE is through the VI to indoor air pathway, which is the movement of vapor from ground water and contaminated soils into buildings or other structures built close to the contaminated sites. PCE and TCE vapors may enter these buildings through gaps or cracks in the building foundation, through porous concrete or through open doors and windows. Figure 1.4 illustrates the concept of VI into a typical home (U.S. EPA, 2015b).

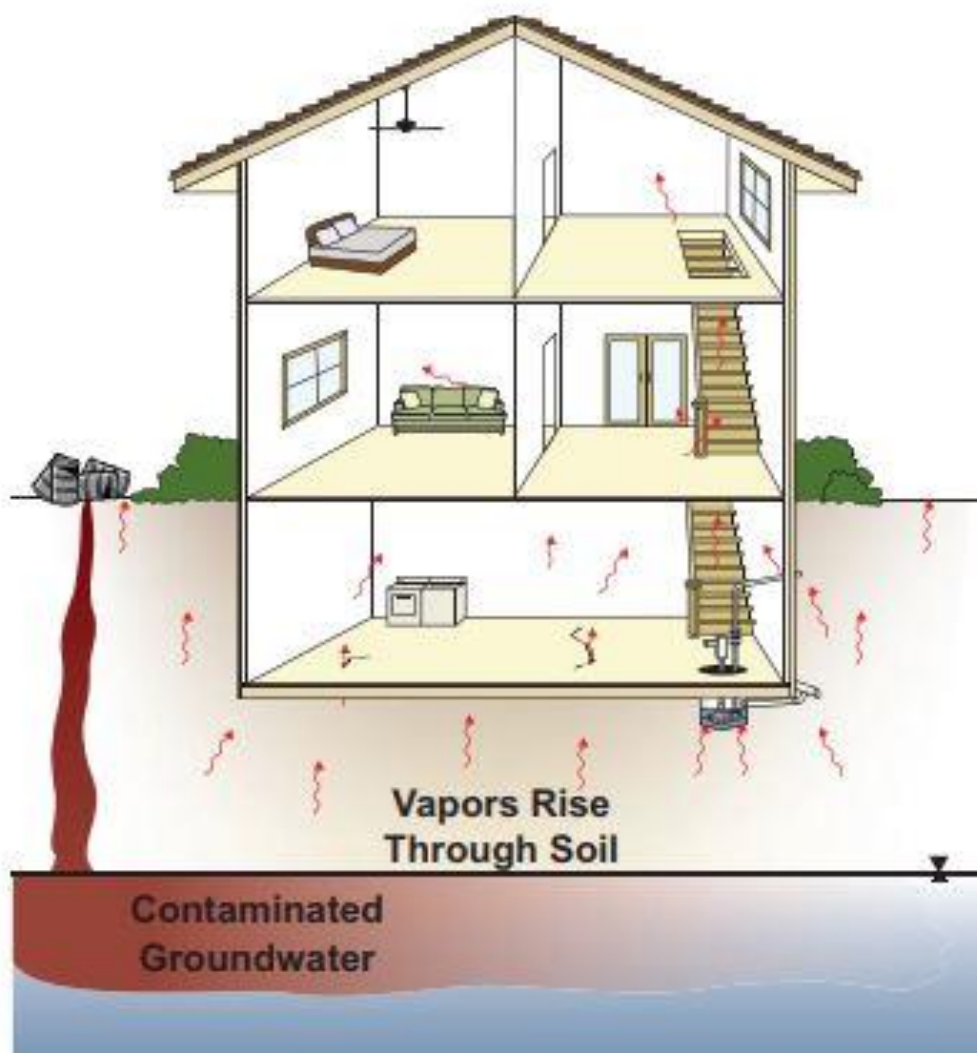


Figure 1.4: Schematic illustrating vapor intrusion into a typical home.

The National Academy of Sciences advocates that careful consideration of the vapor intrusion pathway is warranted at all sites where vapor-forming chemicals are present in the soil or groundwater aquifer. Risk management to address VI when it poses unacceptable human health risks typically entails a combination of response actions, such as remediation to reduce or eliminate subsurface vapor sources, engineered exposure controls for specific buildings to reduce VI, methods to reduce vapor-forming chemicals that have already entered the building, and monitoring to assess the verify the performance and effectiveness of the remediation systems and interim measures. Notifications and risk communication to building occupants and owners can also foster risk management objectives.

The preferred long-term response to the intrusion of vapors into buildings is to eliminate or substantially reduce the level of contamination in the subsurface vapor source (e.g., ground water, subsurface soil, sewer lines) by vapor-forming chemicals to acceptable-risk levels, thereby achieving a permanent remedy. Remediation of the ground water plume or a source of vapor-forming chemicals in the vadose zone will eventually eliminate potential exposure pathways. In cases where subsurface vapor sources cannot be remediated quickly, it may be appropriate to also undertake interim measures in individual occupied buildings (i.e., building mitigation for vapor intrusion) to reduce threats to human health more

quickly. EPA recommends that building mitigation for vapor intrusion be regarded as an interim action that can provide effective human health protection, which may become part of a final cleanup plan.

Mitigation of vapor intrusion in specific buildings generally is not a substitute for remediation of subsurface vapor sources. Thus, EPA recommends that building mitigation generally be conducted in conjunction with vapor source remediation where at all possible.

Conventional methods for determining VI contaminants typically follows EPA Method 21, and involves prescreening potential locations using a portable volatile organic carbon (VOC) analyzer followed by the placement of sample canisters that must be left at a given location for extended periods of time. The atmosphere at the prescreened location is sampled by pumping air at a predetermined rate and a set amount of time into a specially-prepared pre-evacuated stainless-steel canister. After the air sample is collected, the canister valve is closed, and the canister is transported to a laboratory for analysis, where a given volume of air from the canister is passed through a sorbent packing to collect VOCs followed by thermal desorption into a gas chromatograph/mass spectrophotometer (GC/MS) for analysis.

Conventional gas vapor analytical methods are summarized in the EPA Methods TO-14, TO-15 and TO-17 (US EPA, 1999a, 1999b, 1999c). Multiple factors such as heterogeneous geologic conditions, sampling design, gas collection techniques, and seasonal effects may lead to significant spatial and temporal variability in subsurface concentrations, which in combination with other influences such as variable building conditions and occupant habits can lead to significant spatial and temporal variability in gas concentrations in indoor air. The use of portable analyzers or sniffers for screening might introduce uncertainty as these analyzers must be positioned near the VI location to detect the point source where vapors enter and accumulate in occupied buildings, leading to exposures at levels that may pose PCE and TCE public health threats or risks. Consideration of the VI pathway becomes more challenging when assessing industrial and commercial buildings due to other potential sources of indoor pollution. In addition, sampling is very labor intensive, and personnel should be physically present near the leaks during sampling events, and may be exposed to these hazardous chemicals while collecting samples.

As an alternative to using EPA Method 21 for leak detection, in 2015, EPA proposed the use of Optical Gas Imaging (OGI) techniques as one of the systems that may be used for detecting fugitive gas emissions. OGI typically involves the use of infrared (IR) cameras that are designed to capture IR images and video in the IR spectral ranges of the leaking gases. A rule to require the use of OGI technology by the oil and gas industry was finalized by the EPA in 2018 (Federal Register, Vol. 83, No. 48, March 12, 2018; <https://www.gpo.gov/fdsys/pkg/FR-2018-03-12/pdf/2018-04431.pdf>). Advantages of using OGI techniques over conventional methods for detecting leaks include an ability to visually see the leaks and capture images of videos of the leaks, and the ability to detect the leaks farther from the leak source as opposed to being in the vicinity while using conventional methods (Trefiak, 2016). Other advantages include increased efficiency as more locations can be scanned within a set amount of time when compared to conventional methods, and decreased cost due to lower labor and analytical costs (Trefiak, 2016).

IR cameras have more advantages for leak or spill detection rather than a total vapor analyzer (TVA) or “gas sniffers” because they provide area measurement rather than point by point measurement and give a real-time image of the gas plume. In addition, these cameras give the option of OGI inspection of volatile organic compounds that cannot be reached by an organic vapor analyzer or total vapor analyzers. They can detect the motion of the plume and give a good contrast between the absorbing and the background gas which are the key elements for detection. IR imaging cameras allow one to spot several volatile compound gas leaks quickly due to their ability to scan large areas and deliver real-time thermal images of gas leaks. The latest IR cameras are also designed for use in harsh industrial

environments, operate in a wide temperature range of 5-122 °F (-15 to 50 °C) and can withstand water, dust, and vibrations. They have also been tested to detect several volatile compounds such as benzene, butane, ethane, ethyl benzene, ethylene, heptane, hexane, isoprene, methane, methanol, octane, pentane, 1-pentane, propane, propylene, toluene, and xylene. Detection using an IR camera is considered safer than the procedure involving a human-carried sniffing detector because the device can be placed from 5 to 20 feet away compared to the sniffer. Potential disadvantages of OGI may include decreased effectiveness due to background conditions (rain, wind, humidity, etc.), inability to quantitate leak amounts and lower accuracy at concentrations below 1500 ppm (Trefiak, 2016). In addition, current technology in IR imaging cannot provide the true temperature of the gas plume because the emissivity value is always assumed as unity, and the actual emissivity value of the gas is not integrated in the camera's algorithm.

## 1.1 Objectives

The primary objective of this study was to determine if OGI can be used to detect PCE and TCE in VI scenarios. OGI cameras that can detect PCE and TCE gas plumes need detectors that work in the IR spectral ranges of the two chemicals. TCE has an absorbance profile in the mid-IR region (at approximately 3.3  $\mu\text{m}$ ), while PCE and TCE have an absorbance profile in the long-IR region (between 10.5 – 14  $\mu\text{m}$ ). There is no single camera system that works across the whole IR spectral range; the detectors used in the cameras are IR range specific, and typically work in the mid-IR range (2 – 5  $\mu\text{m}$ ) or in the long IR range (7 – 15  $\mu\text{m}$ ). To meet study objectives, two cameras manufactured by FLIR Systems Inc. were used – the FLIR GF-320 camera system, which is a mid-wave IR camera in the 3.2 – 3.4  $\mu\text{m}$  spectral range, and the FLIR GF-306 camera system, which is a long wave IR camera in the 10.3 – 10.7  $\mu\text{m}$  spectral range. Other objectives of this study include:

- 1) Determine if, and to what level, the two EPA-issued FLIR cameras mentioned above can reliably detect PCE and TCE emissions using known PCE and TCE standards in parts per trillion (ppt) to parts per million (ppm) levels;
- 2) Determine how well the FLIR cameras can detect other chemical vapors of interest; and
- 3) If the objectives listed above are met, determine how well the FLIR cameras, when scanned over an area with known VI problems, correlates the results from a conventional VI sampling event.

The research for this project involves three stages. The first segment will encompass use of known concentrations of an accepted set of PCE and TCE standards (concentrations determined/documented by gas vendor), released under controlled environmental conditions, and designed to determine the capabilities of the FLIR camera to see levels of PCE and TCE at specific concentrations. The PCE and TCE standards will be released in known amounts over a specific time at a fixed distance from the camera lens. The camera will be operated in several modes. This will give the camera operators an improved understanding of the capabilities of the camera to detect various levels of PCE and TCE vapors in the environment.

The second segment will involve use of the FLIR cameras to detect other chemical vapors using chemical standards obtained from reputable manufacturers. If the first and second segments are successful, the third segment will involve use of the FLIR cameras at a site where there are documented levels of VI to indoor air. The camera will be methodically scanned over the site, documenting the existence of vapor, and then comparing these results with the sampling results from a conventional sampling approach. This segment may also involve the use of the FLIR camera systems to scan and

screen an industrial/commercial environment that is suspected of having a VI to indoor air problem. Results of the FLIR screen will then be compared to the conventional sampling results.

## 2. BACKGROUND

The electromagnetic spectrum is a range of frequencies (or wavelengths) of electromagnetic radiation that extend from ionizing radiation such as gamma rays and X-rays at one end of the spectrum to radio waves and beyond that have extremely low frequencies at the other end of the spectrum. Each of these waves also have a certain amount of energy associated with them, ranging from 1.24 million electron volts (eV) for gamma rays (ionizing radiation) to 12.4 femto eV for extremely low frequency radio waves (Elert, 2018). Ionizing radiations typically range from 300 EHz (exahertz or  $10^{18}$  Hz) – 30 PHz (petahertz or  $10^{15}$  Hz) frequencies (1 picometer – 10 nanometer (nm)), while the ultra-low frequency radio waves range from 3 – 300 Hz (100,000 kilometers – 1000 kilometers) (Elert, 2018). In between the two extremes lies the visible region comprised of the near ultraviolet to the near infrared, followed by the mid- and far-infrared regions. What we typically think of as “light” is electromagnetic radiation in the frequency range 430 – 750 terahertz (THz; 400 – 700 nm) that our eyes can see, which is perceived in the colors of the rainbow from red through violet. Figure 2.1 shows a schematic of the electromagnetic spectrum ranging from ionizing radiation to the radio waves; beginning at the low frequency (long wavelength) end of the spectrum these are: radio waves, microwaves, terahertz waves, infrared, visible light, ultraviolet, X-rays, and gamma rays at the high-frequency (short wavelength) end.

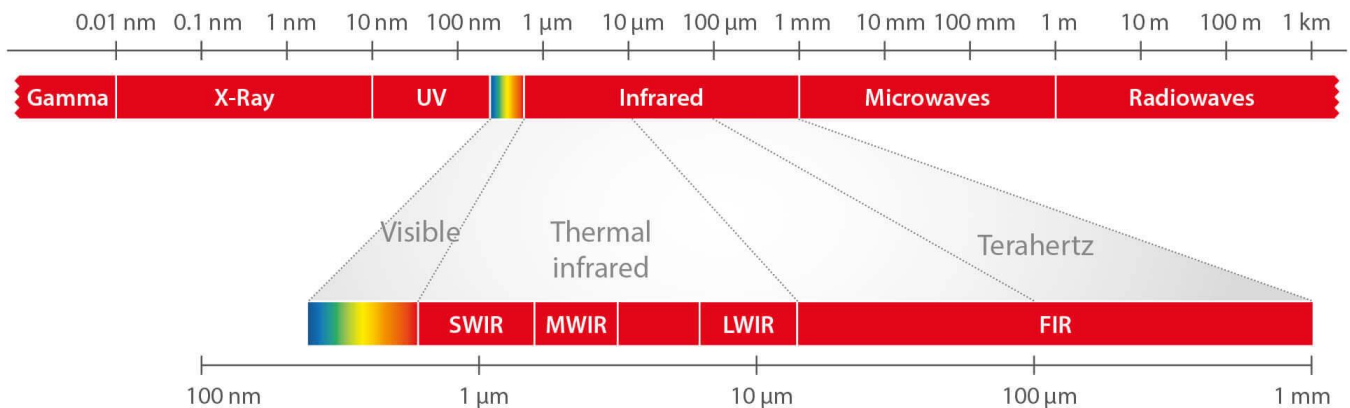


*Figure 2.1: Schematic illustrating the electromagnetic spectrum from ionizing radiation at the far left (high frequency, short wavelength) to radio waves at the far right (low frequency, long wavelength). Source: InfraTec (<https://www.infratec-infrared.com>).*

Humans can see only a very narrow region of the electromagnetic spectrum (‘Visible’ region in Figure 2.1), and specialized equipment is required to extend vision beyond the limitations of the unaided eye. As the energy of electromagnetic spectrum changes, its interaction with matter also changes, resulting in “visibility” at different regions of the electromagnetic spectrum. For example, bones within the human tissue that are invisible in the visible region of the electromagnetic spectrum are visible in the soft X-ray region of the electromagnetic spectrum (approximately 300 petahertz or 1 nm wavelength). Extending human vision with electronic imaging is one of the most powerful techniques available to science and industry, including the ability to see light in the IR portion of the spectrum, which ranges in frequency from 300 gigahertz to 400 THz (1mm – 750 nm wavelength). The IR region of the electromagnetic spectrum is divided into three parts, including the near IR (120 – 400 THz; 750 – 2500 nm), mid IR (30 – 120 THz; 10 – 2.5 μm) and far IR (0.3 – 30 THz; 1mm – 10 μm).

The physicochemical properties of the near IR are similar to those for visible light, while hot (thermal) objects and the human body radiate in the mid IR range. Regions in the mid- and far IR ranges are absorbed by molecular vibrations where atoms in a molecule vibrate around their equilibrium positions, and rotations vibrations where atoms in a molecule twist and turn around their axes. In these cases, the molecules and atoms absorb the electromagnetic radiation and transition from one energy level to another. These transitions are typically strongly coupled to the field via dipole moment changes in the molecule, and are common to many types of gases and vapors. These transitions include symmetric stretches, twisting, scissoring, asymmetric stretches, wagging and rocking among others. The molecular structures for TCE and PCE are shown in Figures 2.2 and 2.3, respectively. In the two figures, the carbon atoms are represented as gray balls, chlorine atoms are represented as green balls, and hydrogen atom is represented as a white ball, and the sticks between the balls represent the type of bonding between the atoms in a molecule. The concept of symmetrical and asymmetrical stretches and bending in illustrated in greater detail in Figure 2.4, while Figure 2.5 illustrates the transitions that occur in a chemical molecule (1,1-difluoroethylene) that is similar to TCE and PCE. The chemical 1,1-difluoroethylene is similar to PCE and TCE in the sense that it has two carbon atoms connected by a double bond, and each of the carbon atoms have two other atoms connected to it by single bonds. Hence, the type of transitions PCE and TCE will undergo will be like 1,1-difluoroethylene. These 6-atom molecules have 12 unique vibrational modes. The arrows in Figures 2.4 and 2.5 indicate the direction of movement of the atoms and/or bonds.

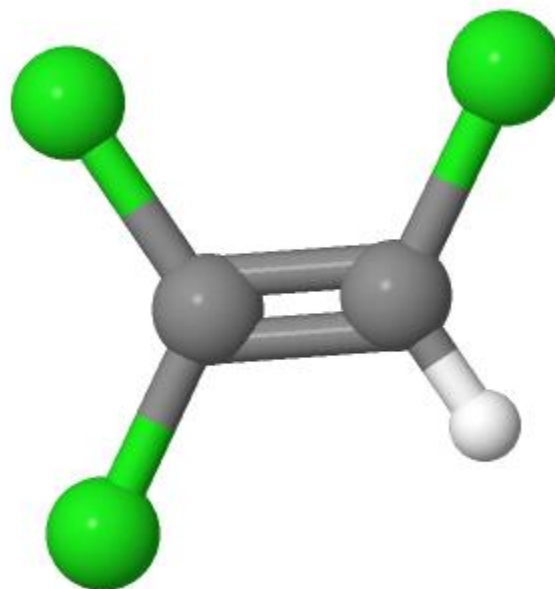


*Figure 2.2: A ball and stick figure of TCE, which has two carbon atoms (gray balls), three chlorine atoms (green balls) and a hydrogen atom (white ball). The sticks connecting the balls represent the type of bond, with the single stick representing a single bond, and the two parallel sticks between the two carbon atoms representing a double bond.*

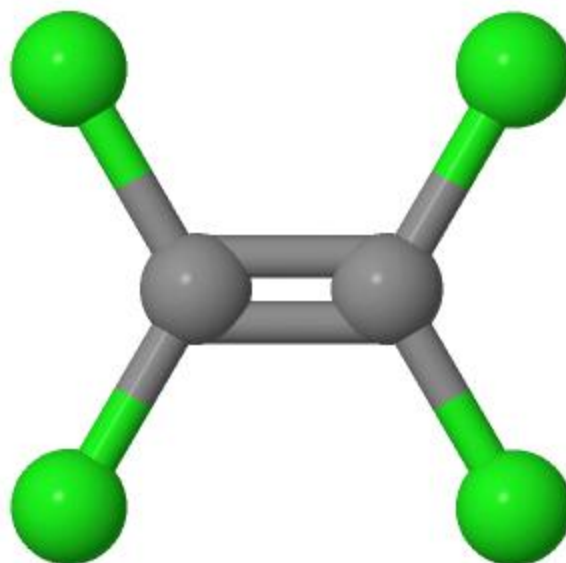


Figure 2.3: A ball and stick figure of PCE, which has two carbon atoms (gray balls) and four chlorine atoms (green balls). The sticks connecting the balls represent the type of bond, with the single stick representing a single bond, and the two parallel sticks between the two carbon atoms representing a double bond.

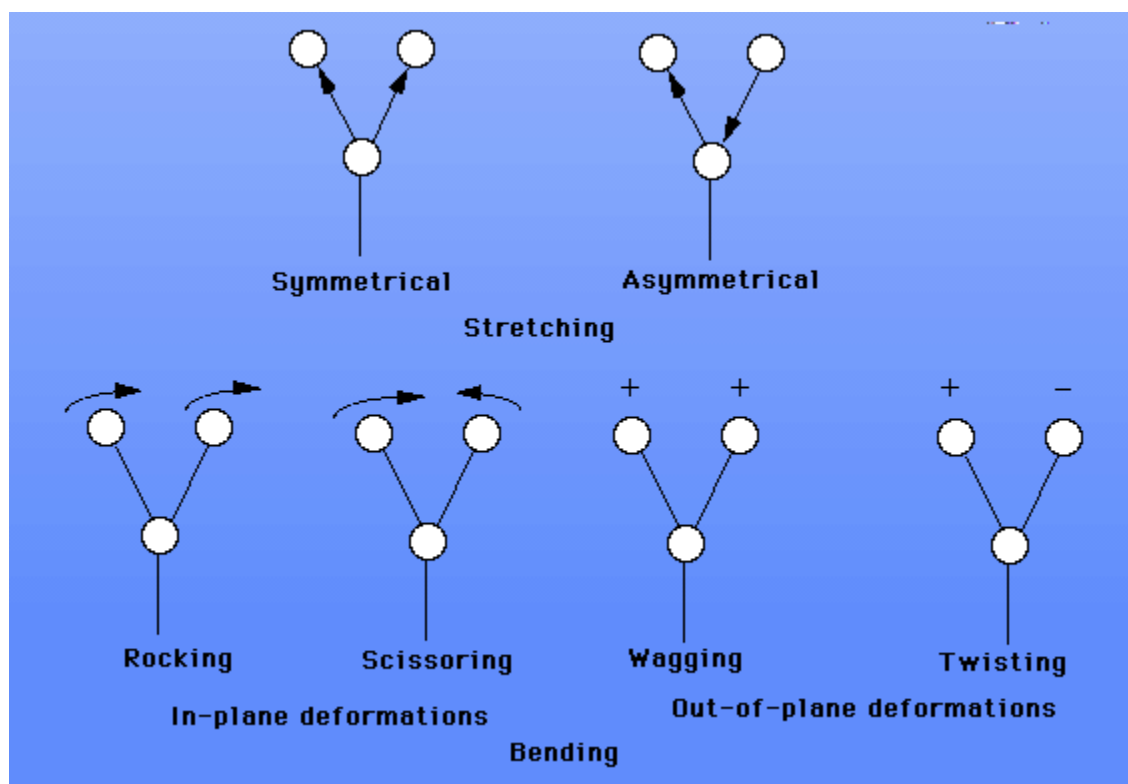


Figure 2.4: Illustration of stretching and bending vibrations in a carbon atom connected to two other atoms via a single bond. Source: <http://shodor.org/succeed-1.0/compchem/labs/vibrations/>

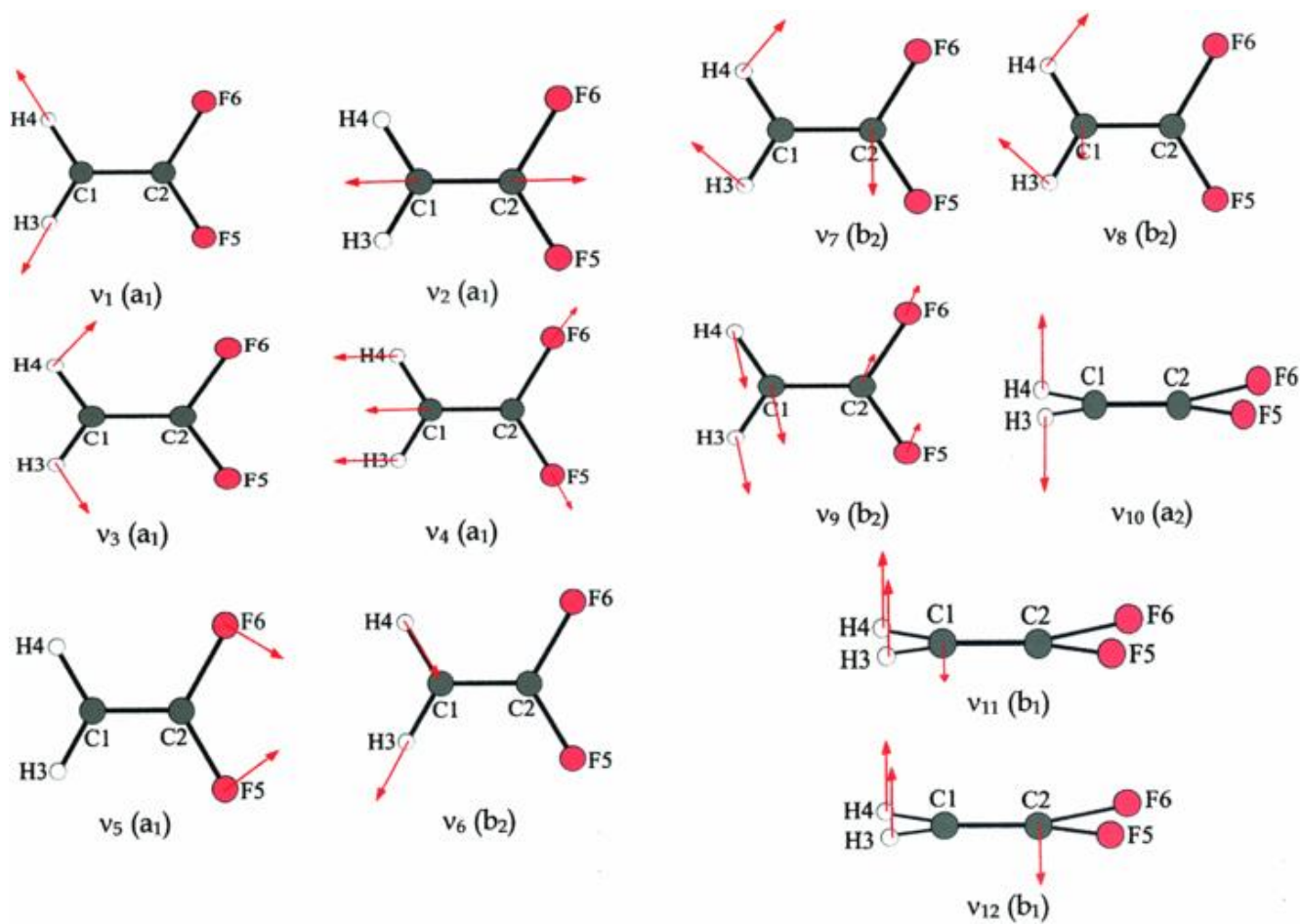


Figure 2.5: Vibrational modes of a chemical molecule that is similar to PCE and TCE. Source: Locht *et al.*, 2012. A molecule like PCE and TCE will have 12 unique vibrational modes, and each of these frequencies will be different for different molecules.

The IR spectrum for 1,1-difluoroethylene is shown in Figure 2.6. In the Figure, the dips in the spectrum correspond to absorbances caused by one of the vibrational modes listed in Figure 2.5.

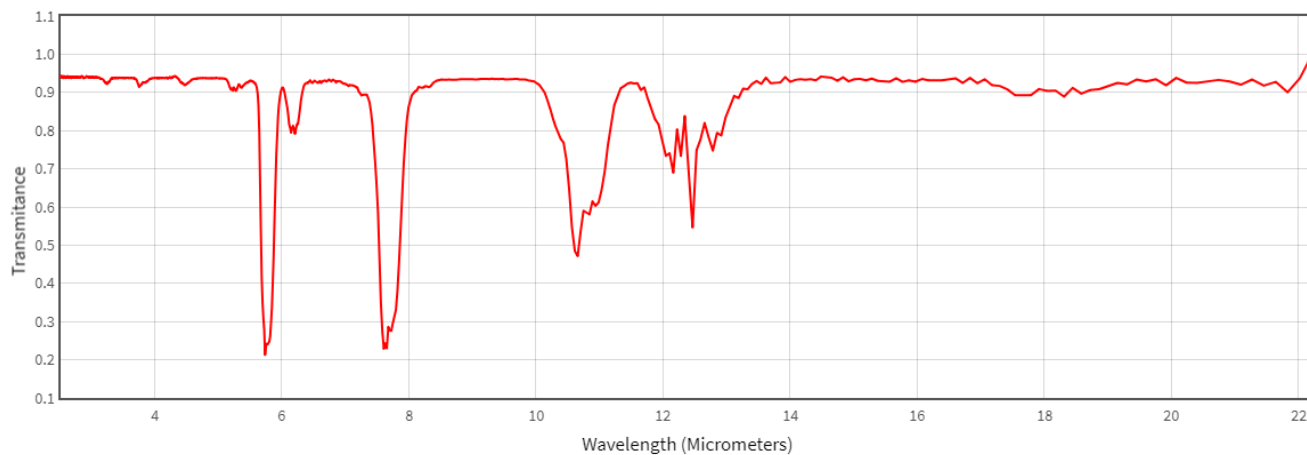


Figure 2.6: IR spectrum of 1,1-difluoroethylene. Radiation wavelength (x-axis) is in mm, while transmittance (y-axis) is unitless.

All objects produce IR energy as a function of temperature. The IR energy that is released by an object is known as its heat signature. The hotter an object is, the more radiation it produces, and the shorter the wavelength of IR light emitted. IR light can penetrate smoke and fog better than visible light, revealing objects that are normally obscured. It can also be used to detect the presence of excess heat or cold that is different from the temperature of the surrounding environment, which can be seen by devices known as thermographic cameras or imagers that are specifically designed to detect light in this area of the electromagnetic spectrum.

A thermal imager is essentially a heat sensor that is capable of picking up tiny differences in temperature. A thermographic camera (also called an infrared camera or thermal imaging camera) is a device that forms an image using infrared radiation, similar to a common camera that forms an image using visible light. The imager collects the infrared radiation from objects in the scene and creates an electronic image based on information about the temperature differences. Because objects are rarely precisely the same temperature as other objects around them, a thermal camera can detect them and they will appear as distinct in a thermal image. Instead of the 400–700 nm range of the visible light camera, infrared cameras operate in wavelengths as long as 14,000 nm (14  $\mu\text{m}$ ). Their use is called thermography. A major difference with optical cameras is that the focusing lenses cannot be made of glass, as glass blocks long-wave infrared light. Special materials such as Germanium or Sapphire crystals must be used. Germanium lenses are quite fragile, so often have a hard coating to protect against accidental contact.

An OGI camera can be considered a highly specialized version of an IR or thermal imaging camera, and has a lens, a detector, and some electronics to process the signal from the detector. The cameras employ a spectral filter that is designed to transmit in a region of the IR spectrum whose wavelength is coincident with the vibrational/rotational energy transitions of VOC molecular bonds. The camera's detectors are designed to have low sensitivity to a wide variety of gases and vapors. Thermally, the camera's sensitivity is <30mK when FLIR's adaptive temporal filter is engaged. The cameras "see" the gas by matching the spectral response of the camera to the peak spectral absorption of the gas. Specific cameras are designed to see specific wavelengths, and hence specific gases. For example, a camera system that is designed to detect 1,1-difluoroethylene would have sensors that match the spectral absorption of the molecule at either 5.8  $\mu\text{m}$  or 7.5  $\mu\text{m}$  (corresponding to the dips in Figure 2.6). Some specification parameters of an infrared camera system are number of pixels, frame rate, responsivity, noise-equivalent power, noise-equivalent temperature difference (NETD), spectral band, distance-to-spot ratio (D:S), minimum focus distance, sensor lifetime, minimum resolvable temperature difference (MRTD), field of view, dynamic range, input power, and mass and volume.

# 3. EXPERIMENTAL APPROACH

## 3.1 Materials

### 3.1.1 Chemicals Used

Laboratory-size gas bottles (58.5L) of PCE and TCE at concentrations ranging from 125 parts per trillion (ppt) to 125 parts per million (ppm) PCE/TCE in nitrogen were obtained from IS GAS (Houston, TX). These concentrations were chosen to encompass residential air exposure and worker air exposure scenarios for PCE and TCE at the  $10^{-6}$  –  $10^{-4}$  risk screening levels (US EPA, 2016). Tables 3.1 and 3.2 list protective levels for PCE and TCE at  $10^{-6}$  –  $10^{-4}$  risk screening levels for the two air exposure scenarios and TCE regional screening levels, respectively. Ammonium hydroxide, n-hexane, and dichloromethane (all ACS grade) were obtained from Fisher Scientific, while a small propane gas bottle was obtained from a local hardware store.

*Table 3.1: Protective levels for PCE and TCE under residential air and worker air exposure scenarios*

Scenario	Risk Screening Level	Protective Level ( $\mu\text{g}/\text{m}^3$ )
PCE Residential Air Exposure	$1 \times 10^{-6}$	11
	$1 \times 10^{-5}$	110
	$1 \times 10^{-4}$	1110
TCE Worker Air Exposure	$1 \times 10^{-6}$	3
	$1 \times 10^{-5}$	30
	$1 \times 10^{-4}$	300

*Table 3.2: Regional Screening Levels for TCE (US EPA, 2016)*

Exposure Scenario	Protective Level (Hazard Quotient = 1)	Protective Level ( $10^{-6}$ – $10^{-4}$ )
Residential	$2.1 \mu\text{g}/\text{m}^3$	$0.48 - 48 \mu\text{g}/\text{m}^3$
Worker	$8.8 \mu\text{g}/\text{m}^3$	$3 - 300 \mu\text{g}/\text{m}^3$

### 3.1.2 Camera Systems

Two types of gas detection camera systems from FLIR (FLIR Systems, Wilsonville, OR) were tested for determining their ability to detect PCE and TCE – FLIR GF 306 and FLIR GF 320 VOC camera. Each of the two experimental camera systems work in a different IR spectral range, and can be used to detect gases whose transmission spectra fall within that range. Typically, longwave IR cameras operate in the 8 – 12  $\mu\text{m}$  range, while medium wave IR cameras operate in the 3 – 5  $\mu\text{m}$  range. FLIR cameras typically require their detectors to be cryogenically cooled using coolers such as a Stirling microcooler for several minutes prior to use, and many camera systems including those by FLIR use some form of digital image processing and color “paletting” to improve detection quality. The purpose of cooling the detector is to reduce the quantum noise, which is generated when electrons can freely move within the atoms that make up the detector material (ITC, 2014). Cooling the detector to near liquid nitrogen temperatures (77 °K) forces the electrons to remain in position, reducing detector noise and increasing the signal to noise ratio. Palettes offered by FLIR cameras include: Iron, Gray, Rainbow, Arctic, Lava, and Rainbow. The two camera systems are described in greater detail in the following subsections.

### 3.1.2.1 FLIR GF 306

The FLIR GF 306 camera system (Figure 3.1) is a long wave IR range camera that was designed for detecting gases such as sulfur hexafluoride (SF<sub>6</sub>), anhydrous ammonia (NH<sub>3</sub>), acetic acid (CH<sub>3</sub>COOH), chlorine dioxide (ClO<sub>2</sub>), dichlorodifluoromethane (CF<sub>2</sub>Cl<sub>2</sub>), superglue (ethyl cyanoacrylate, C<sub>6</sub>H<sub>7</sub>NO<sub>2</sub>) and ethylene (C<sub>2</sub>H<sub>4</sub>). The GF-306 has a focal plane array cooled QWIP (Quantum Well Infrared Photodetector) detector that can accurately measure temperatures up to 500 °C in the 10.3 – 10.7 μm spectral range. A QWIP is an IR detector wherein photons (light) that impinge on quantum wells excite electrons, which is then measured as a current. FLIR reports detection limits as low as 0.026 g/hr. for SF<sub>6</sub> (<http://www.flirthermography.com/cgi/display/?id=55666>) Other specifications for the GF-306 are provided in Table 3.3.

Table 3.3: Technical specifications for the FLIR GF 306 camera

Accuracy	±1 °C (±1.8 °F) for temperature range (0 °C to +100 °C, +32 °F to +212 °F) or ±2% of reading for temperature range (>+100 °C, >+212 °F)
Automatic Gain Control	Continuous/manual, linear, histogram
Battery System	Rechargeable Li-ion battery
Bump/Vibration	25G/2G
Camera Control	Remote camera control via USB
Camera f-number	f/1.5
Color palettes	Iron, Gray, Rainbow, Arctic, Lava, Rainbow HC
Detector Pitch	30 μm
Detector Type	Focal plane array, cooled QWIP
Dynamic Range	14-bit, Real-time non-radiometric recording: MPEG4/H.264 (up to 60 min./clip) to memory card <sup>3</sup>
Encapsulation	IP 54
Field of View	14.5° × 10.8°
Focus	Automatic (one touch) or manual (electric or on the lens)
Frame Rate [Full Window]	60 Hz
Global Positioning System [GPS]	Location data stored with every image
Image Modes	IR image, visual image, High Sensitivity Mode (HSM)
Image Storage Capacity	> 1200 images (JPEG) with post-process capability per GB on memory card
Menu Commands	Level/span, auto adjust continuous/manual/semi-automatic, zoom, palette, start/stop recording, store image, playback/recall image
Mounting	UNC 1/4"-20
NETD	< 15 mK @ +30°C (+86°F)
On Camera Display	Built-in widescreen, 4.3 in. LCD, 800 x 480 pixels
Operating Temperature Range	-20°C to +40°C (-4°F to +104°F)
Packaging Size	400 x 190 x 510 mm (15.7 x 7.5 x 20.1 in.)
Power	AC adapter 90-260 VAC, 50/60 Hz or 12 V from a vehicle
Resolution	320 x 240 pixels
Sensor Cooling	Stirling Microcooler (FLIR MC-3)
Size [L x W x H] w	305 × 169 × 161 mm (12.0 × 6.7 × 6.3 in.)

Lens	
Spectral Range	10.3 – 10.7 $\mu\text{m}$
Storage Media	Removable SD or SDHC memory card; two card slots
Storage Temperature Range	-30°C to +60°C (-22°F to +140°F)
Temperature Range	-40°C to +500°C (-40°F to +932°F)
Video Recording & Streaming	Real-time non-radiometric streaming: RTP/MPEG4
Visual Image	3.2 MP from integrated visible camera
Visual Video	MPEG4 (25 min./clip) to memory card
Weight [incl lens & batteries]	2.48 kg (5.47 lb.)
Zoom	1-8x continuous, digital zoom



*Figure 3.1: A FLIR GF-306 long-range IR camera (Source: FLIR Systems) that can detect ammonia and sulfur hexafluoride among other gases.*

### **3.1.2.2 FLIR GF 320**

The FLIR GF 320 camera system (Figure 3.2) is a medium wave IR range camera that was designed for detecting more than 400 hydrocarbon and other volatile organic compounds (VOCs) gases such as

methane (CH<sub>4</sub>), propane (C<sub>3</sub>H<sub>8</sub>), and other emissions from natural gas production and use. The GF-320 has a cooled Indium antimonide (InSb) detector that can accurately measure temperatures up to 350 °C in the 3.2 – 3.4 μm spectral range. InSb detectors are photovoltaic detectors that generate a photocurrent when exposed to infrared radiation, and are typically sensitive in the 1 – 5 μm wavelength range. FLIR reports detection limits as low as 0.4 g/hr. for C<sub>3</sub>H<sub>8</sub>

(<http://www.flirthermography.com/ogi/display/?id=55671>). Detection limits for other VOCs as measured by a third-party is listed in Table 3.4. Actual detection limits in the field are dependent on environmental factors such as wind speed, temperature, background, and light, and are often more than 1000 times the limits listed in the table.

*Table 3.4: Technical specifications for the FLIR GF 320 camera system*

Accuracy	±1°C (±1.8°F) for temperature range 0°C to +100°C (+32°F to +212°F) or ±2% of reading for temperature range >+100°C (>+212°F)
Adjustable Viewfinder	Tilttable OLED, 800 × 480 pixels
Area Box	5 (min./max./avg.)
Color LCD	4.3"; 800 × 480 Pixels
Delta T	Yes
Detector Type	Cooled InSb
Field of View	14.5° × 10.8°
Focus	Auto & Manual
Global Positioning System [GPS]	Yes
High Temp Option	Yes
Laser Spot	Yes
MPEG Video Recording	Yes
Packaging Size	00 x 190 x 510 mm (15.7 x 7.5 x 20.1 in.)
Profile	1 live line (horizontal or vertical)
Radiometric JPG	Yes
Radiometric Video [15Hz]	No
Resolution	320 × 240
Spectral Response	3.2 – 3.4 μm
Spot Meter	10.0
Temperature Range	-20°C to 350°C (-40°F to 662°F)
Thermal Sensitivity	<15 mK @ +30°C (+86°F)
Total Pixels	76.8
Video Camera wLamp	3.2 MP
Video Out	HDMI
Zoom	1 – 8× continuous digital

### 3.1.2.2.1 Gases Detected and Minimum Detected leak rate (MDLR)

According to FLIR, an independent laboratory testing confirmed the FLIR GF-302 VOC cameras can see the gases listed in Table 3.5 at the minimum detected leak rate (MDLR)

(<http://www.flirthermography.com/ogi/display/?id=55671>). According to the table, the camera is very sensitive towards gases such as propane and butane, which can be detected at concentrations as low as

0.4 g/hr., while it is 10 or more times less sensitive at detecting gases such as pentene (5.6 g/hr.) and isoprene (8.1 g/hr.).

*Table 3.5: Minimum Detected Leak Rate (MDLR) for various VOCs as determined by a third-party laboratory.*

1-Pentene	5.6g/hr.
Benzene	3.5g/hr.
Butane	0.4g/hr.
Ethane	0.6g/hr.
Ethanol	0.7g/hr.
Ethylbenzene	1.5g/hr.
Ethylene	4.4g/hr.
Heptane	1.8g/hr.
Hexane	1.7g/hr.
Isoprene	8.1g/hr.
Methyl Ethyl Ketone	3.5g/hr.
Methane	0.8g/hr.
Methanol	3.8g/hr.
Methyl Isobutyl Ketone	2.1g/hr.
Octane	1.2g/hr.
Pentane	3.0g/hr.
Propane	0.4g/hr.
Propylene	2.9g/hr.
Toluene	3.8g/hr.
Xylene	1.9g/hr.

## 3.2 Methods

### 3.2.1 Leak Detection Experiments

All leak detection experiments were conducted in a standard 4-foot × 4-foot chemical fume hood located at the EPA Region 6 Addison Facility in Texas. A FLIR camera was positioned 8 feet in front of the hood, and the camera lens was in line with the source of the leak inside the chemical fume hood. For PCE and TCE leak detection experiments, a gas canister of known PCE or TCE concentration was placed at the center of the hood. The floor and the fume hood was marked with duct tape to indicate their locations for future leak detection experiments. Each gas standard canister was equipped with a standard regulator, which was connected to a six-inch glass tubing that was shaped like an inverted ‘T.’ The tube ending horizontal to the base of the hood was capped, while the tube ending that was at a ninety-degree angle relative to horizontal was aimed up towards the top of the hood. The height of the camera was 54.5 inches from the floor, and was adjusted such that the center of the camera lens was aimed at the tip of the tube turned towards the top of the hood.

Prior to conducting any leak detection experiments, the camera was powered on, and the detector was allowed to cool. The FLIR GF-320 with the InSb detector took approximately 6 minutes to cool down, while the FLIR GF-306 with the QWIP detector took approximately 10 minutes. After completion of the cool down step (indicated by a bar on the camera LCD screen), the camera was put through a non-

uniformity correction (NUC) process to reduce spatial noise by pressing the ‘NUC’ button on the camera with the lens cap in place. After the completion of the “NUC-ing” process, leak detection experiments were begun.

Leak detection experiments were conducted with six different concentrations for both TCE and PCE, three of which were related to a residential air exposure scenario, and the remaining three were related to a worker air exposure scenario. Prior to initiation of the leak detection experiment with each canister, the chemical fume hood was turned off to prevent the effect of air turbulence on flow paths of the chemical leaks. For each compound, the two cameras described in Sections 3.1.2.1 and 3.1.2.2 were used to “see/view” the leaks. Testing began by viewing PCE and TCE gas canisters with the highest concentration followed by the lesser concentrations. In addition to PCE and TCE, other chemicals that were tested included propane gas, ammonium hydroxide (liquid), and the solvents dichloromethane and hexane. For the gas canisters, the regulator was opened to allow gas flows ranging from 0 (control) to 8 liters per minute (lpm), while for the liquids, the containers containing the liquid were either capped (control) or uncapped. With each chemical “leak,” the camera was operated through four different modes, recording at least one minute of video in each mode: rainbow color palette mode, high sensitivity mode, gray scale mode with white is hot polarity, and gray scale mode with black is hot polarity. At the end of the experiments, the videos were transferred to a computer for further processing.



*Figure 3.2: A FLIR GF-320 medium-range IR camera (Source: FLIR Systems) designed to detect VOC gases.*



*Figure 3.3: Experiment set up at the EPA Region 6 Addison Facility. Gas canisters and vials containing chemicals such as ammonium hydroxide, dichloromethane, and hexanes were opened in the hood, and the camera was focused on the opening. The camera was placed exactly 8 feet from the hood.*

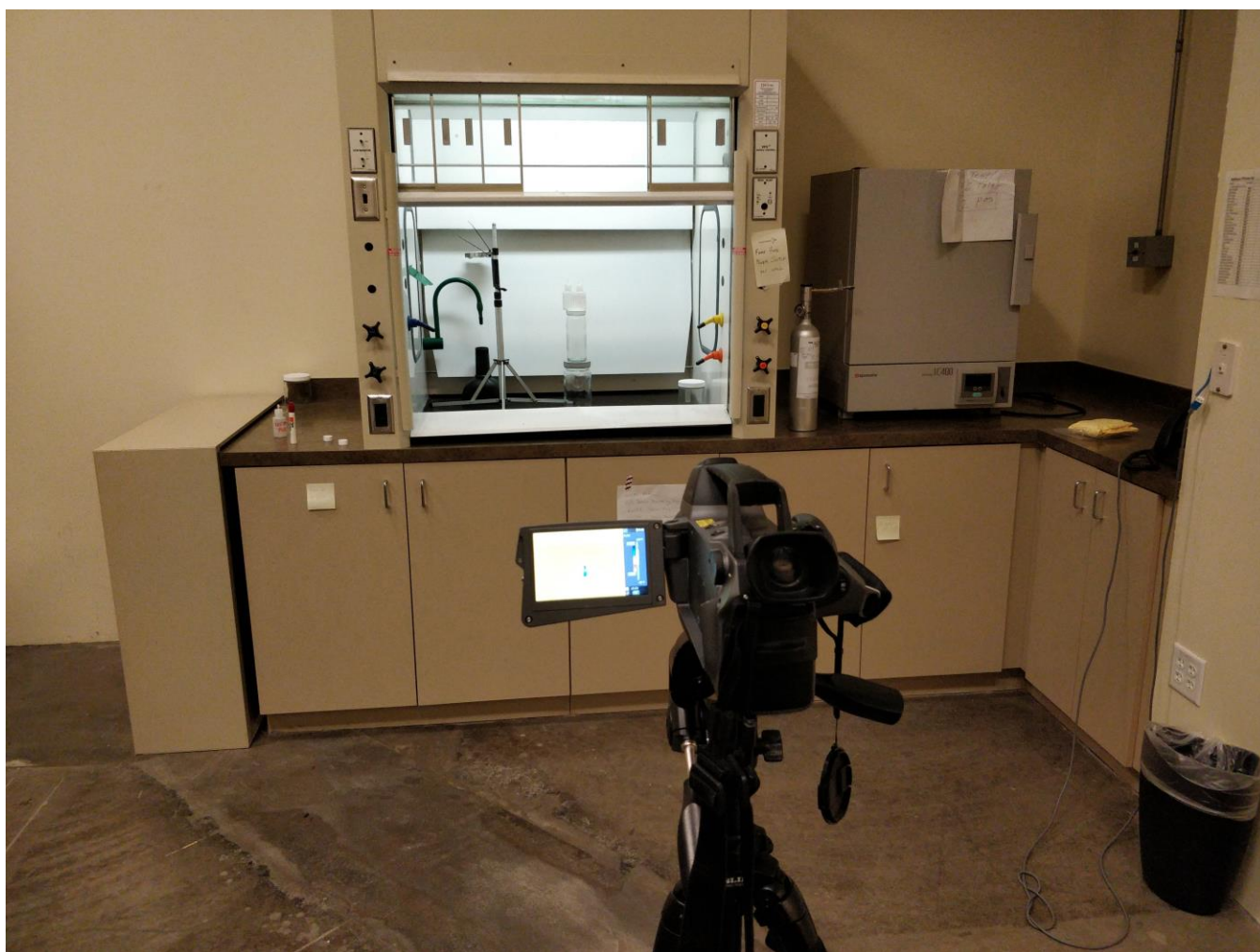


*Figure 3.4: Experiment set up at the EPA Region 6 Addison Facility. Ventilation in the hood was turned off between experiments using the switch that can be seen on the right wall.*

### **3.3 Databases**

#### **3.3.1 National Institute of Standards and Technology (NIST) WebBook**

The NIST Chemistry WebBook (NIST, 2018) is an online database website that provides thermochemical, thermophysical and ion energetics data compiled by the National Institute of Standards and Technology (NIST) under the Standard Reference Data Program. The database is searchable using formula, name, IUPAC identifier, CAS registry number, reaction, author, structure, ion energetic properties, vibrational and electronic energies, and molecular weight. The NIST WebBook was used to obtain IR spectra for the chemicals used in this study, including hexane, propane, ammonia, dichloromethane, PCE and TCE. In addition, the WebBook was used to determine chemicals whose transmittivities fall within the spectral ranges of the two cameras considered in this study. Figure 3.5 shows the web interface for searching chemicals by their IR spectra.

# Search for Species Data by Vibrational Energy Value

Please follow the steps below to conduct your search ([Help](#)):

1. Enter a vibrational energy value or range in  $\text{cm}^{-1}$ :
2. If desired, enter a formula to restrict the search: 
  - Allow elements not specified in formula. ([Help](#))
  - Allow more atoms of elements in formula than specified. ([Help](#))
3. Select the desired units for thermodynamic data:
  - SI  calorie-based
4. Select the desired type(s) of data:

Thermodynamic Data	Other Data
<input type="checkbox"/> Gas phase	<input type="checkbox"/> IR spectrum
<input type="checkbox"/> Condensed phase	<input type="checkbox"/> THz IR spectrum
<input type="checkbox"/> Phase change	<input type="checkbox"/> Mass spectrum
<input type="checkbox"/> Reaction	<input type="checkbox"/> UV/Vis spectrum
<input type="checkbox"/> Ion energetics	<input type="checkbox"/> Gas Chromatography
<input type="checkbox"/> Ion cluster	<input type="checkbox"/> Vibrational & electronic energy levels
	<input type="checkbox"/> Constants of diatomic molecules
	<input type="checkbox"/> Henry's Law
5. Press here to search:

Figure 3.5: Screenshot of the Vibrational Energy search interface of the NIST WebBook database. Cameras can detect chemicals whose vibrational energies fall within their sensor's spectral range.

## 3.3.2 Pacific Northwest National Laboratory IR Database

The Pacific Northwest National Laboratory (PNNL) maintains a vapor phase IR spectral database that contains IR spectra for approximately 450 pure organic chemicals at three different temperatures (5, 25 and 50 °C). The spectral coverage ranges from 600 – 6500  $\text{cm}^{-1}$  (1.5 – 16.2  $\mu\text{m}$ ), and has a resolution of approximately 0.1  $\text{cm}^{-1}$ , and uncertainty  $\leq 0.005 \text{ cm}^{-1}$  (Sharpe et al., 2004). In addition, vapor pressure vs. temperature curves for all chemicals are included in the database. Figure 3.6 shows the IR spectra for PCE at 25 °C, which exhibits its highest absorbance between 890 – 935  $\text{cm}^{-1}$  (10.7 – 11.2  $\mu\text{m}$ ). In addition to the vapor phase IR spectra, the PNNL database contains graphs that illustrate the relation between vapor pressure and temperature, which will be useful for correcting the IR spectra at temperatures other than 5, 25 or 50 °C. Figure 3.7 shows a graph between vapor pressure (Torr) and temperature (°C) for PCE.

## 3.3.3 Response Factor (RF) Calculator

Infrared (IR) Optical Gas Imaging (OGI) cameras are used to image gaseous compounds and detect gas leaks from equipment. A given IR camera may be more sensitive to one compound than another. Response Factor (RF) is a measure of an IR camera's sensitivity for a given compound relative to a reference compound. For example, if the RF value for methane is 0.30 in reference to propane, it means that an image of methane is 30% as strong as propane for this camera, i.e., methane is less easily detected than propane. Similarly, if propene's RF is 1.47, the image of propene is 47% stronger than propane. When RF for a compound is very small, that compound may not be visible in the IR camera.

The values of RF are affected by the type of IR camera and the product of concentration (C) and optical pathlength (L), which is denoted as CL with units of ppm-m. For example, CL=100,000 ppm-m could represent a parcel of pure gas (1,000,000 ppm) that is 0.1-meter-deep, or 100,000 ppm that is 1 meter deep. For practical purposes, three CL values are used in this RF calculator: 2,000 ppm-m for a small/diluted gas plume, 100,000 ppm-m for a large/concentrated gas plume, and 20,000 ppm-m for a condition between the high and low CL. For more information on RF, please refer to paper # 93 in the Proceedings of Air Quality Measurement Methods and Technology, Chapel Hill, NC, March 15-17, 2016 (<http://measurements.awma.org/>).

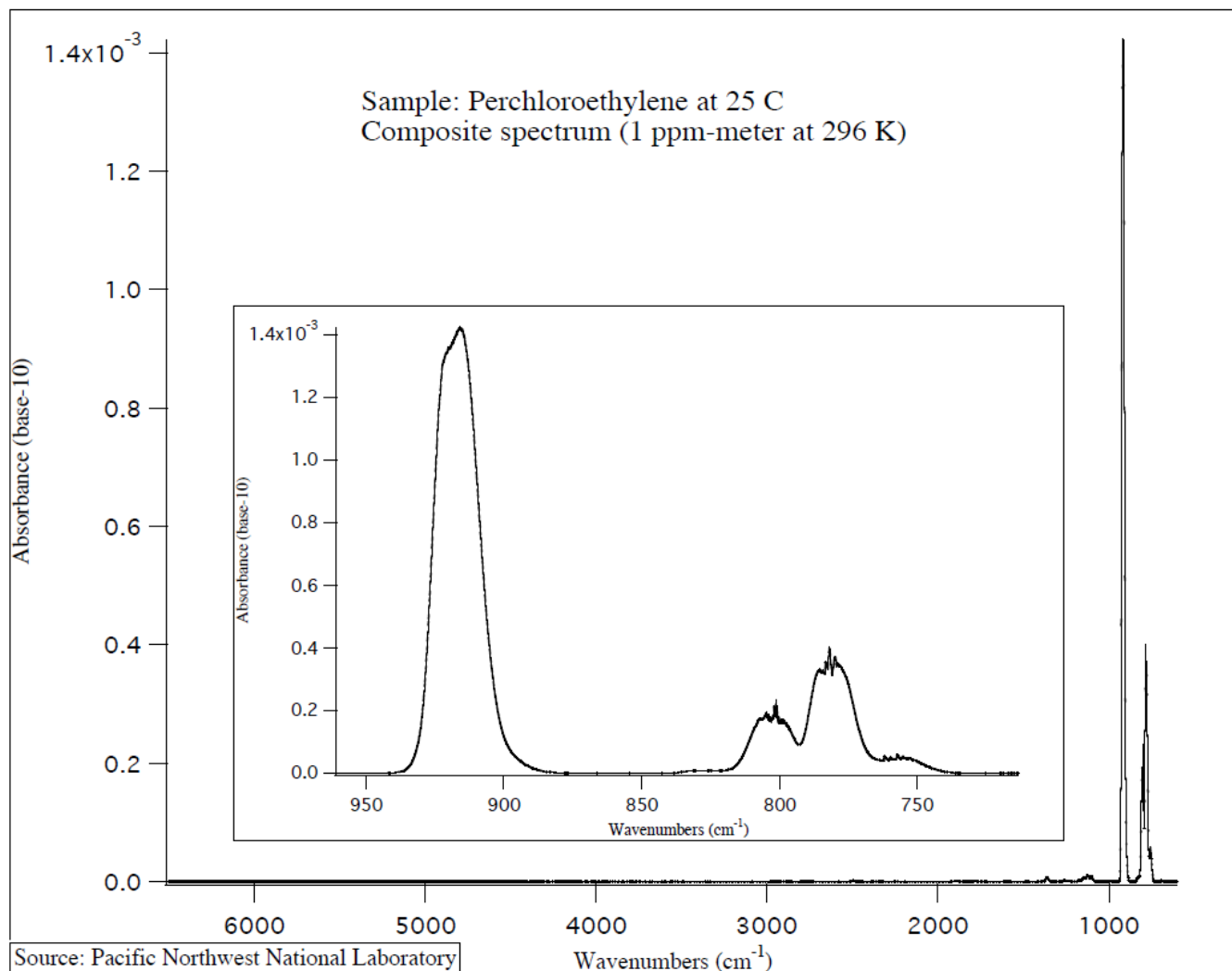


Figure 3.6: IR spectrum of PCE at 25 °C as shown in the PNNL database. PCE is referred to as perchloroethylene (tetrachloroethylene/tetrachloroethene) in the database. The inset shows the highest absorbance of PCE is approximately 920 cm<sup>-1</sup> (wavelength = 1/wavenumber = 1/920 cm<sup>-1</sup> = 10.9 μm).

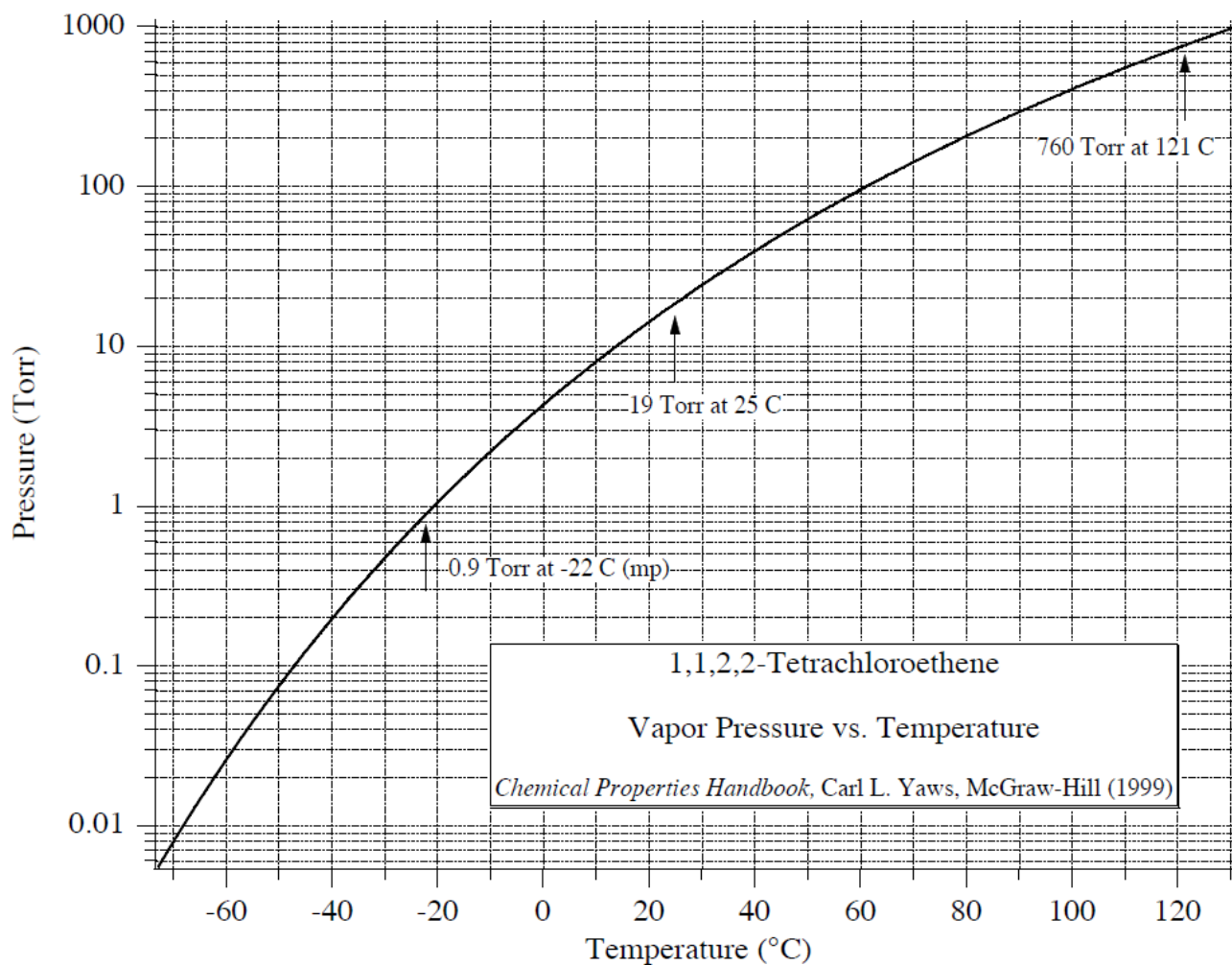


Figure 3.7: Relation between vapor pressure (Torr) and temperature (°C) for PCE as shown in the PNNL database. PCE is referred to as 1,1,2,2-Tetrachloroethene in the database. This relationship can be used to correct the IR spectra for other temperatures.

## 4. QUALITY ASSURANCE/QUALITY CONTROL

This multidisciplinary research project was a collaborative effort of the US EPA ORD's National Risk Management Research Laboratory and the EPA Region 6 Superfund Division. Each organization had project objectives specific to their mission.

The U.S. EPA quality system is integral to this effort, providing policy and procedures that are implemented in all aspects of the project to ensure the data generated from each discipline would be of a type and quality necessary and sufficient to achieve project objectives. The U.S. EPA's quality system encompasses management and technical activities related to the planning, implementation, assessment, and improvement of environmental programs that involve:

- the collection, evaluation, and use of environmental data, and
- the design, construction, and operation of environmental technology.

Consistent with the requirements of the EPA quality system, the participating EPA organizations have implemented Quality Management Plans to define the specific processes and procedures that each EPA organization uses to ensure implementation of the EPA quality system. The following QA tools were implemented during the project:

- A systematic planning approach was applied to develop acceptance or performance criteria for all work covered by the EPA quality system as defined in the QAPP for this project. The QAPP (US EPA, 2017) was developed and approved for use by contract and the EPA quality staff for each project effort before any data collection activities were initiated in the field or laboratory. The title of the QAPP is "RARE Application – Using FLIR Technology as an Effective PCE/TCE Screening Tool for Vapor Intrusion Sampling," with an ORD QA Tracking ID G-STD-0030744.
- Standard operating procedures (SOPs) where available were implemented for all applicable field and laboratory activities to ensure consistency in the collection of samples, operation of environmental technologies, and generation of environmental data in the field and in the laboratory. Manufacturer instructions were followed in cases where SOPs were not available (e.g., for operation of the FLIR GF-306 and GF-320 VOC camera systems).
- Appropriate training was provided for staff to ensure that quality-related responsibilities and requirements as defined in the QAPPs were understood, and that SOPs were implemented for all applicable activities. This practice ensured that research activities are conducted in a consistent and reproducible manner, with the intent the research data produced would meet project data quality objectives and/or acceptance criteria for usability to achieve project objectives.
- All data were reviewed and verified by research staff after collection to ensure the type, quantity, and quality were sufficient to reach conclusions stated in this report and to achieve project objectives.

Furthermore, it is a requirement that all EPA quality system elements "flow down" to the contractor support entities. EPA quality system specifications are incorporated into all applicable EPA-funded agreements and are defined in 48 CFR 46. An important element of this system for contracted analytical services is certification by an independent accrediting organization, such as the National Environmental Laboratory Accreditation Conference. This certification ensures that data are collected according to SOPs and methodologies under a quality system that is equivalent to American National Standards Institute/American Society of Quality Control E4, which is the basis of the EPA quality system.

# 5. RESULTS AND DISCUSSION

## 5.1 Camera Performance Check

The FLIR GF 306 camera system is designed for detecting gases such as SF<sub>6</sub> and NH<sub>3</sub> while the FLIR GF 320 camera system is designed for detecting VOCs. The leak detection capabilities of the FLIR GF-306 and GF-320 camera systems were verified using ammonium hydroxide (NH<sub>4</sub>OH) and propane (C<sub>3</sub>H<sub>8</sub>), respectively. The transmittance IR spectrum for propane is shown in Figure 5.1, while Figure 5.2 shows the transmittance IR spectrum for ammonia. The GF-306 detects gases that have an absorbance peak in the 10.3 – 10.7 μm spectral range, while the GF-320 detects gases that have an absorbance peak in the 3.2 – 3.4 μm spectral range.

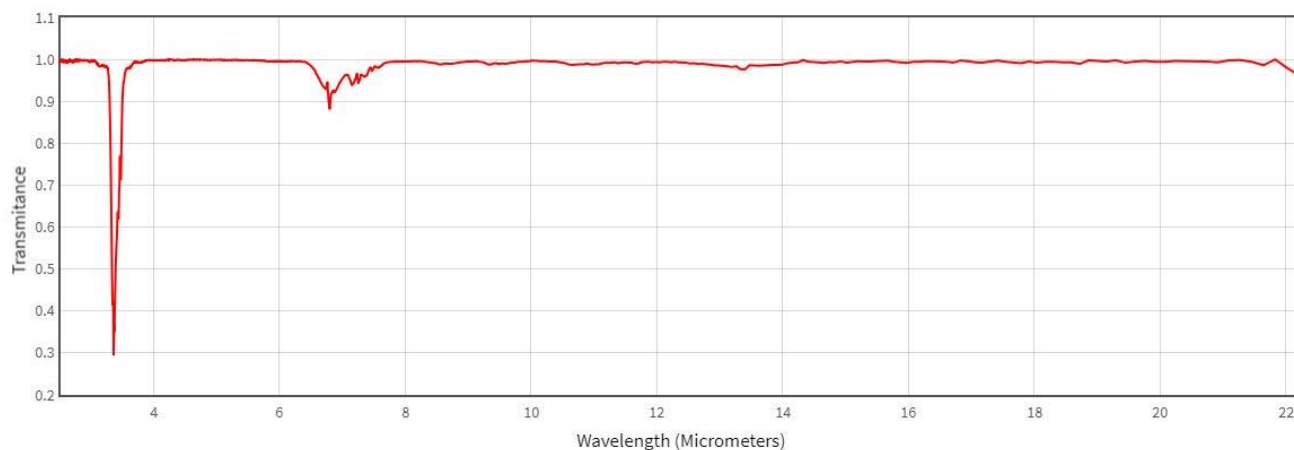


*Figure 5.1: IR spectrum of propane as shown in the NIST WebBook database. The y-axis depicts percent light transmittance (1.0 indicates light is fully transmitted), while the x-axis shows the wavelength in micrometers. The amount of light absorbed is 100% minus the amount of light transmitted. The figure indicates that propane absorbs a majority of the light in the IR region between 2 – 4 μm wavelengths, while minor amounts are absorbed between 6 – 8 μm.*

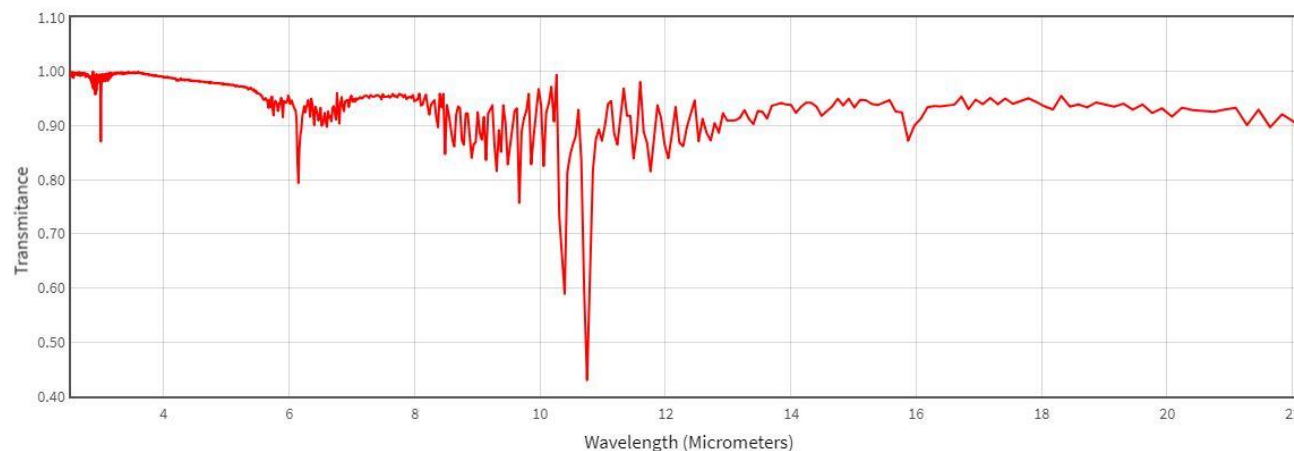


*Figure 5.2: IR spectrum of ammonia as shown in the NIST WebBook database. The y-axis depicts percent light transmittance, while the x-axis shows the wavelength in micrometers. The figure indicates that ammonia absorbs most of the light in the IR range between 10 – 11 μm wavelengths.*

Figures 5.3 – 5.5 show IR images taken from a video of an opened propane tank that was captured with a GF-306 camera using the palettes black is hot (gas vapors are dark in color against a white background), white is hot (gas vapors are white in color against a black background), and rainbow (colors range from red or yellow for background to deep blue for gas vapors). The resolution of the camera sensor is poor ( $320 \times 240$  pixels); hence, one might have to switch amongst the available palettes to distinguish a gas plume from the background. In each of the three figures, the propane plume can be easily seen against the background, though the gas plumes are much easier to see in the video images.

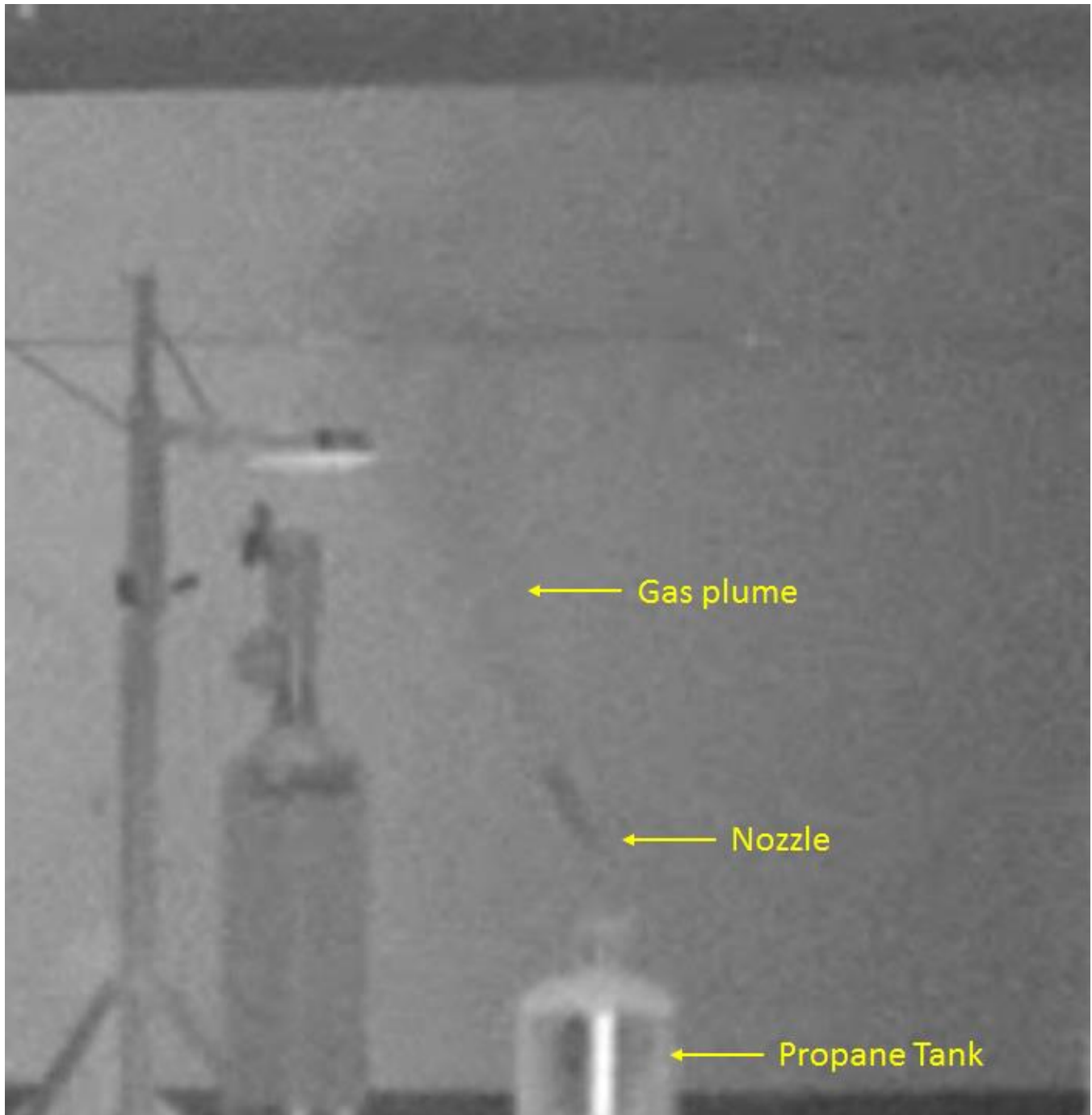


*Figure 5.3: IR image of an open propane tank using the black is hot palette. The gas plume is seen as black clouds against a white background.*

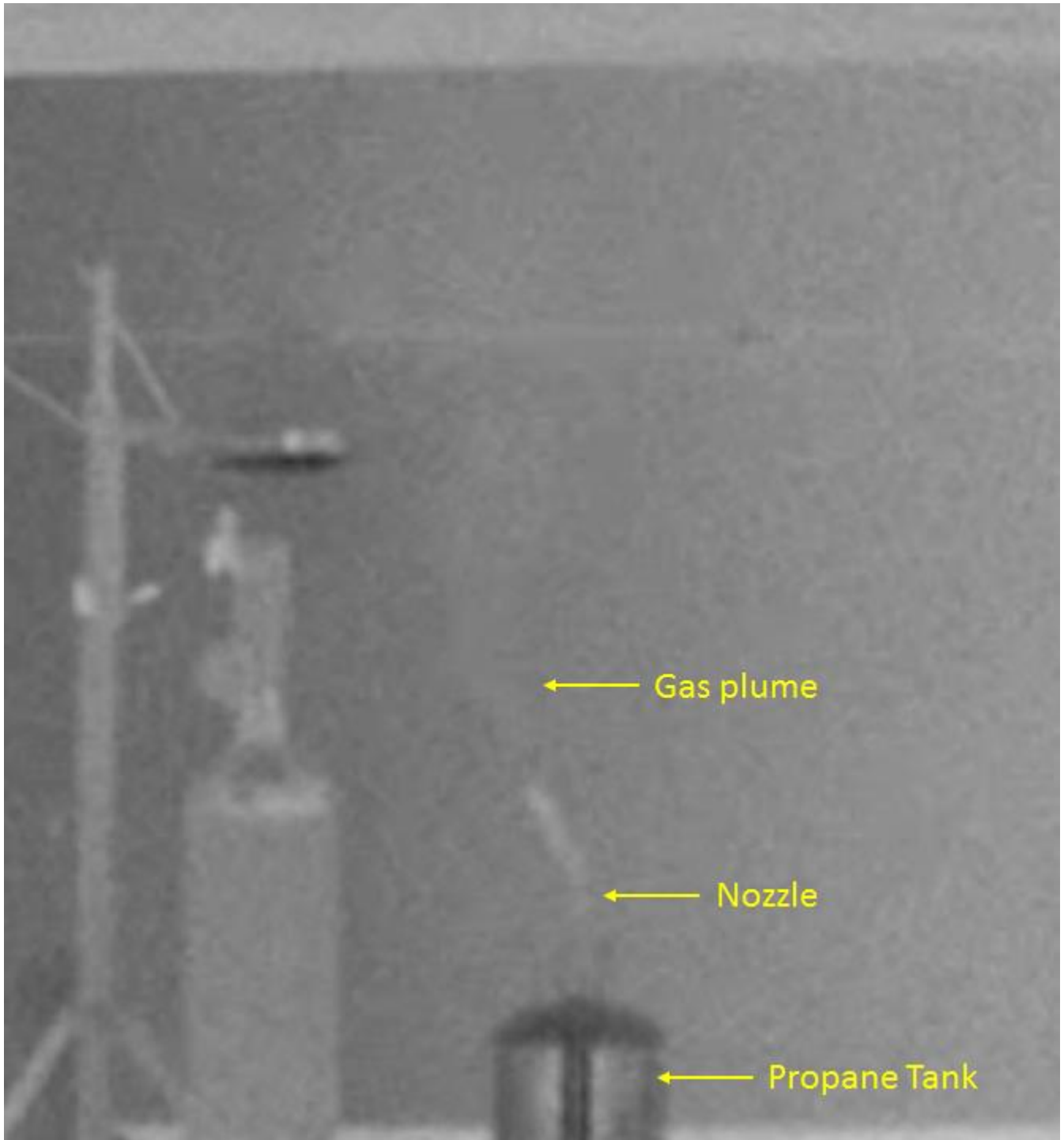


*Figure 5.4: IR image of an open propane tank using the white is hot palette. The gas plume is seen as white clouds against a black background.*



*Figure 5.5: IR image of an open propane tank using the rainbow color palette. The gas plume is seen as a black cloud against a yellow background.*

Figures 5.6 – 5.8 show still IR images taken from a video of a vial containing ammonium hydroxide captured with a GF-320 camera using the palettes black is hot, white is hot, and rainbow. As the vial containing ammonium hydroxide, which is a liquid at room temperature, is opened, the liquid vaporizes and is released into the air. Since the air in the hood was turned off during this experiment, the ammonia vapors appear undisturbed and undiluted, and the plume can be seen to rise straight towards the top of the hood. In addition, the air-liquid interface where the evaporation occurs can be easily distinguished inside the vial containing the liquid.



*Figure 5.6: IR image of an open vial containing ammonium hydroxide using the black is hot palette. A black plume is seen at the top of the vial as the liquid ammonium hydroxide vaporizes and is released into the air.*



*Figure 5.7: IR image of an open vial containing ammonium hydroxide using the white is hot palette. A white plume is seen rising from the top of the vial.*



*Figure 5.8: IR image of an open vial containing ammonium hydroxide using the rainbow color palette. The ammonia vapors are harder to see with the rainbow or any of the other available color palettes.*

## **5.2 PCE and TCE Leak Detection**

Preliminary experiments were conducted at the 1 in a million ( $10^{-6}$ ) risk range action level (125 ppt) for both PCE and TCE using both the FLIR GF-320 and GF-306 cameras. Gas flow rates ranging from 1 to 8 liters per minutes (lpm) were tested for both gases. Palettes tested included black is hot, white is hot, and the rainbow color palette. In all cases, the cameras were not able to distinguish PCE and TCE vapors

from the background. The experiments were repeated at the 1 in 10,000 ( $10^{-4}$ ) risk range action level (25 ppb). The two cameras were not able to distinguish the VOC vapors from the background at these higher concentrations either. PCE gas canisters at higher concentrations (125 ppb, 1.25 ppm and 125 ppm) were also procured, and the experiments were repeated at the highest available concentration for both PCE (125 ppm) and TCE (125 ppb). The results were similar to those obtained at the lower concentrations, i.e., the two cameras were not able to distinguish the two gases from the background. Figures 5.9 – 5.11 illustrate IR images of the top of the TCE cylinder in three different color palettes, with 8 lpm of 25 ppb TCE flowing out of the top of the nozzle. The area on the top of the nozzle in all three images is of similar color to the rest of the background, indicating the camera was not able to detect the TCE vapors.



*Figure 5.9: IR image of the top of a TCE gas canister using the black is hot palette. TCE, if detected, would show up as a black cloud above the nozzle that is pointed upwards.*



*Figure 5.10: IR image of the top of a TCE gas canister using the color palette. TCE, if detected, would show up as a blue cloud above the nozzle that is pointed upwards.*



*Figure 5.11: IR image of the top of a TCE gas canister using the white is hot palette. TCE, if detected, would show up as a white cloud above the nozzle that is pointed upwards. A lack of a white cloud above the nozzle indicates the camera was not able to detect TCE.*

### **5.3 Determination of Gas Detection Capabilities for each Camera System**

As mentioned previously, the detection capabilities of the two camera systems are highly dependent on the spectral range of the camera sensors, with the GF-306 being able to detect gases in the 10.3 – 10.7  $\mu\text{m}$  spectral range, while the GF-320 can detect gases in the 3.2 – 3.4  $\mu\text{m}$  spectral range. IR spectra databases such as the ones from PNNL and the NIST WebBook may be used to determine if a given camera system can detect gases of a type by comparing the spectral range of the camera sensor with any absorbance (inversely proportional to transmittance) in that range. For example, Figures 5.12 – 5.15 show the IR spectra from the NIST WebBook for both propane and ammonia in the 3.2 – 3.4  $\mu\text{m}$  and 10.3 – 10.7  $\mu\text{m}$  spectral ranges. Figure 5.12 shows approximately 30% transmittance for propane in the 3.2 – 3.4  $\mu\text{m}$  while the transmittance is close to 100% in the 10.3 – 10.7  $\mu\text{m}$  spectral range (Figure 5.13). This indicates the GF-320 camera system will be able to detect propane, while the GF-306 will not be able to detect the gas. Similarly, the GF-320 camera cannot detect ammonium hydroxide vapors as the transmittance is close to 100% in the camera's spectral range (Figure 5.15), while the GF-306 camera is able to detect the vapors. Unlike propane, ammonia has transmittance close to 75% at 10.3  $\mu\text{m}$ , which then decreases to approximately 60% at 10.4  $\mu\text{m}$  before increasing to approximately 93% at 10.63  $\mu\text{m}$  (Figure 5.14). The transmittance then decreases to approximately 42% at 10.75  $\mu\text{m}$ , which is outside the

spectral range of the GF-306 camera. However, the camera can still detect ammonium hydroxide whose transmittance is in the shaded region shown in Figure 5.14, including the region up to  $10.7\ \mu\text{m}$ , which has a transmittance of approximately 60%.

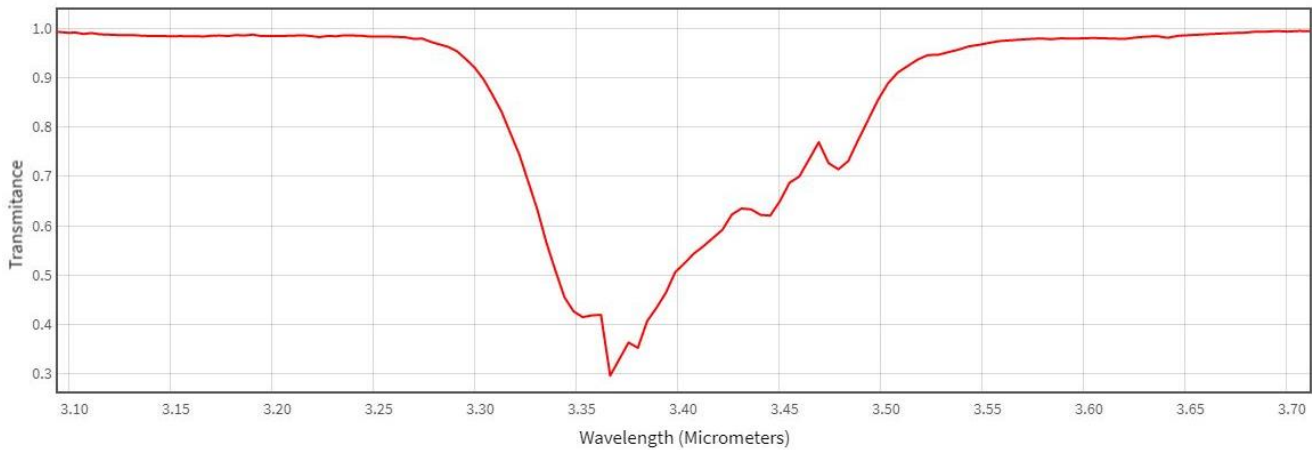


Figure 5.12: IR spectra of propane close to the  $3.2 - 3.4\ \mu\text{m}$  spectral range. Since propane has a transmittance peak with a minima at approximately  $3.36\ \mu\text{m}$  with approximately 30% transmittance (the minima are close to the 0.3 transmittance line in the y-axis), the GF-320 VOC camera can detect propane.

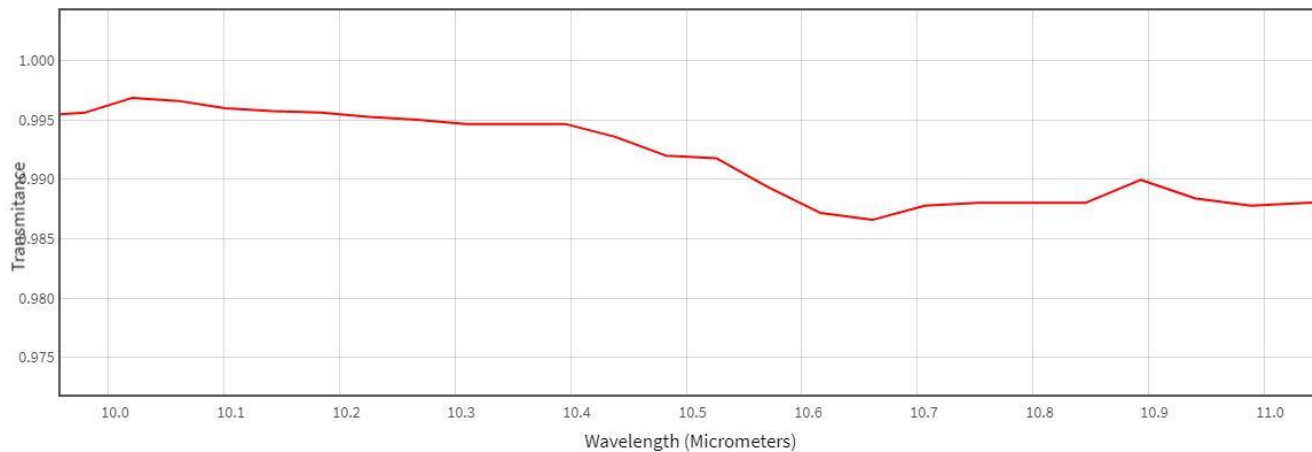


Figure 5.13: IR spectra of propane close to the  $10.3 - 10.7\ \mu\text{m}$  spectral range. Since the transmittance is very close to 1 for propane in this spectral range, the GF-306 camera, whose absorbance falls within this spectral range, cannot detect propane.

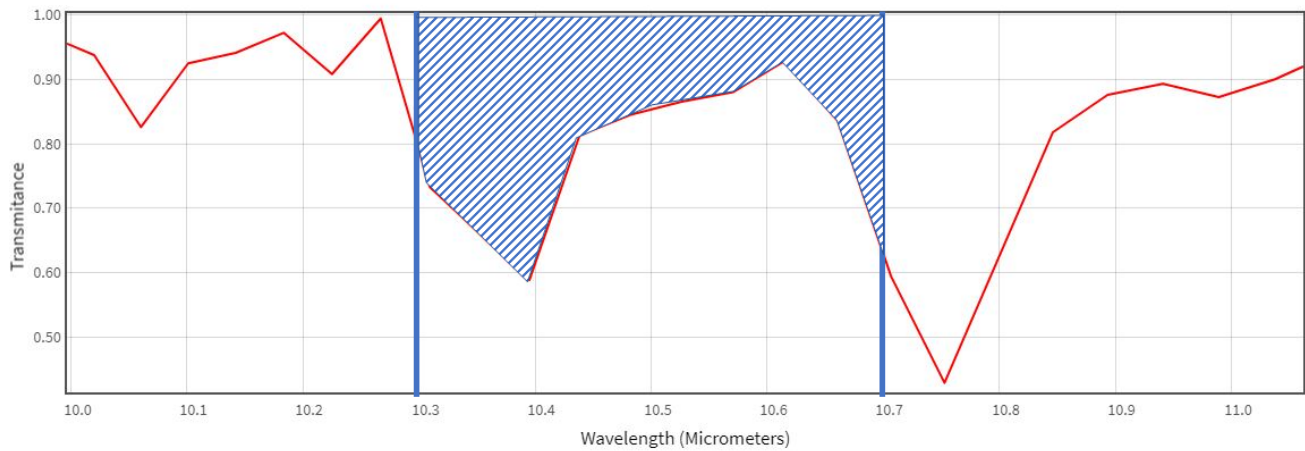


Figure 5.14: IR spectra of ammonia close to the 10.3 – 10.7  $\mu\text{m}$  spectral range (shown using dark blue lines parallel to the y-axis). Even though ammonia has a transmittance peak with the minima at approximately 10.75  $\mu\text{m}$ , which is outside the spectral range of the GF-306 camera, the gas has some absorbance within the spectral range (60% transmittance close to 10.4  $\mu\text{m}$  and approximately 60% transmittance at 10.7  $\mu\text{m}$ ), the GF-306 camera can detect ammonium hydroxide vapors, which has a spectra similar to ammonia.

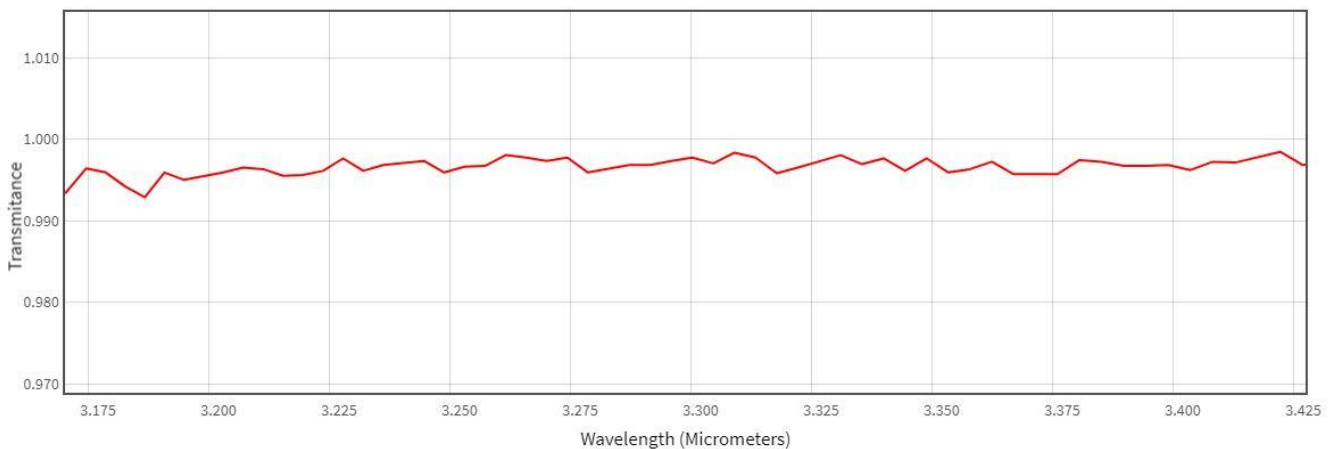


Figure 5.15: IR spectra of ammonia close to the 3.2 – 3.4  $\mu\text{m}$  spectral range. Since the transmittance is very close to 1 for ammonia in this spectral range, the GF-320 VOC camera, whose absorbance falls within this spectral range, cannot detect ammonium hydroxide vapors.

#### 5.4 PCE and TCE Gas Detection Capabilities for each Camera System

Figure 5.16 shows the IR spectra from the NIST WebBook for TCE while Figure 5.17 shows the IR spectra for PCE. TCE has several low transmittance regions in the 10 - 13  $\mu\text{m}$  range, with a minimal transmittance less than 5% at around 11.8  $\mu\text{m}$  wavelength as well as a peak with 70% transmittance close to 3.2  $\mu\text{m}$  wavelength (Figure 5.16). PCE has its lowest transmittance (approximately 10%) close to 10.9  $\mu\text{m}$ , and a second region with approximately 55% transmittance in the 12 – 13.5  $\mu\text{m}$  spectral range (Figure 5.17). Figures 5.18 and 5.19 show the transmittance for TCE in the 10.3 – 10.7  $\mu\text{m}$  and 3.2 – 3.4  $\mu\text{m}$  spectral ranges, respectively. TCE has a very low transmittance of approximately 10%

between 10.55 and 10.7  $\mu\text{m}$ , which is within the range of the GF-306 sensor, indicating the camera is capable of detecting TCE molecules whose spectra are in the shaded region shown in Figure 5.18. In addition, TCE has a smaller transmittance region between 3.22 and 3.26  $\mu\text{m}$  (Figure 5.19), which is within the range of the GF-320 sensor, indicating that this camera is capable of detecting TCE. However, the detection capabilities of the two experimental camera systems are proportional to the area of the shaded regions in Figures 5.18 and 5.19, with the area in Figure 5.19 being approximately 5 – 10% of the shaded area in Figure 5.18, indicating the FLIR GF-320 is approximately 5 – 10% less sensitive at detecting TCE than the FLIR GF-306. Hence, for example, if the minimum detection limit for TCE using the GF-306 camera system is 1000 parts per million (ppm), the concentration will have to be between 10,000 – 20,000 ppm to detect TCE using the GF-320 VOC camera system.

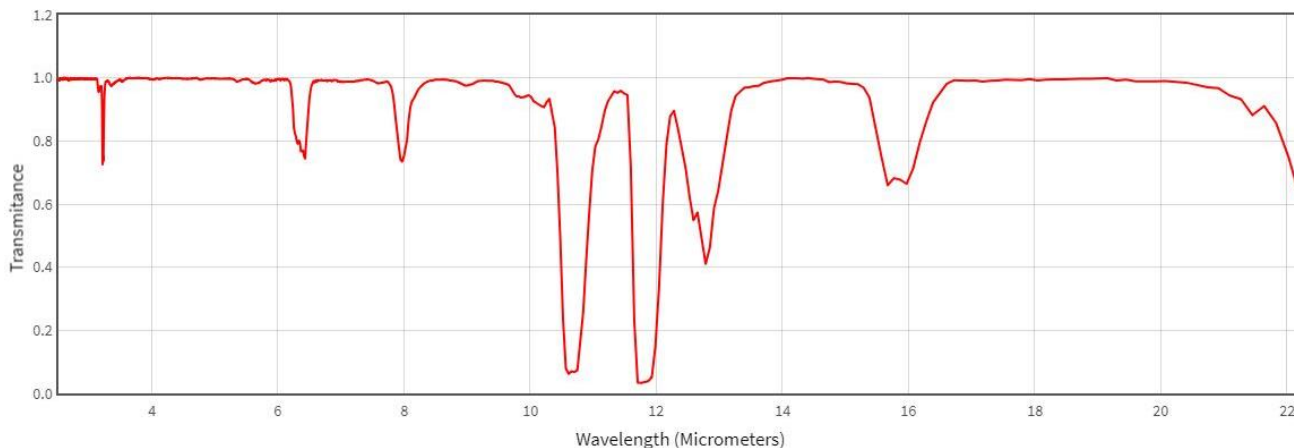


Figure 5.16: IR spectrum of TCE from the NIST WebBook database.

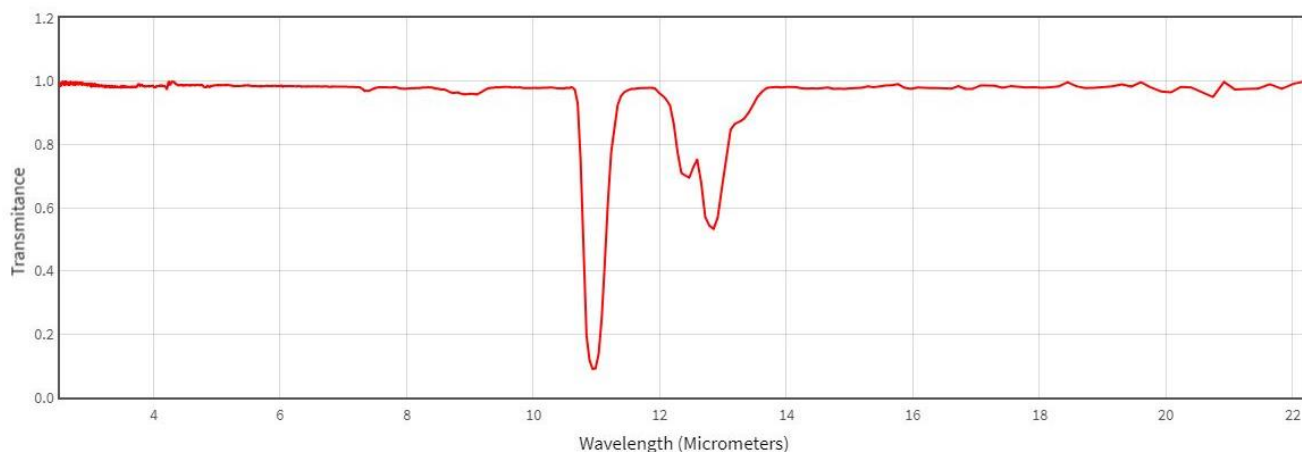


Figure 5.17: IR spectrum of PCE from the NIST WebBook database.

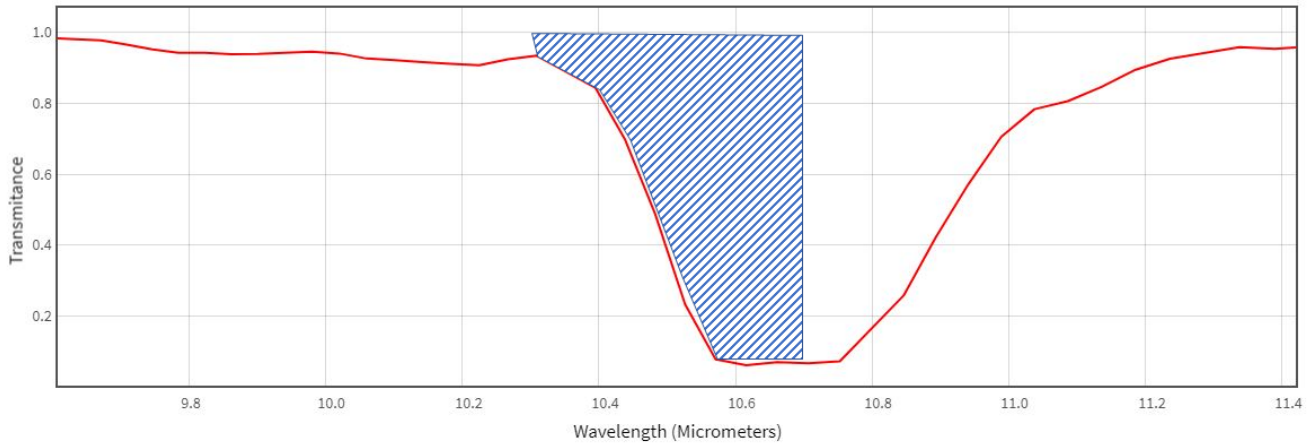


Figure 5.18: IR spectrum of TCE in the 10.3 – 10.7  $\mu\text{m}$  spectral region. The GF-306 camera can detect TCE molecules whose transmittance is in the shaded region.

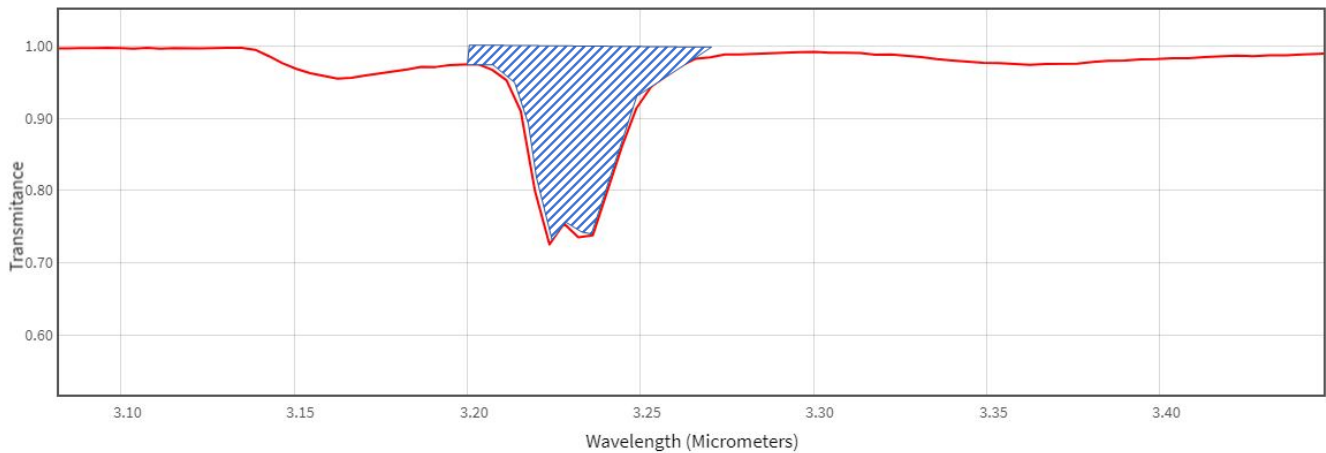


Figure 5.19: IR spectrum of TCE in the 3.2 – 3.4  $\mu\text{m}$  spectral region. The GF-320 VOC camera can detect TCE molecules whose transmittance is in this region.

Figures 5.20 and 5.21 show the transmittance for PCE in the 10.3 – 10.7  $\mu\text{m}$  and 3.2 – 3.4  $\mu\text{m}$  spectral ranges, respectively. The transmittance for PCE is close to 100% in both the 10.3 – 10.7  $\mu\text{m}$  and 3.2 – 3.4  $\mu\text{m}$  spectral ranges, indicating that neither of the two camera systems will be effective at detecting PCE however high the concentration. Hence, it was not surprising that the reason PCE was not detected by the two cameras while conducting leak experiments using 125 ppm PCE gas canisters at the EPA Region 6 Addison Facility. A camera system whose sensor covers the 10.7 – 11.4  $\mu\text{m}$  spectral range will have to be used instead to detect PCE.

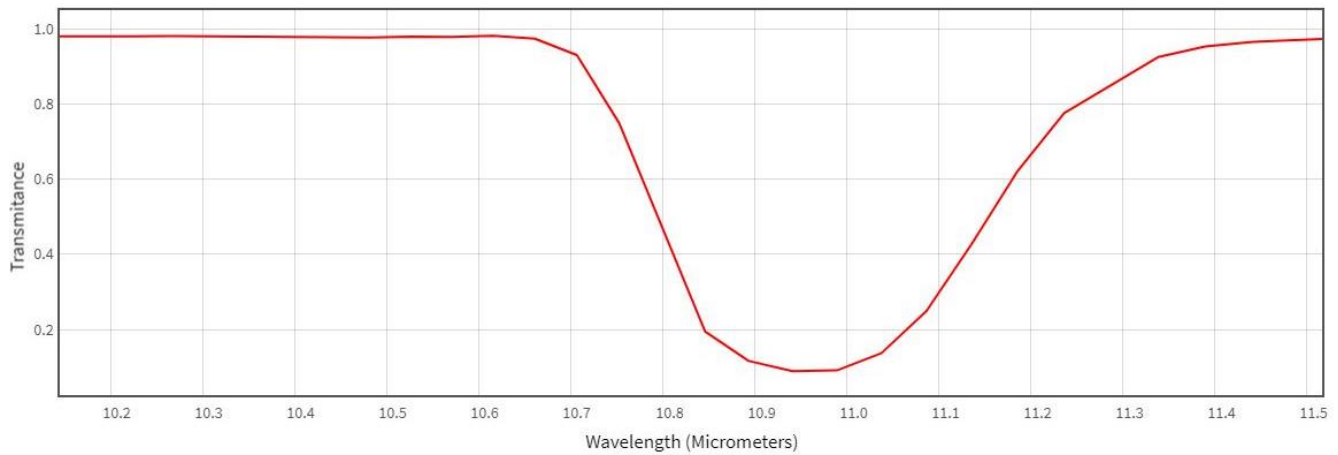


Figure 5.20: IR spectrum of PCE in the 10.3 – 10.7  $\mu\text{m}$  spectral region. Though the PCE IR spectrum shows a transmittance peak in the figure, the dip in the transmittance starts at approximately 10.7  $\mu\text{m}$ . The transmittance is close to 100% in the 10.3 – 10.7  $\mu\text{m}$  spectral region, which is the spectral range of the GF-306 camera sensor. Hence, the camera is not able to detect PCE.

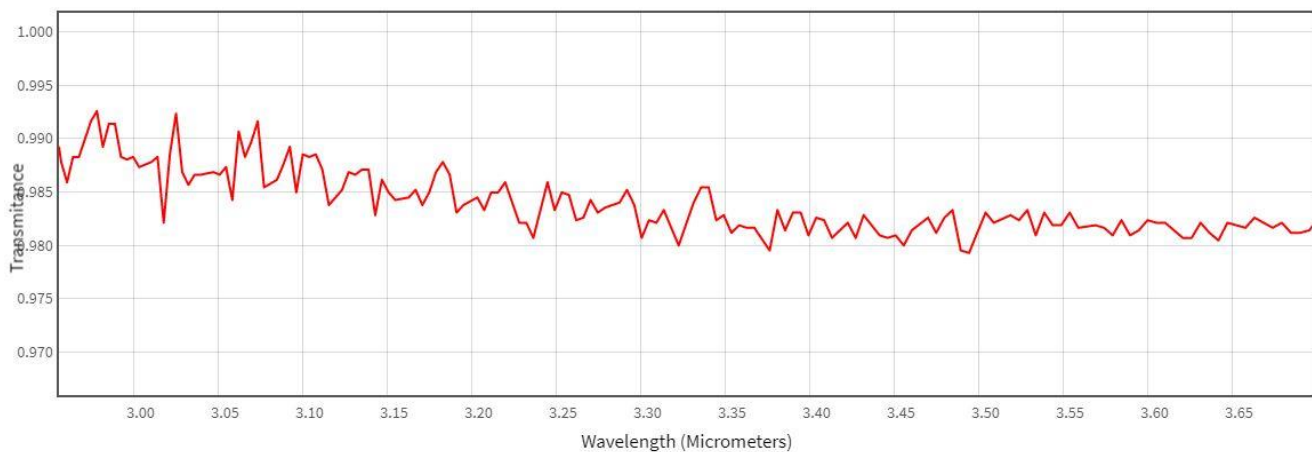


Figure 5.21: IR spectra of PCE in the 3.2 – 3.4  $\mu\text{m}$  spectral region. The transmittance is close to 100% in the 3.2 – 3.4  $\mu\text{m}$  spectral region, which is the spectral range of the GF-320 VOC camera sensor. Hence, the VOC camera is not able to detect PCE.

## 5.5 Determination of Gas Leak Detection Limits

FLIR provides minimum detectable leak rates (MDLR) for some gases as determined by a third-party lab. For example, FLIR mentions an MDLR of 0.026 grams/hour (g/hr.) for SF<sub>6</sub> while using a GF-306 camera system (<http://www.flirthermography.com/ogi/display/?id=55666>), while MDLRs for various VOCs while using a GF-320 VOC camera system were determined to be between 0.04 – 8.1 g/hr. (<http://www.flirthermography.com/ogi/display/?id=55671>). MDLRs for the gases reported on the FLIR website were typically determined under optimal conditions including zero wind speed, no rain, low moisture, and optimal lighting conditions that simulate a bright blue sky among other conditions. However, MDLRs for the two chemicals that are of interest in this study, PCE and TCE, were not reported by FLIR nor are they available in the literature. Despite the lack of this information, it is

theoretically possible to estimate MDLRs for PCE and TCE based on the MDLRs reported on the FLIR site for VOCs as well as physicochemical properties and IR spectra of PCE and TCE. Two methods to estimate detection limits for PCE and TCE are described below.

### 5.5.1 Determination of Detection Limits using the Response Factor (RF) Calculator

An IR camera may be more sensitive or less sensitive to one gas over another depending on the physicochemical properties of the gases. The RF is a measure of an IR camera's sensitivity for a given gas when compared to a reference gas. Any of the gaseous forms of the chemicals listed on the FLIR website for which MDLRs are reported such as benzene, methane, toluene, etc. may be used as the reference chemical. For example, the MDLR for methane is listed as 0.8 g/hr., while the MDLR for propane is listed as 0.4 g/hr. while using the GF-320 VOC camera. Hence, if propane is used as the reference compound, the RF for methane would be 0.5, as methane is 50% less sensitive than propane, and implies that methane is less easily detected than propane. This implies that that an image of a methane gas will be 50% as strong as propane using a GF-320 VOC camera. The opposite is true for RF values greater than 1. When the RF for a chemical is very small relative to a reference chemical, that chemical might not be visible while using the IR camera.

RF values for more than 300 chemicals are available for the FLIR GF-300 and GF-320 cameras on the Providence Photonics website (<http://rfcalc.providencephotonics.com/>). The RFs on the website were calculated using the IR spectra from the PNNL database. To determine the RF for a chemical of interest, an email address is entered, an IR camera is selected (currently, information is available for GF-300 and GF-320 cameras, with additional cameras to be added later) followed by the selection of a chemical via a pull-down menu. In addition, a CL value is selected via a pull-down menu. Per the RF calculator website, "The values of RF are affected by the type of IR camera and the product of concentration (C) and optical pathlength (L), which is commonly denoted as CL with units of ppm-m. For example, CL=100,000 ppm-m could represent a parcel of pure gas (1,000,000 ppm) that is 0.1 meter deep, or 100,000 ppm that is 1 meter deep. For practical purposes, three CL values are used in this RF calculator: 2,000 ppm-m for a small/diluted gas plume, 100,000 ppm-m for a large/concentrated gas plume, and 20,000 ppm-m for a condition between the high and low CL. For more information on RF, please refer to paper # 93 in the Proceedings of Air Quality Measurement Methods and Technology, Chapel Hill, NC, March 15-17, 2016 (<http://measurements.awma.org/>)." (<http://rfcalc.providencephotonics.com/>).

Figure 5.22 shows a screenshot of the RF calculator website with selections made for the camera type (FLIR GF-320), chemical (PCE) and CL (2000 ppm-m). A CL of 2000 ppm-m was chosen as it is the lowest available CL value in the RF calculator tool, and will be representative of a small gas leak. Figure 5.23 shows a screenshot of the output for PCE, which shows an RF of 0.001 in reference to propane. Hence, the calculated RF indicates that PCE as detected by the GF-320 camera is approximately 1000 times less sensitive than propane.

## RESPONSE FACTOR CALCULATOR

Infrared (IR) Optical Gas Imaging (OGI) cameras are used to image gaseous compounds and detect gas leaks from equipment. A given IR camera may be more sensitive to one compound than another. Response Factor (RF) is a measure of an IR camera's sensitivity for a given compound relative to a reference compound. For example, if the RF value for methane is 0.30 in reference to propane, it means that an image of methane is 30% as strong as propane for this particular camera, i.e., methane is less easily detected than propane. If propene's RF is 1.47, the image of propene is 47% stronger than propane. When RF for a compound is very small, that compound may not be visible in the IR camera.

The values of RF are affected by the type of IR camera and the product of concentration (C) and optical pathlength (L), which is commonly denoted as CL with units of ppm-m. For example, CL=100,000 ppm-m could represent a parcel of pure gas (1,000,000 ppm) that is 0.1 meter deep, or 100,000 ppm that is 1 meter deep. For practical purposes, three CL values are used in this RF calculator: 2,000 ppm-m for a small/diluted gas plume, 100,000 ppm-m for a large/concentrated gas plume, and 20,000 ppm-m for a condition between the high and low CL. For more information on RF, please refer to paper # 93 in the Proceedings of Air Quality Measurement Methods and Technology, Chapel Hill, NC, March 15-17, 2016 (<http://measurements.awma.org/>).

This online RF Calculator is provided to the OGI user community by Providence Photonics free of charge. Users simply need to enter their email address in order to use this tool.

Enter Email:

No Spam emails will be sent!

Select Camera:

More cameras coming soon

Select Chemical

Enter CAS number

Select CL

Figure 5.22: The Response Factor (RF) Calculator website (<http://rfcalc.providencephotonics.com/>). Appropriate selections were made for the camera, chemical and CL.

Enter Email:

No Spam emails will be sent!

Select Camera:

More cameras coming soon

Select Chemical

Enter CAS number

Select CL

RF: 0.001 for Tetrachloroethylene (CAS #: 127-18-4)

(in reference to Propane)

Acknowledgement: the IR spectral data used to calculate the RF is downloaded on November 18, 2015 from the IR database maintained by Pacific Northwest National Lab (PNNL).

Figure 5.23: RF calculations results for PCE. Calculated results indicate that PCE is 1000 times less sensitive than the reference chemical, propane.

The FLIR website lists the MDLR for propane while using a FLIR GF-320 VOC camera to be 0.4 g/hr. (<http://www.flirthermography.com/ogi/display/?id=55671>). Based on this, the MDLR for PCE, which has an RF of 0.001 with respect to propane is estimated to be (0.4/0.001) or 400 g/hr. of 100% PCE (or 400 g/hr. of 1,000,000 ppm PCE).

An alternate method for calculating the minimum flow rate of PCE required to be detected using a FLIR GF-320 VOC camera would be to use the physicochemical properties of propane and PCE. The density of propane gas is approximately 0.0018 g/ml at STP (standard temperature and pressure of 25 °C and 1 atm, respectively), and its specific volume is 0.552 m<sup>3</sup>/kg or 552 ml/g ([https://www.engineeringtoolbox.com/propane-d\\_1423.html](https://www.engineeringtoolbox.com/propane-d_1423.html)). For a detection limit of 0.4 g/hr. of 100% propane, the flow will be 0.4 g/hr. × 552 ml/g or ~ 221 ml/hour or 3.68 ml/min.

Given that the RF for PCE is 0.001 with respect to propane, this translates to a detection limit of 3.68 × 1000, or 3680 ml/min of 100% pure PCE. Hence, for detecting a 1 ppm PCE gas stream (at a depth of 1 m) using a GF-320 camera system, the minimum flow rate should be 3.68 × 10<sup>6</sup> l/min. Given the high transmittance as shown in Figure 5.21 in the GF-320 camera's 3.2 – 3.4 μm spectral range, the necessity for such a high flow rate is not surprising. For detecting PCE at the 10<sup>-6</sup> risk range action level (125 ppt), for a PCE plume that is 1 m in depth, the flow rate must be 8000 times higher or approximately 29.4 billion liters per minute.

## 5.5.2 Estimation of Detection Limits using IR Spectra

The sensitivity of an IR camera may be estimated using transmittance percentages in the IR camera's spectral range. Hence, if a given chemical has a low transmittance in each camera's spectral range, the camera should be able to detect the chemical. The opposite is true for chemicals that have close to 100% transmittance in the camera's spectral range. Detection limits for chemicals may be determined by comparing the IR spectra of the chemical to the IR spectra of a reference chemical for which MDLRs are available on the FLIR website. The percent of IR absorbed in the spectral range of a camera for a given chemical is compared to the percent of IR absorbed for a reference chemical. For example, Figure 5.24 shows the IR spectra for propane in the spectral range of the GF-320 VOC camera (3.2 – 3.4 μm), while Figure 5.25 shows the IR spectra for TCE in the same spectral range.

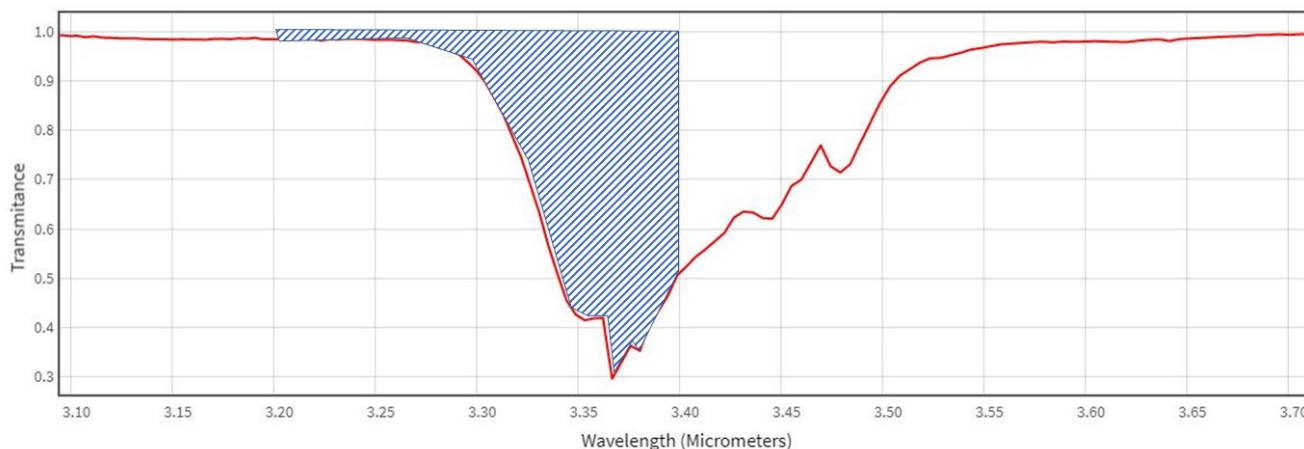
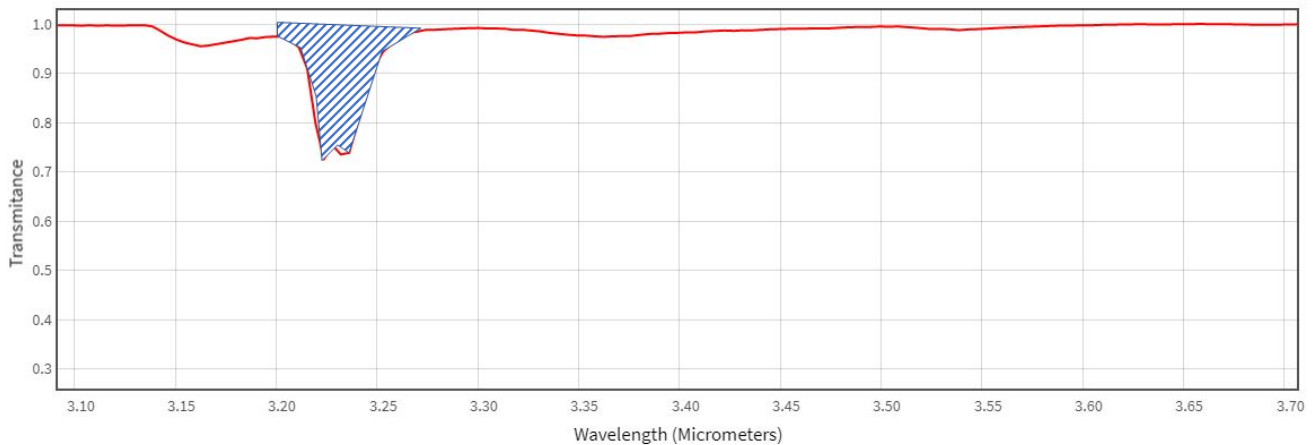


Figure 5.24: IR spectrum for propane in the spectral range of the FLIR GF-320 VOC camera system.



*Figure 5.25: IR spectrum for TCE in the spectral range of the FLIR GF-320 VOC camera system. The area of the shaded region for TCE in this figure is approximately 5% of the area for propane (shown in Figure 5.24), suggesting the sensitivity of TCE is approximately 5% of that of propane as detected by the GF-320 VOC camera.*

The sensitivity of a target chemical with respect to a reference chemical can be compared to the absorbance or transmittance area (area under the curve) of the two chemicals within the spectral range of a camera. For example, the shaded area in Figure 5.24 represents the sensitivity of propane, the reference chemical, in the spectral range of the FLIR GF-320 VOC camera system (3.2 – 3.4  $\mu\text{m}$ ), while the shaded area in Figure 5.25 represents the sensitivity of TCE in the same spectral range. The x- and y-axis ranges in the two figures are approximately the same; hence, according to the shaded areas for the two chemicals, the sensitivity of TCE is approximately 5% of the sensitivity of propane. Similarly, the MDLR of TCE is expected to be approximately 5% of the MDLR of propane, which indicates the MDLR of TCE is 0.4 g/hr./0.05, or approximately 8 g/hr. of 100% (1,000,000 ppm) TCE. Based on the IR images of a fully open propane tank shown in Figures 5.3 – 5.5, the flow rate of TCE should be approximately 20 times greater for the GF-320 VOC camera to detect pure TCE at the same level as propane in the 3 figures (the flow rate of propane from the tank is many times higher than the MDLR or 0.4 g/hr.). For TCE at a concentration of 1000 ppm, the flow rates would be 20,000 times higher than the flow rate of propane from the propane tank.

Based on the IR spectrum of TCE at the spectral ranges of the FLIR GF-306 and GF-320 cameras, and based on the absorbance or transmittance area, the FLIR GF-306 camera is expected to be approximately 100 times or more sensitive towards detecting TCE than the FLIR GF-320 VOC camera. For the same reason, the MDLR for TCE would be 100 or more times lower for the FLIR-306 camera than the FLIR-320 VOC camera.

## 5.6 Static Detection of Gas using the Two Camera Systems

As mentioned previously, the sensitivity, and hence the detection limit is highly dependent on the concentration of gas in the plume and the distance (length) over which light travels through the plume to reach the camera sensor. Hence, the response of a given camera towards a gas plume that is at a concentration of 1000 ppm and 1 m in length will be the same as a plume that is at a concentration of 10,000 ppm and 100 cm in length. Figure 5.26 illustrates the concept of the camera sensor being dependent on the concentration and the length of the plume in the same direction as the camera sensor.

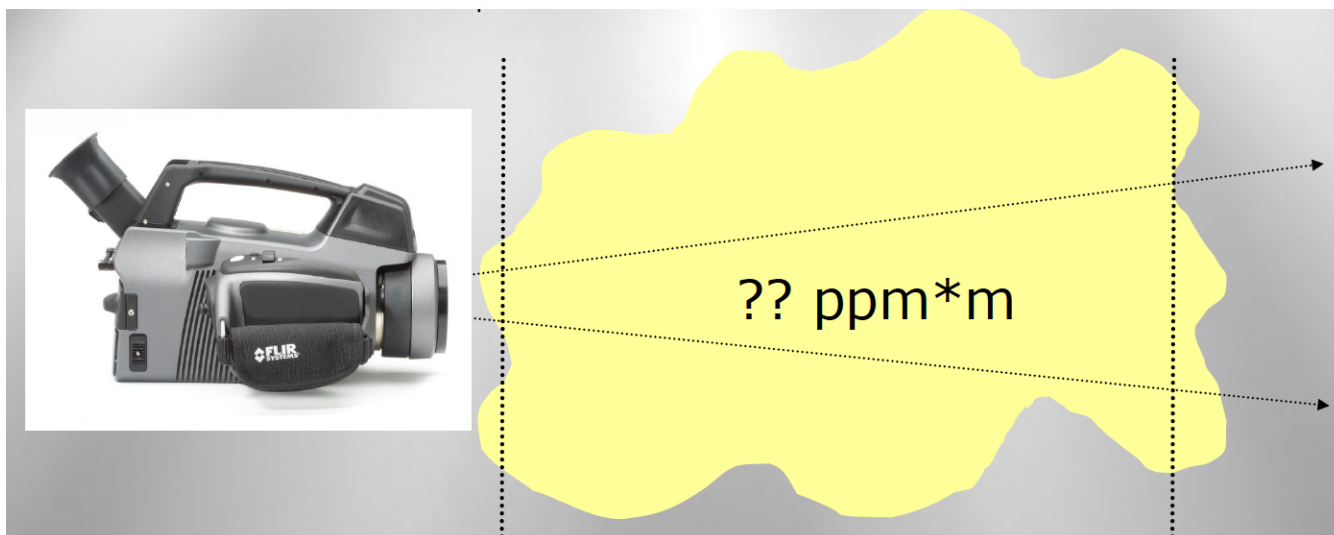


Figure 5.26: A schematic illustrating the importance of concentration and dimensions of the plume on the sensitivity of the camera towards a gas plume (Source: FLIR Systems, Inc.). If the vertical line closest to the camera lens can be considered to be the 100 cm line, and the line farthest away can be considered the 1 m line, the amount of gas seen by the camera at the 100 cm line is much smaller than the amount of gas seen at the 1 m line, leading to better sensitivity at the 1 m line.

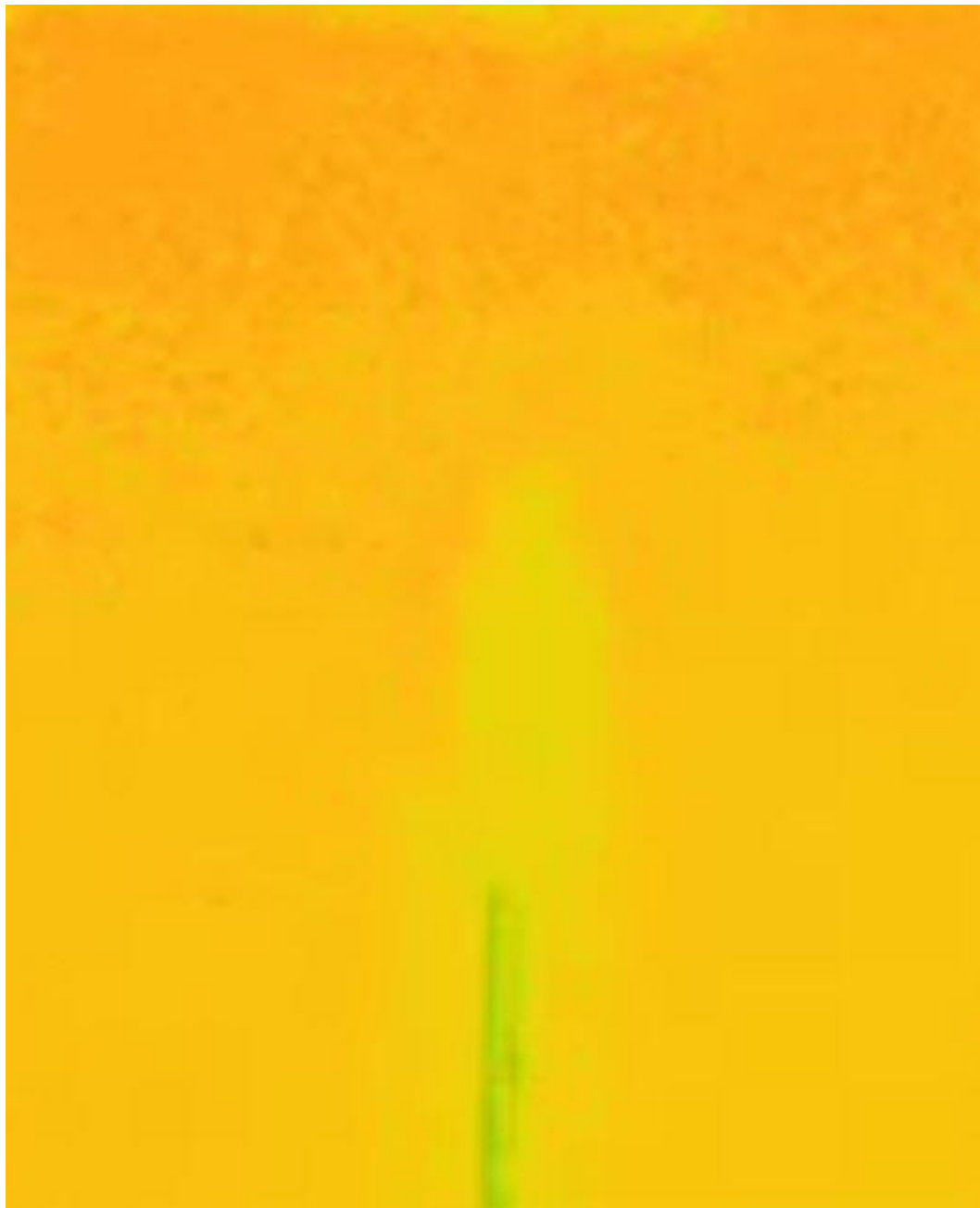
Since the size of the nozzle from the gas canisters was very small, and the concentration of the gas plume was low (ppt – ppm levels), experiments that considered an increased cross section of the gas plume were conducted. However, since the volume of gas available in the canisters was limited (approximately 58 liters, which would yield about 5 – 6 minutes of a gas “leak” at sufficient pressure and a flow rate of around 8 lpm), an effort was made to capture the gas in an enclosed container with a wider cross section. This way, the width of the gas “plume” in the enclosed container would be wider than the width of gas coming out of a nozzle. In addition, the plume of gas in the bottle remains undiluted by air with time and distance unlike the plume of gas coming out the nozzle. Hence, the camera sensor would “see” a constant cross-section of the undiluted gas in an enclosed container. To this effect, various enclosed containers were tested for capturing gas including 1L glass jars, inverted beakers and plastic bottles of various types and sizes. Ultimately, it was determined the glass containers that were tested, which were made of borosilicate glass, would not allow IR radiation to pass through (the 40 ml TOC vial on the other hand was not made of borosilicate glass, which allowed the FLIR GF-306 camera system to “see” the level of ammonium hydroxide in the vial as well as ammonia vapors in the vial; see Figures 5.6 – 5.8 for IR images of a TOC vial that contained ammonium hydroxide liquid and vapors). Figure 5.27 shows some of the containers that were tested, including an inverted glass beaker, glass jars, and an open vial containing ammonium hydroxide that was placed inside an open glass jar. In this scenario, the camera was not able to “see” the ammonium hydroxide fumes that were released from the open vial (figure not shown). Some of the plastic bottles tested blocked IR radiation (the plastic material was unknown); however, the testing lab at the EPA Region 6 Addison Facility had several thin-walled 60 ml high density polyethylene (HDPE) bottles with caps that contained a nozzle that could be capped. These bottles were found to allow IR radiation to pass through. In addition, these bottles with capped nozzles served the dual purpose of either completely enclosing the captured gas or liquid when capped or allowing gas to escape as a jet stream when uncapped, especially when squeezed along the sides of the bottle. Figure 5.28 shows an IR image of an empty 60 ml HDPE bottle (control) using the rainbow color palette that was taken using the FLIR GF-306 camera system. Multiple experiments were conducted with the 60 ml HDPE bottles that were filled with gases, solvents, or

ammonium hydroxide. In all experiments, the FLIR GF-306 camera system was used to capture the IR images.



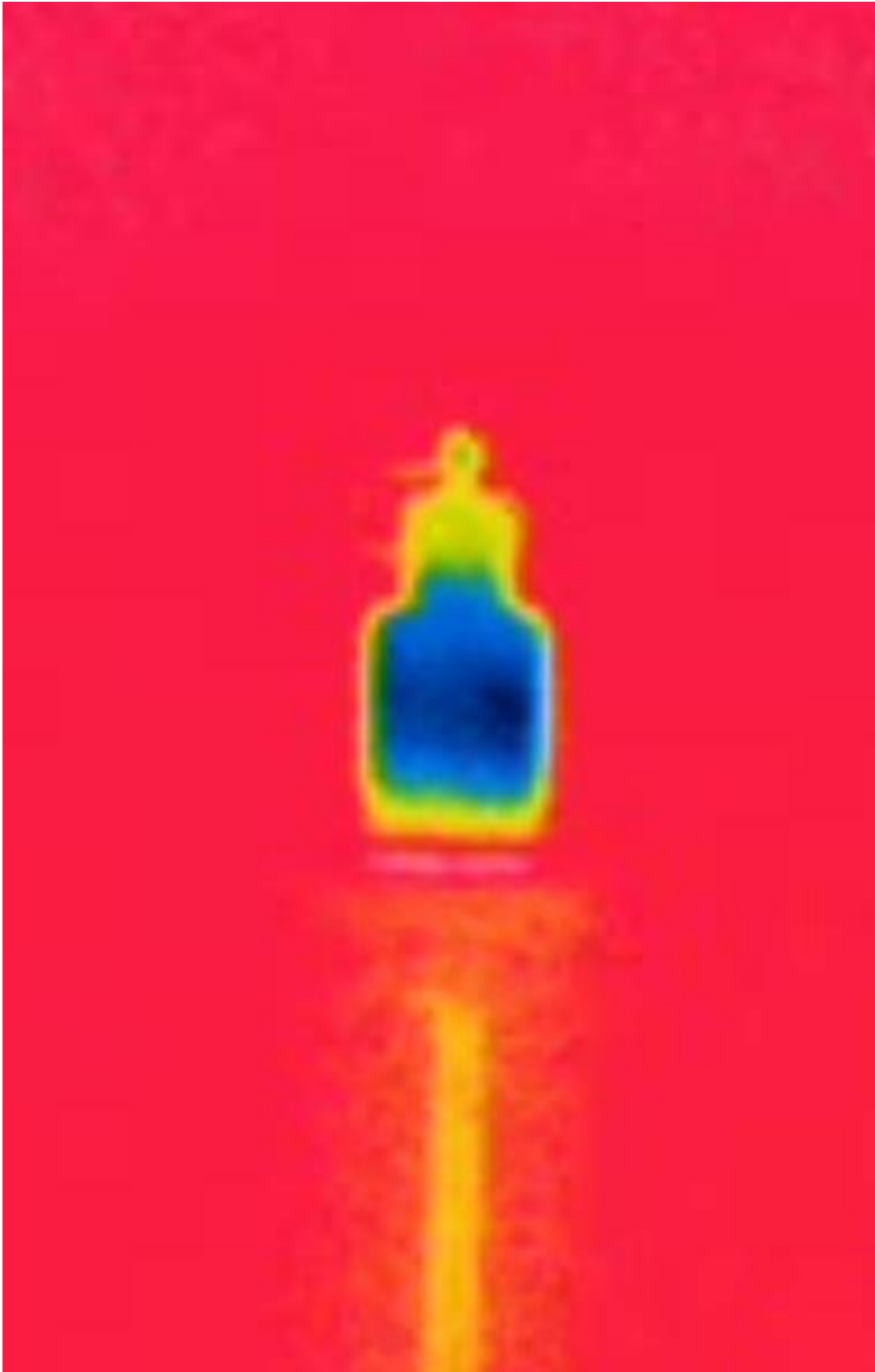
*Figure 5.27: An inverted beaker and other glass jars were tested to “capture” PCE or TCE gas. In the picture, an open bottle containing ammonium hydroxide that was placed inside one of the glass jars could not be “seen” by the FLIR GF-306 camera as the outside glass jar was made of borosilicate*

glass, which blocks IR radiation from passing through.

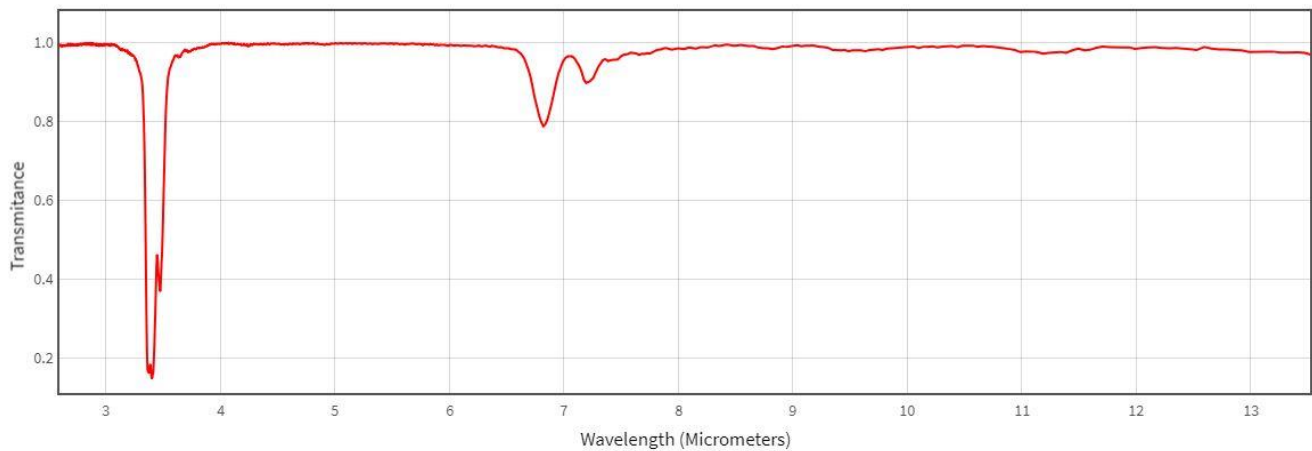


*Figure 5.28: An IR image of an empty 60 ml HDPE bottle using the rainbow color palette taken with the FLIR GF-306 camera. The bottle containing air was indistinguishable from the background (back pane of the fume hood made up of porcelain material).*

The 60 ml HDPE bottle was filled with a few drops of ammonium hydroxide and capped. Figure 5.29 shows the HDPE bottles filled with ammonia vapors. The IR image shows the vapors inside the bottle as deep blue against a pink background. To determine if the camera was detecting the ammonia and not some other artifact, a second 60 ml HDPE bottle was filled with a few drops of hexane. The IR spectrum of hexane is shown in Figure 5.30, which shows a transmittance close to 10% in the 3.2 – 3.4  $\mu\text{m}$  spectral region, which is within the spectral range of the FLIR GF-320 VOC camera. However, the transmittance in the 10.3 – 10.7  $\mu\text{m}$  spectral region is close to 100%, indicating the FLIR GF-306 camera system will not be able to detect hexane.



*Figure 5.29: An IR image of a 60 ml HDPE bottle containing a few drops of ammonium hydroxide using the rainbow color palette. The ammonia vapor inside the HDPE bottle was easily distinguished by the FLIR GF-306 camera.*



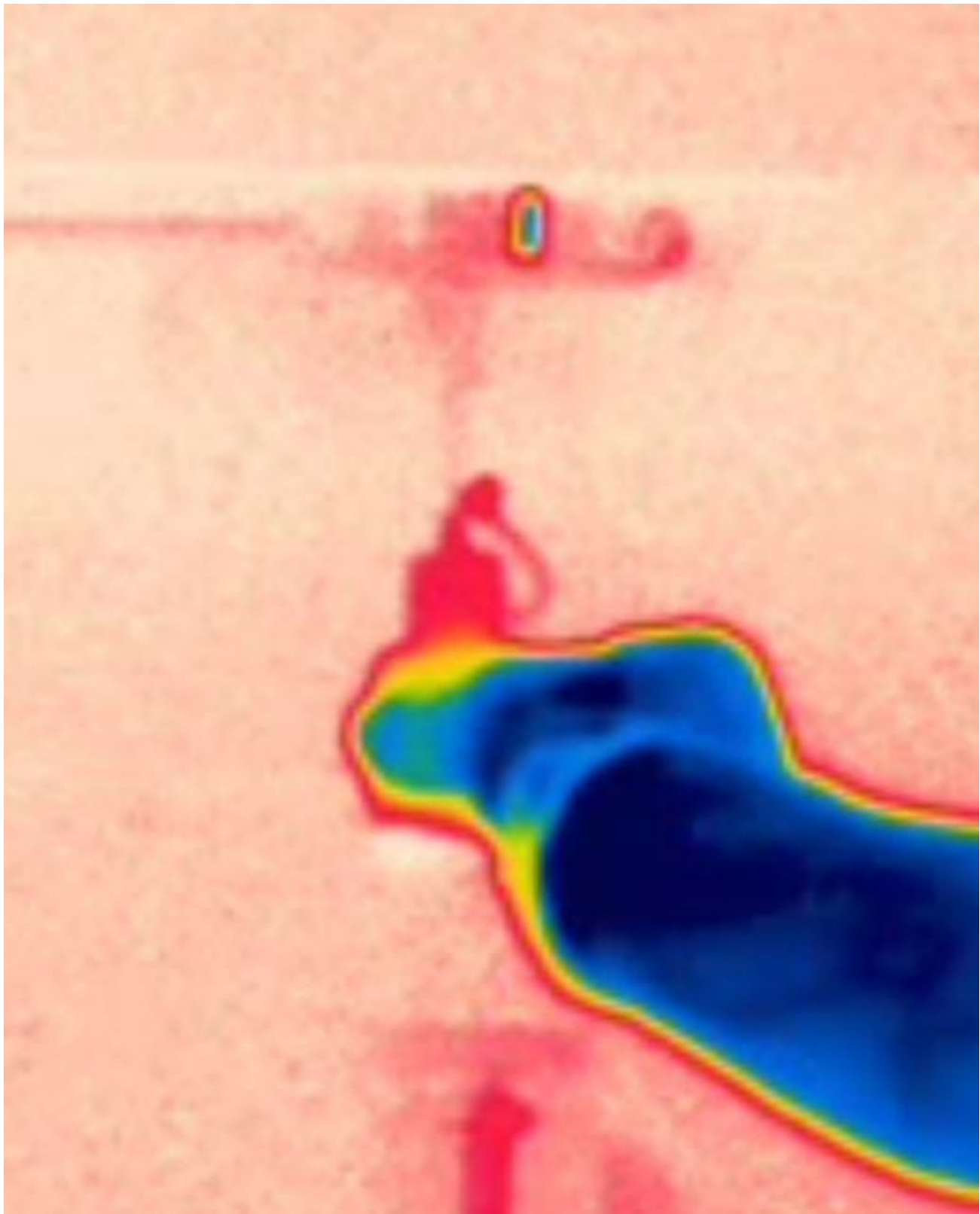
*Figure 5.30: IR spectrum of hexane from the NIST WebBook database. The transmittance of hexane decreases in the 3.2 – 3.4  $\mu\text{m}$  spectral region, which can be detected by the FLIR-320 VOC camera. There is no reduction in transmittance in the 10.3 – 10.7  $\mu\text{m}$  spectral region, which indicates the GF-306 camera will be not be able to detect hexane.*

Figure 5.31 shows an IR image of a HDPE bottle containing a few drops of hexane using the rainbow color palette. Unlike the bottle containing ammonium hydroxide, which showed the vapor inside the bottle in a deep blue color, the bottle containing hexane is yellow in color, indicating the GF-306 camera could not detect the hexane inside the HDPE bottle.

To test a “leak” scenario with the FLIR GF-306 camera system, the nozzle of the bottle containing ammonium hydroxide was uncapped, and the sides of the bottle was gently squeezed, releasing a gently stream of ammonia through the nozzle. Figures 5.32 and 5.33 show IR images of the squeezed bottle. The investigator’s hand holding the bottle can be seen (in blue), and the vapor stream from the nozzle is seen as a red plume on top of the bottle. In addition, a cap from one of the jars was inverted (bottom facing down) and tied to a stand a few inches from the tip of the nozzle. The ammonia fumes from the nozzle can be seen accumulating inside the inverted cap, and flowing out around the sides of the inverted cap as a red cloud.



*Figure 5.31: An IR image of a 60 ml HDPE bottle containing a few drops of hexane using the rainbow color palette. The hexane and its vapor inside the HDPE bottle was not detected by the FLIR GF-306 camera.*



*Figure 5.32: An IR image of a 60 ml HDPE bottle containing a few drops of ammonium hydroxide using the rainbow color palette. The cap on the nozzle was opened, and the bottle gently squeezed, releasing ammonia vapor in a jet stream, which is seen as a red plume. (The investigator's hand and arm are seen as color palette with blue is hot.)*

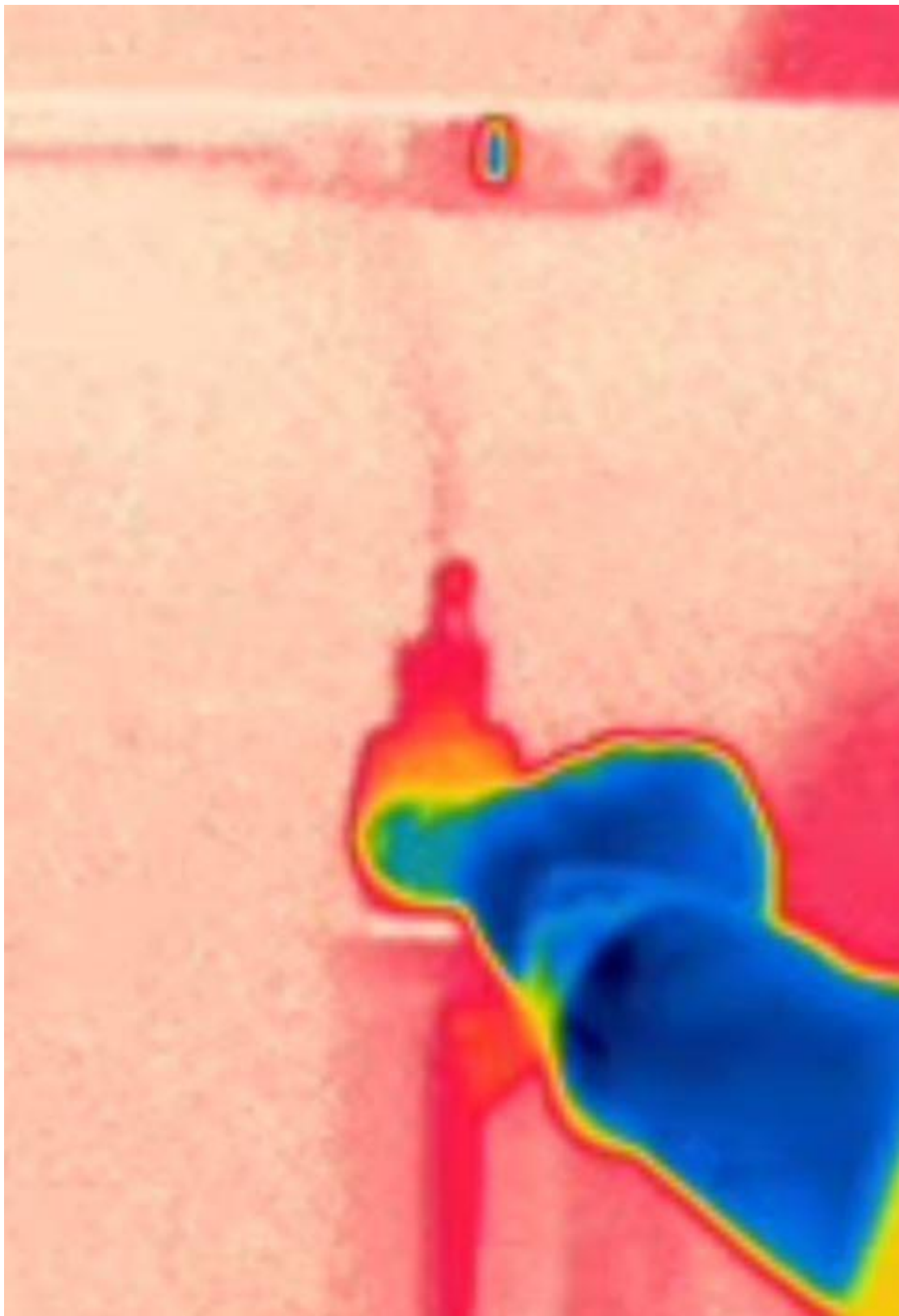


*Figure 5.33: An IR image of a 60 ml HDPE bottle containing a few drops of ammonium hydroxide using the rainbow color palette. The cap on the nozzle was opened, and the bottle gently squeezed, releasing ammonia vapor in a jet stream, which is a red plume emanating from the nozzle. (The investigator's hand and arm are seen as color palette with blue is hot.)*

To determine if the FLIR GF-306 camera can detect TCE vapor in a bottle, a new 60 ml HDPE bottle was flushed with several volumes of gas from a 125 ppb TCE gas canister by running a tube from the canister to the inverted bottle. The bottle was then capped and placed alongside a control 60 ml HDPE bottle that contained air. The set up can be seen in Figure 5.34.

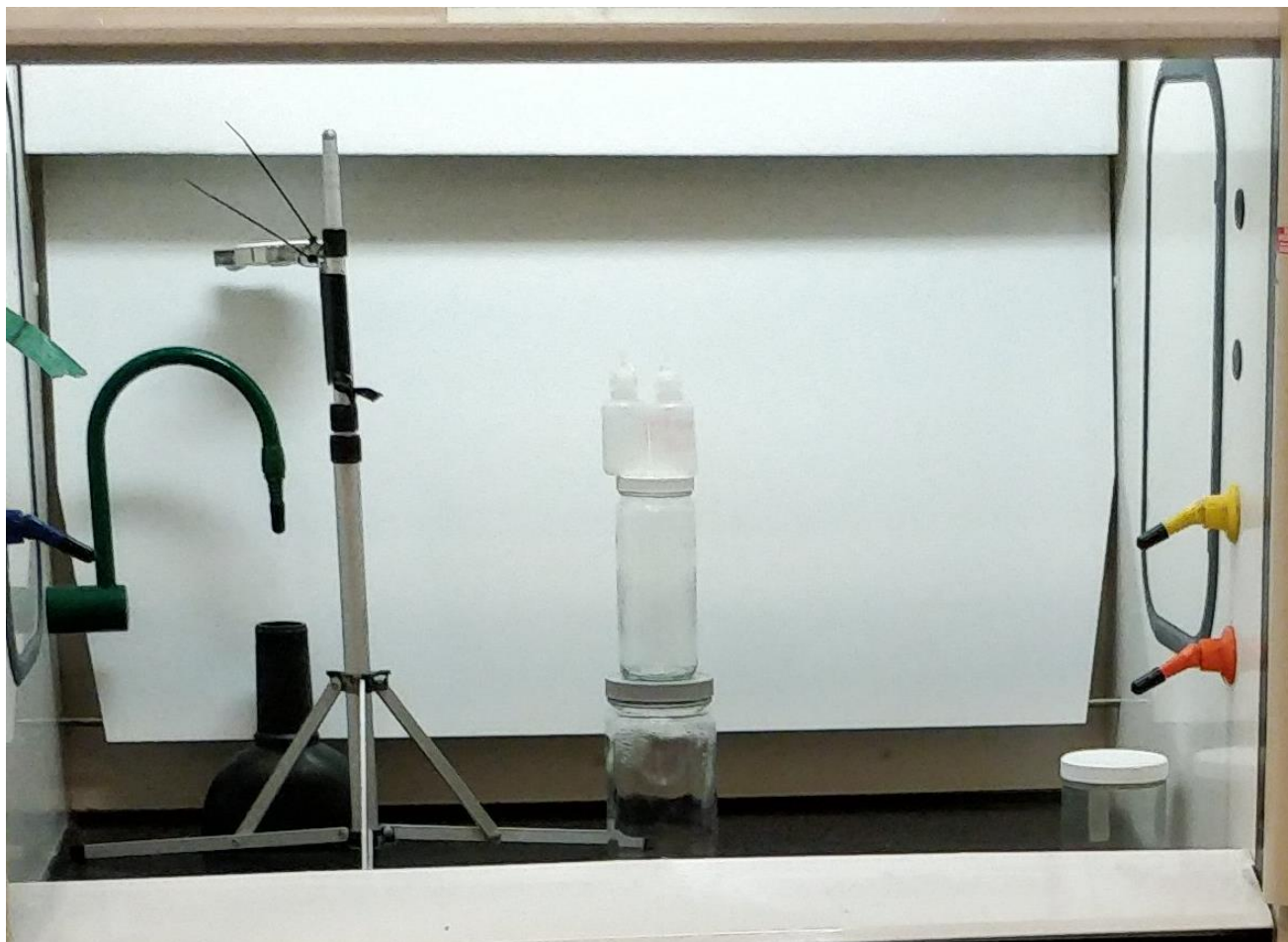


*Figure 5.34: A setup to detect TCE gas in a 60 ml HDPE bottle. Two bottles were placed side by side on top of two glass jars to keep the HDPE bottles in line with the camera lens. The bottle on the left contained air while the bottle on the right contained 125 ppb TCE.*

Figures 5.35 – 5.37 show IR images of the two bottles using a rainbow color palette, a black is hot palette and a white is hot palette, respectively. In Figure 5.35, the HDPE bottle containing TCE vapor is bluish green, while the control bottle is yellow in color (similar to the background). Optical images of this setup, including those with IR images on the camera screen are shown in Figures 5.38 and 5.39. Figure 5.38 focuses on the bottles in the hood while Figure 5.39 focuses on the camera's LCD screen, with the bottles in the background.



*Figure 5.35: An IR image of two 60 ml HDPE bottles, the one on the right containing 125 ppb TCE, and the one on the left containing air using the rainbow color palette. The bottle containing TCE is bluish green, while the one containing air is yellow.*



*Figure 5.36: An IR image of two 60 ml HDPE bottles, the one on the right containing 125 ppb TCE, and the one on the left containing air using the “black is hot” palette. The bottle containing TCE is darker in color, while the background and the one containing air are lighter in color.*



*Figure 5.37: An IR image of two 60 ml HDPE bottles, the one on the right containing 125 ppb TCE, and the one on the left containing air using the “white is hot” palette. The bottle containing TCE is lighter in color, while the background and the one containing air are darker in color.*



*Figure 5.38: A setup to detect TCE gas in a 60 ml HDPE bottle. Two bottles were placed side by side on top of two glass jars to keep the HDPE bottles in line with the camera lens. The bottle on the left contained air while the bottle on the right contained 125 ppb TCE. An IR image of the two bottles can be seen on the camera's LCD screen in the foreground.*

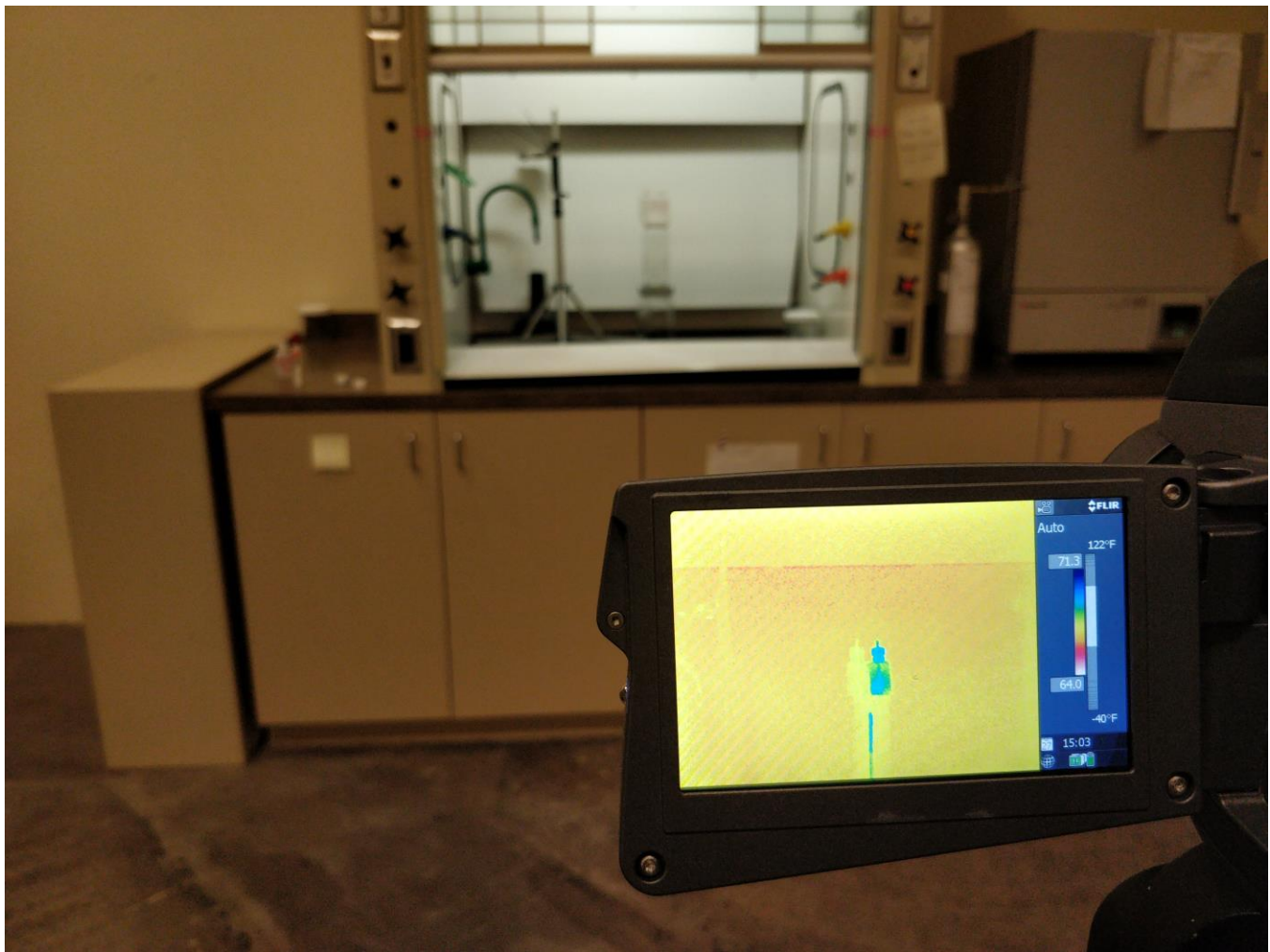


*Figure 5.39: A setup to detect TCE gas in a 60 ml HDPE bottle. Two bottles were placed side by side on top of two glass jars to keep the HDPE bottles in line with the camera lens. The bottle on the left contained air while the bottle on the right contained 125 ppb TCE. An IR image of the two bottles can be seen on the camera's LCD screen in the foreground.*

Results from these “static” experiments seem to indicate the FLIR GF-306 camera might be able to detect TCE when the CL values are sufficiently high.

## **5.7 Implications for Testing Vapor Intrusion Scenarios**

Recently, the EPA proposed regulations requiring use of optical gas imaging (OGI) technologies to identify and repair leaks. While this is true mostly for the oil and gas industry, several vendors participated in EPA’s Environmental Technology Verification (ETV) program to verify their advanced monitoring technologies for monitoring air (<https://archive.epa.gov/nrmrl/archive-etv/web/html/vrvs.html>). FLIR was one of the vendors that participated in this program in 2010 (U.S. EPA, 2010). The tests under this verification program were conducted with a GasFindIR™ camera, which is the predecessor to the FLIR mid-wave GF-320 VOC camera. As part of the verification test, the gas leaks detected by the camera for various chemicals such as acetic acid, benzene, methylene chloride and propane were compared to U.S. EPA Method 21 under both laboratory conditions and field conditions at 10 different locations, with a minimum leak rate of 500 ppm by volume. Test results indicate that detection by the IR camera agreed with conventional monitoring methods for 7 vapors (1,3-butadiene, acetic acid, acrylic acid, benzene, ethylene, pentane, and styrene) under laboratory settings,

the camera could not detect some of these vapors that had concentrations as high as 100,000 ppm by volume at a distance of 10 ft. in the field, primarily because of some confounding factors (U.S. EPA, 2010) that are typically encountered in the field. FLIR camera systems typically rely on the physical characteristics of the environment, which has its own IR signature, and the physicochemical properties of the gas; this temperature and emissivity difference between background IR radiation and absorption spectra of the leaking gas causes the camera sensor to “see” the gas leak. Though the IR spectra of the gas remains the same, the IR spectra of the background will be different between a laboratory setting and each of the field settings, leading the camera to miss field detection of a gas that was successfully detected in a laboratory setting. In addition, the leaking gas may not have sufficient thermal emission or absorption in each spectral region (e.g., TCE in the mid-wave spectral region compared to the long-wave spectral region), leading the IR camera to not detect a leak against the ambient thermal background. During ETV laboratory testing conducted by the EPA (2010), the effect of experimental factors such as background materials, wind speed, and standoff distance on the leak detection capabilities for various gases were tested.

Among the factors tested, the imaging distance was shown to be one of the most important parameters affecting IR detection effectiveness (Ravikumar *et al.*, 2017; US EPA, 2010). For example, Ravikumar *et al.* (2017) showed that a GF-320 camera could detect over 80% of emissions from a simulated well-site from an imaging distance of 10 meters, and that increasing the imaging distance increased method detection limits and decreased detector sensitivity. Ravikumar *et al.* (2018) reported the size of a leak that will be required for detection is proportional to the square of distance from the leak as the apparent size of a plume, as seen by the detector sensor (in pixels), is inversely proportional to the square of the imaging distance. Similar effects were noticed due to windspeed. An increase in windspeed from 0 to 2.5 mph increased the detection limits of most of the tested chemicals by a factor of 10 or more, while an increase in windspeed from 2.5 to 5 mph doubled the detection limits for most of the chemicals (U.S. EPA, 2010), resulting in a decrease in detector sensitivity by a factor of 20 or more. Other factors that may negatively impact detector sensitivity include humidity or moisture content in the atmosphere as water vapor will reduce atmospheric transmission (Ravikumar *et al.*, 2017). Factors that positively affect detector sensitivity include the use of camera lenses with a higher focal length or those that have optical magnification and the presence of “superemitters” in the gas plume, which are gases that show high absorbance in the spectral range of a camera. For example, FLIR reports the detection limit of sulfur hexafluoride as 0.026 g/hr. (<http://www.flirthermography.com/ogi/display/?id=55666>), while methylene chloride is less sensitive with a reported detection limit of 18 g/hr. (U.S. EPA, 2010). Hence, the presence of approximately 1% SF<sub>6</sub> in a gas plume containing methylene chloride would increase the detection capability of the camera towards the gas mixture. In addition, modeling results by Ravikumar *et al.* (2017) show the background has an outside influence on leak detection capability, with land-based detection against the sky or low-emissivity backgrounds having a much higher detection efficiency compared to aerial measurements. According to the authors, the emissivity of the background plays an important role in improving contrast, especially when there is little temperature difference between a gas plume and its background.

As mentioned previously, the sensitivity, and hence the detection limit is highly dependent on the concentration of gas in the plume and the distance (length) over which light travels through the plume to reach the camera sensor. Hence, the response of a given camera towards a gas plume that is at a low concentration but that is spread over a wide distance would be equivalent to a highly concentrated gas plume a few centimeters thick. This implies that while the PCE and TCE leak detection experiments conducted in this study were not detected by the FLIR GF-306 and GF-320 VOC camera systems, in a vapor intrusion scenario, the camera systems, especially the long-wave GF-306 camera might be able to detect a room full of TCE vapor. For example, the lowest TCE concentration tested was using a 125 ppt

gas canister. Given the nozzle size at the point of gas release was 1/16" (~ 0.16 cm), the GF-306 camera sensor was trying to see a TCE cloud at approximately 19.8 ppt \* cm. For a 10-ft long room filled with TCE at 125 ppt, the camera sensor will now see the TCE cloud at 37,500 ppt \* cm, which is approximately 1900 times more sensitive than seeing the gas at the tip of the nozzle. Unfortunately, neither of the two experimental camera systems can detect PCE at any concentration since the spectral ranges of the two cameras do not match the IR spectra of PCE.

The sensitivity towards seeing this gas plume can be further increased by working with a camera with a slightly larger spectral range. The GF-306 camera has a spectral range of 10.3 – 10.7  $\mu\text{m}$ , while TCE has an absorbance range from approximately 10.5 – 13.5  $\mu\text{m}$  (Figure 5.16). Working with a wider spectral range is expected to increase sensitivity towards detecting TCE by a factor of 100 or more (based on the area under the curve as shown in Figure 5.18).

The FLIR GF-306 and GF-320 camera systems will be able to detect other chemical vapors. Using the NIST WebBook search feature shown in Figure 3.5, the list of chemicals that can be seen by the GF-306 in their vapor state is given in Table 5.1, while a partial list of chemicals that be seen by the GF-320 VOC camera is provided in Table 5.2. In both cases, the sensitivity of the cameras towards a chemical can be determined by following the procedure described in Section 5.5.

*Table 5.1: List of chemicals that can be detected by the FLIR GF 306 camera*

Wave number ( $\text{cm}^{-1}$ )	Wavelength (mm)	Chemical Name
935	10.70	Titanium dioxide (anatase)
939	10.65	2-Butanone
940	10.64	Propane
940	10.64	Silane, methyl-
943	10.60	Benzene-D6
943	10.60	Ethylene
944	10.59	Titanium dioxide (anatase)
947	10.56	Titanium dioxide (anatase)
948	10.55	Butane
948	10.55	Ethane, 1,2-dichloro-
949	10.54	Ethylene
950	10.53	Ammonia
952	10.50	2-Butanone
955	10.47	Butane
955	10.47	Methane, bromo-
959	10.43	2-Propenal
959	10.43	Titanium dioxide (anatase)
959	10.43	1-Propyne, 3-iodo-
961	10.41	1-Propyne, 3-bromo-
961	10.41	Ethane, 1-bromo-2-chloro-
962	10.40	Titanium dioxide (anatase)
964	10.37	Butane
964	10.37	Ethyl bromide
965	10.36	Carbonic difluoride

Table 5.2: List of chemicals that can be detected by the FLIR GF 320 VOC camera

Wave number (cm <sup>-1</sup> )	Wavelength (mm)	Chemical Name
2941	3.40	1-Propene, 2-methyl-
2941	3.40	2-Butanone
2943	3.40	Methyl formate
2943	3.40	Formic acid
2944	3.40	Acetic acid
2945	3.40	1-Propene, 2-methyl-
2946	3.39	Methyl Alcohol
2946	3.39	Ethyl Chloride
2952	3.39	Dimethyl ether
2953	3.39	Ethane, 1,2-dibromo-
2954	3.39	Ethane
2954	3.39	Acetonitrile
2955	3.38	Propanenitrile
2957	3.38	Ethane, 1,2-dichloro-
2958	3.38	1-Propyne, 3-iodo-
2960	3.38	Ethane, 1-bromo-2-chloro-
2960	3.38	Methyl Alcohol
2961	3.38	Methylamine
2962	3.38	Propane
2963	3.37	Acetone
2964	3.37	Acetic acid, methyl ester
2965	3.37	Butane
2966	3.37	2-Butyne
2966	3.37	Acetic acid, methyl ester
2967	3.37	Propane
2967	3.37	Ethyl Chloride
2967	3.37	Acetaldehyde
2968	3.37	Butane
2968	3.37	Propanedinitrile
2968	3.37	1,4-Dioxane
2968	3.37	Methane, isocyanato-
2968	3.37	Propane
2969	3.37	Methyl formate
2969	3.37	Ethane
2970	3.37	1-Propene, 2-methyl-
2970	3.37	1,4-Dioxane
2972	3.36	Ethane, 1,2-dibromo-
2972	3.36	Acetone
2973	3.36	2-Butyne
2973	3.36	Propane
2974	3.36	Ethane, 1,2-dibromo-
2976	3.36	1-Propyne, 3-bromo-
2977	3.36	Propane
2980	3.36	1-Propene, 2-methyl-
2980	3.36	Methyl Alcohol

2982	3.35	Silane, methyl-
2983	3.35	Ethane, 1,2-dichloro-
2983	3.35	2-Butanone
2984	3.35	1,3-Butadiene
2985	3.35	Ethane
2985	3.35	Methylamine
2986	3.35	Ethyl Chloride
2988	3.35	Ethyl bromide
2989	3.35	1-Propene, 2-methyl-
2989	3.35	Ethylene
2992	3.34	1,3-Butadiene
2994	3.34	Acetic acid, methyl ester
2996	3.34	Dimethyl ether
2996	3.34	Acetic acid
2999	3.33	Methylene chloride
3000	3.33	2-Propenal
3000	3.33	Methyl Alcohol
3001	3.33	Propanenitrile
3003	3.33	1,3-Butadiene
3003	3.33	Methane, bromochloro
3005	3.33	Ethane, 1,2-dibromo-
3005	3.33	Ethane, 1,2-dichloro-
3005	3.33	Acetaldehyde
3005	3.33	Acetic acid, methyl ester
3006	3.33	1-Propyne, 3-bromo-
3006	3.33	Methyl fluoride
3006	3.33	Ethylene oxide
3007	3.33	Allene
3008	3.32	1-Propyne, 3-iodo-
3008	3.32	Propyne
3009	3.32	Methane, dibromo-
3009	3.32	Acetonitrile
3010	3.32	Ethane, 1-bromo-2-chloro-
3012	3.32	Methyl formate
3013	3.32	Ethane, 1,2-dibromo-
3014	3.32	Ethyl Chloride
3015	3.32	Ethylenimine
3015	3.32	Allene
3017	3.31	Methane, isocyanato-
3018	3.31	Ethyl bromide
3019	3.31	Acetone
3019	3.31	Methane
3025	3.31	Cyclopropane
3026	3.30	Ethylene
3028	3.30	2-Propenal
3031	3.30	Acetic acid, methyl ester
3034	3.30	Trichloromethane

3035	3.29	Ethene, 1,1-dichloro-
3035	3.29	Acetic acid, methyl ester
3036	3.29	Fluoroform
3037	3.29	Ethane, 1,2-dibromo-
3038	3.29	Cyclopropane
3039	3.29	Chloromethane
3040	3.29	Methylene chloride
3042	3.29	Methane, isocyanato-
3042	3.29	Methane, tribromo-
3045	3.28	Methyl formate
3047	3.28	Benzene
3051	3.28	Acetic acid
3055	3.27	1,3-Butadiene
3056	3.27	Methane, bromo-
3060	3.27	Methane, iodo-
3062	3.27	Benzene
3063	3.26	Benzene
3063	3.26	Ethylene oxide
3065	3.26	Ethylene oxide
3066	3.26	Methane, bromochloro-
3068	3.26	Benzene
3072	3.26	Ethylene, 1,2-dichloro-, (Z-isomer)-
3073	3.25	Ethylene, 1,2-dichloro-, (E-isomer)-
3073	3.25	Methane, dibromo-
3077	3.25	Ethylene, 1,2-dichloro-, (Z-isomer)-
3079	3.25	Ethylenimine
3082	3.24	Cyclopropane
3086	3.24	Thiophene
3086	3.24	1-Propene, 2-methyl-
3086	3.24	Allene
3087	3.24	1,3-Butadiene
3090	3.24	Ethylene, 1,2-dichloro-, (E-isomer)-
3098	3.23	Thiophene
3101	3.22	1,3-Butadiene
3103	3.22	2-Propenal
3103	3.22	Ethylene
3103	3.22	Cyclopropane
3106	3.22	Ethylene
3125	3.20	Thiophene

Though the FLIR GF-306 and GF-320 VOC camera systems can detect gases qualitatively (i.e., the gases are either ‘detect’ or ‘non-detect’), FLIR Systems, in partnership with Providence Photonics, has a quantitative module, the Providence Photonics’ QL320™, that is designed to work with FLIR cameras, including the FLIR GF-306 and GF-320 VOC camera systems. The intent behind the development of a quantitative module is to eliminate the need for conventional analysis techniques such as EPA Method 21 to quantify the amount of gas in a plume. Similar to the GF-300 series camera systems, including the GF-306 and GF-320 cameras, the response of the quantitative module is dependent on the IR spectra of the gas compound, and as with the GF-300 series cameras, sensitivity can be determined by calculating a

response factor or the methods described in Section 5.4. The Providence Photonics' QL320™ in conjunction with a FLIR GFx320 or FLIR GF320 camera can measure mass leak rates (lb/h or g/h) or volumetric leak rates (cc/min or L/min) for most hydrocarbons. Recently, Thoma *et al.* (2016) tested two prototype QOGI systems in a collaborative study at the EPA's optical remote sensing range in Research Triangle Park, NC. Using both known and unknown controlled gas release rates, the authors successfully simulated leaks of methane and propane for a variety of scenarios.

## 6. CONCLUSIONS

The primary objective of this study was to determine if a FLIR camera system can serve as an alternative to traditional methods for reliably detecting point sources of PCE and TCE vapors released into the environment. To test the objective, PCE and TCE gas canisters of known concentration ranging from 125 ppt to 125 ppm were obtained from IS GAS in Houston, TX. Leak detection experiments were conducted wherein each gas canister of known concentration was connected to a gas regulator, placed in a chemical fume hood, and gas was released through a 1/16" nozzle perpendicular to the ground at flow rates ranging from 0 (control) to 8 liters per minute. For each of the leak detection experiments, a FLIR GF-306 long wave IR camera or a GF-320 mid-wave IR camera was set up 8 feet in front of the source, and the lens was focused on the tip of the nozzle. In all cases, including the highest concentrations of PCE (125 ppm) and TCE (125 ppb) tested, neither of the two experimental camera systems could detect any gas plume in any of the four camera settings tested: gray scale with black is hot polarity, gray scale with white is hot polarity, high sensitivity mode, and a rainbow color palette. In the case of PCE, this is because the absorbance range of PCE (10.8 – 13  $\mu\text{m}$ ) was just outside the spectral range of the GF-306 camera, while PCE does not have any absorbance in the spectral range of the GF-320 VOC camera (3.2 – 3.4  $\mu\text{m}$ ). In the case of TCE, though the spectral ranges of both the mid- and the long-wave camera system encompass at least a portion of TCE's absorbance wavelengths, this is because the concentration of the highest standard used (125 ppb) was much lower than the detection limit (500 ppm by volume or higher according to Trefiak *et al.*, 2016). This is especially true of the absorbance peak in the mid-wave IR range as it is approximately 1 – 5% of the absorbance peak in the long-wave IR range. Hence, the FLIR GF-306 will theoretically be 20 – 100 times more sensitive towards detecting TCE vapor than the FLIR GF-320 VOC camera. Though neither of the two cameras will be able to detect PCE at any concentration, a camera system with a wider spectral range in the long wave IR region might be able to detect both vapors.

The performance of the FLIR GF-306 and GF-320 cameras were tested against a list of chemicals they are known to detect. For example, the manufacturer of the camera lists ammonia as one of the chemicals that can be detected by the FLIR GF-306 camera, while propane is one of the chemicals that is listed as being able to be detected by the FLIR GF-320 camera. For the GF-320 camera, a setup like the one used for PCE/TCE gas canisters was used, while for the GF-306 camera, a bottle containing ammonium hydroxide was placed inside a hood with the cap off. In both cases, the two cameras could detect propane (for GF-320) and ammonia (for GF-306) under gray scale with black is hot polarity, gray scale with white is hot polarity, high sensitivity mode, and a rainbow color palette, indicating the two cameras were operating as intended.

The detection capability or the sensitivity of a camera system is highly dependent on the concentration of gas in the plume and the cross-sectional length of the plume along the camera axis. Hence, the response of a given camera towards a gas plume that is at a concentration of 1000 ppm and 1 meter in length will be the same as a plume that is at a concentration of 10,000 ppm and 100 cm in length. Since the testing lab did not have the means to increase the plume size and the amount of gas for testing purposes was limited, the path length of a gas plume was artificially increased by capturing the gas (or liquids) in a plastic bottle. Under this scenario, the GF-306 camera could detect ammonia gas inside the plastic bottle, while the GF-320 VOC camera was able to detect TCE inside the plastic bottle. In the case of TCE, IR images of a bottle containing TCE was taken side by side with a bottle containing air. The bottle containing air had the same color as the background under gray scale with black is hot polarity, gray scale with white is hot polarity, and a rainbow color palette, while the bottle containing TCE had a different hue, thus differentiating the two. The ability to detect vapors under this so-called "static"

scenario will be useful in situations such as confined spaces where a lack of air movement will cause the gas to remain in place long enough to be detected by an IR camera.

Though this study was not successful in detecting PCE and TCE vapor intrusion at both the worker and residential air exposure scenarios, this study was successful in demonstrating the capability of FLIR technology to safely detect gas leaks from a location far from the source. In addition, the study was useful in determining the effect of flow rates of gas plumes and cross-sectional length of the plume with respect to the camera axis on a camera's detection capabilities. However, based on their IR spectra and information provided by the manufacturer, detection of gases such as methane, propane, and butane; gasoline fumes; solvents such as benzene and methylene chloride; and common water pollutants such as trihalomethanes are well within the capabilities of the two experimental camera systems. Other means to increase detector sensitivity include using a camera lens with a longer focal length, and controlling environmental factors such as wind, humidity, and background.

# 7. RECOMMENDATIONS

The FLIR GF-306 long wavelength camera system has a very narrow spectral range from 10.3 – 10.7  $\mu\text{m}$ , primarily because it was designed for the detection of gases such as sulfur hexafluoride and ammonia. Though one of TCE's absorbance peaks is partially covered by this range (Figure 7.2), none of PCE's absorbance peaks are covered by the camera's spectral range (Figure 7.1), leading to limited detection of these two chemicals, especially at low concentrations. Using a camera that has a slightly wider spectral range in the long wave IR region might help detect these two vapor-forming compounds at the concentrations that were tested in this study. For example, the VarioCAM HDx head 600 by InfraTEC offers an IR camera with a spectral range of 7.5 – 14  $\mu\text{m}$ , which covers most of the absorbance peaks for both PCE and TCE, and may have lower detection limits than the FLIR GF-306 camera system. In addition, the company has higher resolution detectors, including  $640 \times 480$  on the VarioCAM model all the way up to a  $2560 \times 2048$  resolution as opposed to a detector resolution of  $320 \times 240$  on the GF-306 camera system. One potential downside of using an IR camera with a wider spectral range is reduced specificity in detecting vapors, i.e., the camera will pick up any chemical whose IR spectrum falls within the wider spectral range.

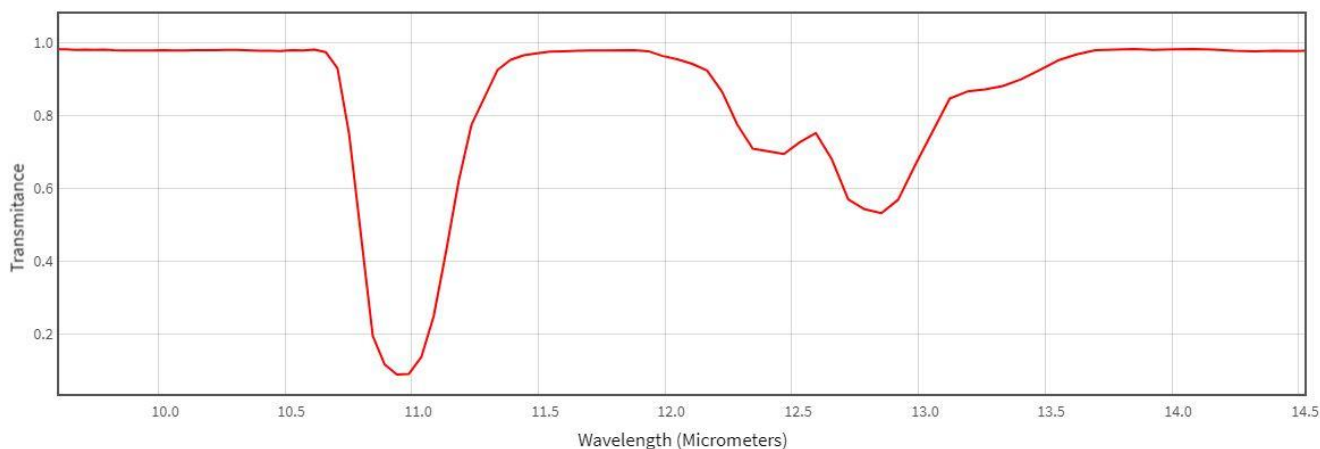


*Figure 7.1: PCE IR spectrum in the 10 – 14 mm range. A VarioCAM with the wider spectral range will be able to take advantage of both transmittance peaks.*

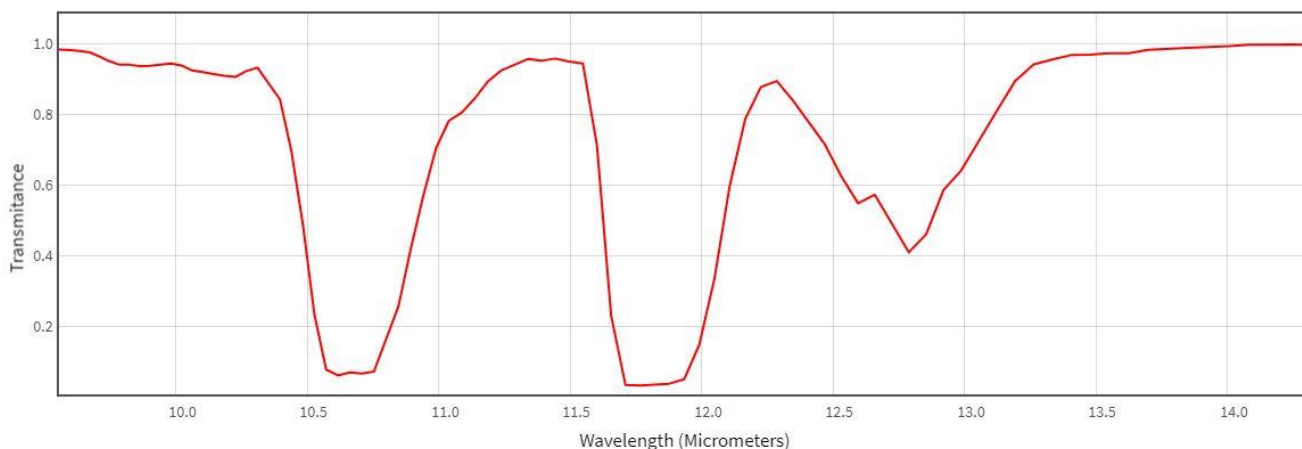


*Figure 7.2: TCE IR spectrum in the 10 – 14 mm range. A VarioCAM with the wider spectral range will be able to take advantage of all three transmittance peaks as opposed to half of one for the GF-306 camera.*

The highest concentration of TCE tested in the lab using the FLIR GF-306 camera system was 125 ppb. Given the camera could detect this concentration of TCE in a static setting, i.e., when a plastic bottle was filled with TCE, it is likely the camera will be able to detect TCE at mid- to high-ppm levels in a flow setting. In addition, given the detection capabilities of a camera are dependent on both concentration and the cross-sectional length of a plume, using a bigger nozzle size may help the camera sensor detect the plume at lower concentrations.

A camera's ability to detect gas leaks is highly dependent on its sensor's ability to detect temperature differences between the gas plume and the background. Hence, physical characteristics of the gas plume and the background may help increase the sensitivity of detection. For example, certain gases have a cooling effect when released from a gas canister, which will be picked up by the camera sensor. In addition, having a background different from the metal plate used in a hood might help differentiate the gas plume from the background. Future studies might consider providing more contrast by trying to focus on the leak from different camera locations (closer and farther from the leak source as well as testing different angles), testing other background materials such as cardboard, drywall, brick, cement, or blue sky among others.

Caution should be exercised when attempting to translate the findings in this report into field performance as various environmental factors such as background, wind speed, humidity and distance from the leakage affect a camera's leak detection capabilities. For example, increasing the stand-off distance from the leak will increase the method detection limits (make the camera less sensitive) as will increasing the wind speed. This work is to be used to establish a starting point for a screening protocol, but not necessarily as an indication of how well products may perform in the field.

## 8. REFERENCES

- Elert, G. 2018. The Electromagnetic Spectrum, The Physics Handbook. Available at <http://hypertextbook.com/physics/electricity/em-spectrum/>. Accessed September 2018.
- Locht, R.; Dehareng, D.; Leyh, B. 2012. The Spectroscopy of the Germinal Ethylene Difluoride (1,1-C<sub>2</sub>H<sub>2</sub>F<sub>2</sub>): the Hel, Threshold and Constant Ion State Photoelectron Spectroscopies. *Journal of Physics B: Atomic, Molecular and Optical Physics*, 45(11), 115101
- McDonald, G.J. and W.E. Wertz. 2007. PCE, TCE, and TCA Vapors in Subslab Soil Gas and Indoor Air: A Case Study in Upstate New York. *Ground Water Monitoring and Remediation* 27(4): 86-92.
- Niemet, M.R.; Lund, L.; Torres, M. 2012. Accounting for Active Dry Cleaner Emissions and Re-entrainment of Subslab Exhaust Vapors in a Site-Wide Vapor Intrusion Mitigation System Design. Eighth International Conference on Remediation of Chlorinated and Recalcitrant Compounds, Monterey, CA.
- Ravikumar, A.P.; Wang, J., and Brandt, A.R. 2017. Are Optical Gas Imaging Technologies Effective for Methane Leak Detection? *Environmental Science & Technology* 51: 718-724.
- Ravikumar, A.P.; Wang, J.; McGuire, M.; Bell, C.S.; Zimmerle, D. and Brandt, A.R. 2018. “Good versus Good Enough?” Empirical Tests of Methane Leak Detection Sensitivity of a Commercial Infrared Camera. *Environmental Science & Technology* 52: 2368-2374.
- Sharpe, S.W.; Johnson, T.J.; Sams, R.L.; Chu, P.M.; Rhoderick, G.C. and Johnson, P.A. 2004. Gas-Phase Databases for Quantitative Infrared Spectroscopy. *Applied Spectroscopy* 58(12): 1452-1461.
- Thoma, E.D.; DeWees, J.; Keser, R.; Hagan, N.; Zeng, Y. and Morris, J. 2016. Progress in Evaluating Quantitative Optical Gas Imaging. Air & Waste Management Association Air Quality Measurement Methods and Technology Conference, March 15-17, 2016, Chapel Hill, North Carolina.
- Trefiak, T. 2016. LDAR Case Study: Comparison of Conventional Method 21 vs Alternative Work Practice. <https://www.epa.gov/sites/production/files/2016-04/documents/20trefiak.pdf>. Accessed August 2018.
- US EPA. 1999a. Compendium of Methods for the Determination of Toxic Organic Compounds in Ambient Air, Second edition: Compendium Method TO-14A, Determination of Volatile Organic Compounds (VOCs) in Ambient Air Using Specially Prepared Canisters with Subsequent Analysis by Gas Chromatography. EPA 625/R-96/010b. Office of Research and Development, Cincinnati, OH. January. Available at <http://www.epa.gov/ttnamti1/files/ambient/airtox/to-14ar.pdf>.
- US EPA. 1999b. Compendium of Methods for the Determination of Toxic Organic Compounds in Ambient Air, Second edition: Compendium Method TO-15, Determination of Volatile Organic Compounds (VOCs) in Air Collected in Specially Prepared Canisters and Analyzed by Gas Chromatography/Mass Spectrometry (GC/MS). EPA 625/R-96/010b. Office of Research and

Development, Cincinnati, OH. January. Available at <http://www.epa.gov/ttnamti1/files/ambient/airtox/to-15r.pdf>.

US EPA. 1999c. Compendium of Methods for the Determination of Toxic Organic Compounds in Ambient Air, Second edition: Compendium Method TO-17, Determination of Volatile Organic Compounds (VOCs) in Ambient Air Using Active Sampling Onto Sorbent Tubes. EPA 625/R-96-010b. Office of Research and Development, Cincinnati, OH. January. Available at <http://www.epa.gov/ttnamti1/files/ambient/airtox/to-17r.pdf>.

US EPA. 2006. Assessment of Vapor Intrusion in Homes Near the Raymark Superfund Site Using Basement and Sub-Slab Air Samples. EPA/600/R-05/147. Office of Research and Development, Cincinnati, OH. March.

US EPA. 2010. Environmental Technology Verification Report. FLIR Systems. GasFindIR™ Midwave (MW) Camera. <https://archive.epa.gov/nrmrl/archive-etv/web/pdf/p100el8v.pdf>. Accessed August 2018.

US EPA. 2015a. OSWER Technical Guide for Assessing and Mitigating the vapor Intrusion Pathway from Subsurface Vapor Sources to Indoor Air. OSWER Publication 9200.2-154.

US EPA. 2015b. A Citizen's Guide to Vapor Intrusion Mitigation. [https://www.epa.gov/sites/production/files/2015-04/documents/a\\_citizens\\_guide\\_to\\_vapor\\_intrusion\\_mitigation\\_.pdf](https://www.epa.gov/sites/production/files/2015-04/documents/a_citizens_guide_to_vapor_intrusion_mitigation_.pdf). Accessed August 2018.

US EPA. 2016. Regional Screening Levels (RSLs) – Generic Tables. <https://www.epa.gov/risk/regional-screening-levels-rsls-generic-tables-may-2016>. Accessed September 2018.

US EPA. 2017. RARE Application – Using FLIR Technology as an Effective PCE/TCE Screening Tool for Vapor Intrusion Sampling. Measurement Project Quality Assurance Project Plan. ORD QA Tracking ID: G-STD-0030744.

US EPA. 2018. Superfund National Priorities List (NPL) Sites – by State. <https://www.epa.gov/superfund/national-priorities-list-npl-sites-state>. Accessed September 2018.

# ISSUE DEN OFF



PRESORTED  
STANDARD POSTAGE  
& FEES PAID EPA  
PERMIT NO. G-35

Office of Research and  
Development (8101R)  
Washington, DC 20460

Offal Business  
Penalty for Private Use  
\$300